



UNIVERSITY OF NAIROBI

**SYNTHESIS, CHARACTERIZATION AND APPLICATION OF NOVEL PALLADIUM
COMPLEXES**

BY

WYCLIFFE ODHIAMBO


I56/15698/2018

**A Research Thesis Submitted in Partial Fulfillment of the Requirements for the Degree of
Master of Science in Chemistry of the University of Nairobi**

2021

DECLARATION

I declare that this thesis is my original work and has not been submitted elsewhere for examination. Where other people's works have been used, this has properly been acknowledged and referenced in accordance with the University of Nairobi's requirements.

Signed..... Date ...29th November 2021.....

Wycliffe Odhiambo

I56/15698/2018

This thesis is submitted for examination with our approval as supervisors:


Dr. Ruth Odhiambo,
Department of chemistry,
University of Nairobi
odhiambor@uonbi.ac.ke

Signed  Date ...30/11/2021.....

Prof. Lydia Njenga,
Department of chemistry,
University of Nairobi
lnjenga@uonbi.ac.ke

Signed.....  Date ...30/11/2021.....

Prof. Martin Onani,
Department of chemistry,
University of the Western Cape (SA)
monani@uwc.ac.za

Signed ... Date.....30-11-2021....

DEDICATION

I would like to first dedicate this work to Almighty God for good health, protection and the blessing of life. To my loving and caring family; my lovely daughter Nylla Hawii Achieng, my parents Mr. Dickson Misigo and Mrs Eunice Achieng and my siblings Simon, Laventine, Ferdinand, Owen, Swanga, Zuri, Val and Aron for the patience and tireless support you have given me. Your unrelenting prayers towards this work are highly appreciated.

ACKNOWLEDGEMENT

First of all I would like to thank the Almighty God for the free gift of life, provision, good health and the energy to do this. 'I can do all things through Christ who gives me strength.

Sincere thanks to all my hardworking supervisors: Dr Ruth Odhiambo, Prof Lydia Njenga and Prof Martin Onani for incalculable comments, high skillful training and supervision to enable me successfully complete this research project. Your tireless support including guidance via phone calls is much appreciated. Weekly pizza and lunch outs after progress report presentations were awesome. Thanks to University of Nairobi, Department of Chemistry, University of the Western Cape, Department of Chemical Sciences, University of the Western Cape organometallics and nanochemistry research group, my classmates and all who contributed to this work.

I would wish to thank Prof. Marvin Mayer, Dr. Nicole Sibuyi and Dr. Swartz Lauren Department of Biotechnology, University of Western Cape for your immense support in biological investigation. Thanks to Prof RodgersLalancette, Rutgers University-New York, for the great work in solving crystal structures.

May I take this opportunity to thank Dr. Peter Waweru, Dr. Wycliffe Wanyonyi and Mr Nelson Khan for paying my masters program school fee. Special thanks to my beloved uncle Mr. Desmond Wagumba together with his lovely wife Mrs. Rebecca Wagumba for housing me during my entire study and providing anything I needed to finish this work.

Thanks to International Science Program (ISP), through KEN-01 and NRF-South Africa for both material and financial support. This work could have not been possible without your support.

ABSTRACT

Palladium(II)thiosemicarbazone complexes are known to be good anticancer agents. However, their stability is a challenge during biological application because of faster ligand exchange kinetics. This research focused on synthesis of palladium complexes with bulky ligands to improve their stability. Thiosemicarbazone (TSC) ligands were synthesized via condensation reaction of aldehydes and respective amines. The following ligands were synthesized; (*E*)-*N,N'*-dimethyl-2-((5'-methyl-[2,2'-bithiophen]-5-yl)methylene)hydrazine-1-carbothioamide (**L1**), (*E*)-*N*-ethyl-2-((5-phenylthiophen-2-yl)methylene)hydrazine-1-carbothioamide (**L2**) and (*E*)-2-((5'methyl)-[2,2'-bithiophen]-5-yl)methylene)-*N*-phenylhydrazine-1-carbothioamide (**L3**). Corresponding Pd(II) complexes were synthesized by reacting equimolar amounts of ligands and Pd(cod)Cl₂. Complexes synthesized were; (*E*)-*N,N'*-dimethyl-2-((5'-methyl-[2,2'-bithiophen]-5-yl)methylene)hydrazine-1-carbothioamide palladium(II)chloride complex (**C1**), (*E*)-*N*-ethyl-2-((5-phenylthiophen-2-yl)methylene)hydrazine-1-carbothioamide palladium(II)chloride complex (**C2**) and (*E*)-2-((5'methyl)-[2,2'-bithiophen]-5-yl)methylene)-*N*-phenylhydrazine-1-carbothioamide palladium(II)chloride complex (**C3**). Stability test for ligands and complexes were done using ¹H NMR in DMSO-d₆ within a period of 72 hours at an interval of 6 hours monitoring any peak change. Both ligands and complexes were characterized by UV-Vis, FTIR, ¹H NMR, ¹³C NMR, elemental analysis and single crystal X-ray diffraction for **L2**. Single crystal X-ray crystallography revealed that the prepared ligand had *E* conformation and existed as thione tautomer. Elemental analysis result indicated that **L1** and **L2** coordinated to palladium metal in N S bidentate fashion while **L3** in SNS tridentate fashion. UV-Vis studies were done on ligand to confirm formation of imine around 300nm ($\pi \rightarrow \pi^*$ transition). UV-Vis also revealed Ligand to metal charge transfer (LMCT) transition confirmed successful coordination of ligands through S-M bond. The anticancer activities of ligands and complexes were screened against Caco-2, HT-29, HeLa and KMST cell lines using *cisplatin* as a positive control. The ligands displayed low anticancer potency compared to corresponding complexes except for **L1**. **L3** had the lowest inhibition to all cell lines with IC₅₀ > 100 $\mu\text{g/mL}$. However after complex formation, **C3** showed inhibition; Caco-2 (IC₅₀=84.32 $\mu\text{g/mL}$), HT-29 (IC₅₀=49.10 $\mu\text{g/mL}$), HeLa (IC₅₀=0.73 $\mu\text{g/mL}$) and KMST (IC₅₀>100 $\mu\text{g/mL}$). All the cell lines displayed high susceptibility to **L1**; Caco-2 (IC₅₀=6.814 $\mu\text{g/mL}$), HT-29 (IC₅₀=6.449 $\mu\text{g/mL}$), HeLa (IC₅₀=0.2619 $\mu\text{g/mL}$) and KMST (IC₅₀=10.7900 $\mu\text{g/mL}$). Among the ligands and complexes **C3** had selective anticancer properties. Caco-2 cell displayed some resistance to inhibition to all the compounds. The complexes had enhanced anticancer activities compared with the respective ligands except for **L1**. Synthesized palladium(II) complexes with bulky ligands were stable and were cytotoxic towards cancer cell lines.

TABLE OF CONTENTS

DECLARATION	ii
DEDICATION	iii
ACKNOWLEDGEMENT	iv
ABSTRACT	v
LIST OF FIGURES	x
LIST OF SCHEMES	xii
LIST OF TABLES	xiii
LIST OF ABBREVIATIONS	xiv
CHAPTER ONE	1
INTRODUCTION	1
1.0 Coordination compounds	1
1.1 Platinum Group Metals	2
1.2 Thiosemicarbazone palladium complexes	3
1.2.5 Heterocyclic thiosemicarbazone complexes of palladium (II)	3
1.4 Cancer	5
1.5 Statement of the problem	5
1.6 Objectives.....	6
1.6.1 General Objective	6
1.6.2 Specific Objectives	6
1.7 Justification of the study	6
CHAPTER TWO	8
LITERATURE REVIEW	8
2.0 Transition metal complexes	8
2.1 Stability of transition complexes	9

2.2 Transition metal complexes in catalysis	10
2.2.1 Iridium complexes	11
2.2.2 Copper complexes.....	13
2.2.3 Palladium complexes	13
2.3 Metal complexes in medicine	15
2.3.1 Gold complexes	15
2.3.2 Ruthenium complexes.....	16
2.3.3 Nickel complexes.....	17
2.4 Metals complexes in cancer treatment.....	19
2.5 Schiff base ligands	20
2.5. 1 Thiosemicarbazones.....	21
2.5.2 Heterocyclic thiosemicarbazones.....	24
2.5.3 Thiophene substituted thiosemicarbazones.....	26
2.6Anticancer activities of palladiumcomplexes	27
CHAPTER THREE	31
MATERIALS AND METHODS.....	31
3.0 instrumentation	31
3.1 Chemicals.....	31
3.2 Synthesis of ligands	32
3.2.1 (<i>E</i>)- <i>N,N'</i> -dimethyl-2-((5'-methyl-[2,2'-bithiophen]-5-yl)methylene)hydrazine-1-carbothioamide (L1).....	32
3.2.2 (<i>E</i>)- <i>N</i> -ethyl-2-((5-phenylthiophen-2-yl)methylene)hydrazine-1-carbothioamide (L2).....	32
3.2.3 (<i>E</i>)-2-((5' methyl)-[2,2'-bithiophen]-5-yl)methylene)- <i>N</i> -phenylhydrazine-1-carbothioamide (L3).....	32
3.3 Synthesis ofthiosemicarbazone complexes of palladium	33
3.3.1 Synthesis of <i>cis</i> -cyclooctadienepalladium(II) chloride precursor.....	33

3.3.2 Synthesis of (<i>E</i>)- <i>N,N'</i> -dimethyl-2-((5'-methyl-[2,2'-bithiophen]-5-yl)methylene)hydrazine-1-carbothioamide palladium(II)chloride (C1)	33
3.3.3 Synthesis of (<i>E</i>)- <i>N</i> -ethyl-2-((5-phenylthiophen-2-yl)methylene)hydrazine-1-carbothioamide palladium(II)chloride (C2)	34
3.3.4 Synthesis of (<i>E</i>)-2-((5'-methyl)-[2,2'-bithiophen]-5-yl)methylene)- <i>N</i> -phenylhydrazine-1-carbothioamide palladium(II)chloride (C3).....	34
3.4 Characterization of ligands and complexes	34
3.4.1 Melting point.....	34
3.4.2 Fourier Transform Infrared spectroscopy	34
3.4.3 UV-Visible spectroscopy	35
3.4.4 Nuclear Magnetic Resonance	35
3.4.5 Elemental analysis	35
3.4.6 Single X-ray crystallography	35
3.5 Determination of stability	36
3.6 Determination of anticancer activities	36
CHAPTER FOUR.....	37
RESULTS AND DISCUSSION	37
4.0 Thiosemicarbazones ligands	37
4.2 Physical properties for ligand L1	37
4.3 Characterization and structural confirmation of ligand L1	38
4.4 Physical properties for ligand L2	40
4.5 Characterization Structural confirmation of ligand L2	40
4.6 Physical properties for ligand L3	47
4.7 Characterization and structural confirmation of ligand L3	47
4.8. Palladium (II) thiosemicarbazone complexes	48
4.9 Physical properties for complex C1	51

4.10 Characterization and structural confirmation of complex C1	52
4.11 Physical properties for complex C2.....	54
4.12 Characterization and structural confirmation of complex C2.....	55
4.13 Physical properties for complex C3.....	56
4.14 Characterization and structural confirmation of complex C3.....	56
4.15 Cytotoxicity studies	58
CHAPTER FIVE	63
CONCLUSION AND RECOMMENDATIONS.....	63
5.0 Conclusion	63
5.1 Recommendations.....	64
REFERENCES.....	65
APPENDICES.....	83

LIST OF FIGURES

Figure 2.1: Bonding modes of thiosemicarbazone	24
Figure 4.1: FT-IR spectrum for L1	38
Figure 4.2: UV-Vis spectrum for L1	39
Figure 4.3: ^1H NMR spectra for L2	41
Figure 4.4: ^{13}C NMR spectrum for ligand L2	42
Figure 4.5: DEPT spectra for L2	43
Figure 4.6: Crystal structure for L2	45
Figure 4.7: Tortion angles in thiophene and intramolecular H-bonding	46
Figure 4.8: FTIR spectra of prepared Pd(cod)Cl ₂	49
Figure 4.9: FTIR spectra of Pd(cod)Cl ₂ from the authentic source.	50
Figure 4.10: FTIR spectra for complex C1	52
Figure 4.11: UV-Vis spectrum for complex C1	53
Figure 4.12: ^1H NMR spectrum for complex C1	54
Figure 4.13: Viability of HeLa cell line to compounds	59
Figure 4.14: Response of KMST cell line to treatment.....	59
Figure 4.15: Response of colon cancer (HT-29) upon treatment	60
Figure 4.16: Response of Caco-2 upon treatment.....	61
Figure 1: UV-Vis spectra for C2	83
Figure 2: UV-Vis spectra for C3	83
Figure 3: UV-Vis spectra for L2	84
Figure 4: UV-Vis spectra for L3	84
Figure 5: FTIR spectra for L3	85
Figure 6: FTIR spectra for C3	85
Figure 7: FTIR spectra for L2	86
Figure 8: FTIR spectra for C2	86
Figure 9: ^1H NMR for L1	87
Figure 10: ^{13}C NMR spectra for L1	87
Figure 11: ^1H NMR spectra for C2	88
Figure 12: ^{13}C NMR spectra for L3	88
Figure 13: ^1H NMR spectra for L3	89

Figure 14: ^1H NMR spectra for **C3**..... 89

LIST OF SCHEMES

Scheme 1.1: Neutral and Anionic forms	3
Scheme 2.1: Diels alder catalysis using copper (I) oxide	11
Scheme 2.2: Methoxytrifluoromethylation of styrene	12
Scheme 2.3: Mechanism of Suzuki coupling	14
Scheme 2.4: Reaction in thiosemicarbazone synthesis	22
Scheme 2.5: Reaction mechanism for aldehyde and primary amines	22
Scheme 3.1: Synthesis of Pd(cod)Cl ₂	33
Scheme 4.1: Synthesis of thiosemicarbazone ligands	37
Scheme 4.2: Synthesis of the complexes	51

LIST OF TABLES

Table 4. 1: 1D and 2D NMR data for L2	43
Table 4.2: Single-Crystal Data and Structure Refinement Parameters for L2	44
Table 4.3: Geometric parameters for ligand L2	47
Table 4.4. IC ₅₀ values (µg/mL) of compounds	61

LIST OF ABBREVIATIONS

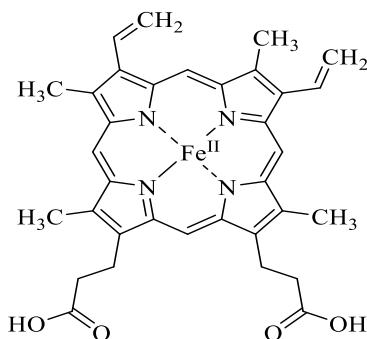
DCM	Dichloromethane
DMF	Dimethylformamide
DMSO	Dimethylsulfoxide
DNA	Dioxyribonucleic acid
EWG	Electron withdrawing group
FTIR	Fourier-transform infrared spectroscopy
HIV	Human Immunodeficiency Virus
HOMO	High Occupied Molecular Orbital
LUMO	Low Unoccupied Molecular Orbital
MDR	Multidrug resistance
NMR	Nuclear magnetic resonance
PMG	Platinum Group Metal
ppm	parts per million
THF	Tetrahydrofuran
TLC	Thin Layer Chromatography
TSC	Thiosemicarbazone
UV-Vis	Ultraviolet-visible

CHAPTER ONE

INTRODUCTION

1.0 Coordination compounds

Coordination compounds have proved to be important in various aspects of life based on their wide application. These compounds are formed when ligands (electron donors) coordinate to the central metal through coordinate bonds. The chemistry of coordination compounds is naturally witnessed in hemoglobin (**1**) which is a coordination complex of polyporphyrin and iron. Iron is coordinated to polyporphyrin compounds via nitrogen because of the presence of more labile lone pair of electrons for donation to form coordinate bonds.



1

It is responsible for oxygen transportation from the lungs to other parts of the body and carbon (IV)oxide from the body to the lungs. Other naturally available compounds include chlorophyll which is responsible for photosynthesis and metalloenzymes for biocatalysis (Helland *et al.*, 2019).

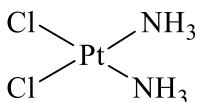
Transition elements like iridium have versatile applications due to their ability to accept lone pairs of electrons into their empty d-orbitals. Iridium ion exists in three stable oxidation states; Ir⁺, Ir³⁺ and Ir⁴⁺. Iridium ion is considered good catalyst in industrial application because they are resistant to corrosion; they are used in both acidic and basic medium. besides corrosion resistant, iridium complexes are used as industrial green catalyst because they are not environmental pollutants (Singh, 2016). For instance triscyclometalated iridium(III)2-(1-naphthyl)pyridine is

used as a catalyst in methoxytrifluoromethylation of styrene (Njogu *et al.*, 2019). Other catalytic applications include hydrogenation of benzene, amination of primary alcohols and 1,3-dipolar cycloaddition (Bayram *et al.*, 2010).

Other reactions catalyzed by transition elements include Wacker process where PdCl₂ is used in the conversion of olefins to aldehyde and Suzuki coupling where C-C bonds are formed. Palladium is used in Suzuki coupling and the reaction proceeds via Pd⁰-Pd²⁺ route (Lennox & Lloyd-Jones, 2014).

1.1 Platinum Group Metals

Platinum group metals, also known as platinum metals are elements of group VIII B. They consist osmium, palladium, platinum, iridium, rhodium and ruthenium. The electronic configurations of these elements are Ru (4d⁷ 5s¹); Rh (4d⁸ 5s¹); Pd (4d¹⁰/ 4d⁸5s²); Os (5d⁶ 6s²); Ir (5d⁷ 6s²); Pt (5d⁹ 5s¹). They have close nuclear sizes making them to have similar chemical and physical characteristics. Platinum group metals have various oxidation states however their stable oxidation states are; Ru²⁺/Ru³⁺/Ru⁴⁺, Rh³⁺, Pd²⁺/ Pd⁴⁺, Os³⁺/ Os⁴⁺, Ir⁴⁺/Ir³⁺, Pt²⁺./Pt⁴⁺, and (Jain & Chauhan, 2016). These group of metals form sigma bonds with electron donors (ligands) like H₂O, Cl⁻, NH₃ and sulphur. They also bond with donors in pi-systems like aromatic heterocyclics, azometine, thiocarbonyls and carbonyls. They have wide industrial applications because of their high heat resistance, resistance to corrosion, high melting point and catalytic activities. This group of metals have wide application in medicinal field example is *cisplatin* (**2**), platinum complexes used to treat cancer.



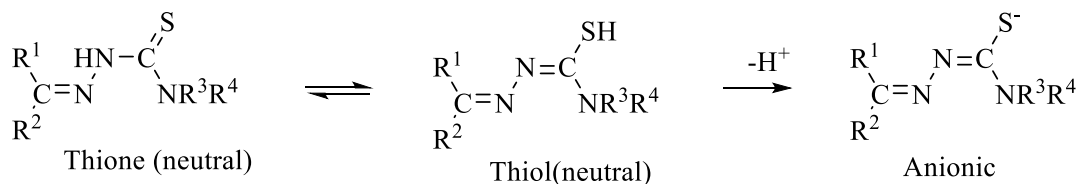
2

Palladium(II) complexes are also emerging as anticancer drugs as a result of platinum (II) complexes setbacks. One of the major setbacks of platinum(II) complexes as anticancer drug is that they are kinetically inert. Palladium(II) chelates especially with N,S donor ligands (for example thiosemicarbazones) are thermodynamically stable, they have high lability in bringing metal towards DNA and allowing it to interact with it. For these reasons, they are used as

anticancer, antimalarial and antiviral drugs. Their mode of action is to prevent conversion of ribonucleotides to deoxyribonucleotides through inhibition of enzyme ribonucleotide reductase. (Munikumari *et al.*, 2019).

1.2 Thiosemicarbazone palladium complexes

Thiosemicarbazones are Schiff base ligands with majorly sulfur and nitrogen as donor atoms. They are derived from a condensation reaction of aldehydes/ketones and thiosemicarbazides. Bidentate thiosemicarbazone ligands coordinate with the central metal forming five membered chelates. Their applications are due to their selectivity in coordination and good coordination tendency. They can interact with the metal either in anionic or in neutral form. The neutral forms are its two tautomers; thione and thiol and anionic after deprotonation of thiol as shown in Scheme 1.1 below. The Rs can be alkyl group or H (Pal *et al.*, 2002).

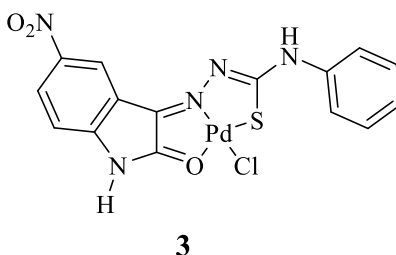


Scheme 1.1: Neutral and Anionic forms

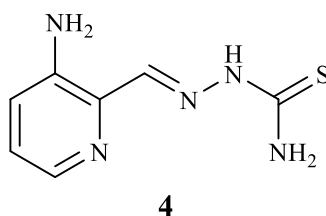
1.2.5 Heterocyclic thiosemicarbazone complexes of palladium (II)

Pd^{2+} thiosemicarbazone complexes with heterocyclic substituents such as thiophene have attracted interest in bioinorganic chemistry due to their potential biological activities such as antifungal, antimalarial, antiviral and anticancer. Pd^{2+} coordinates with ligands in the same mode as Pt^{2+} hence they are likely to form square complexes with thiosemicarbazone ligands. However, Pt^{2+} complexes are more kinetically and thermodynamically stable than the corresponding Pd^{2+} complexes. Ligand exchange rate for Pd^{2+} complexes are 10^4 times quicker than platinum because it readily forms 5-coordinate intermediate complex. Faster kinetic property of palladium is related to its small atomic size compared to platinum, causing steric repulsion of ligands (Ali *et al.*, 2017). Many Pd^{2+} complexes have been synthesized using the standard condensation method, characterized and investigated to be potent towards cancer cells.

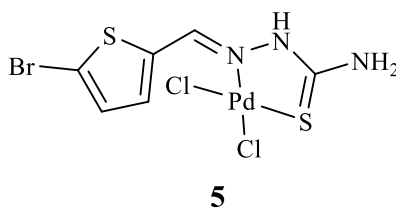
Some of these complexes include 5-nitroisatin thiosemicarbazone complex of palladium (**3**) which proved to be active towards colorectal cancer (Munikumari *et al.*, 2019).



The biological activities of thiosemicarbazone ligands which improves when coordinated with a metal make this group of compounds to be used as anticancer agents. Triapine (**4**) (3-aminopyridine-2-carboxaldehyde thiosemicarbazone) is one of thiosemicarbazone group of compounds currently on clinical trials against breast, leukemia, and cervical cancer (Nunes *et al.*, 2020).



Its combination with *cisplatin* has improved the effectiveness of *cisplatin* as far as Multi Drug Resistance (MRD) is concerned. Triapine-*cisplatin* combination is currently showing exemplary anticancer activities on vaginal and cervical cancers (Enyedy *et al.*, 2020). Thiophene substituted thiosemicarbazones have also proved to be cytotoxic against a number of cancer cell lines Mbugua *et al.*(2020) found that (*E*)-1-((5-bromothiophen-2-yl)methylene)thiosemicarbazidepalladium(II) chloride (**5**) had anticancer activities against human cervical (HeLa), human colon (Caco-2) and breast cancer (MCF-7). The cytotoxicity of the complex was more enhanced compared to free ligand.



1.4 Cancer

Cancer is one of the leading causes of deaths world wide. Cancer incidences and mortality cases are rapidly increasing due to aging and population growth. The rate at which population increases, cancer is likely to be the leading cause of deaths replacing coronary heart diseases and stroke (Wilson *et al.*, 2019). The malady is a burden to many nations because a lot of funds have to be allocated to curb it. The increasing cases of cancer are related to exposure to carcinogenic agents, some due to poverty and *westernized* lifestyles in developed nations according Bray *et al.* (2018). According to world health organization (WHO) 2018 statistics, lung cancer is the leading cause of deaths followed by breast cancer (Bray *et al.*, 2018; Wilson *et al.*, 2019).

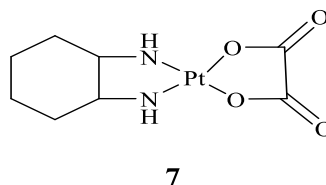
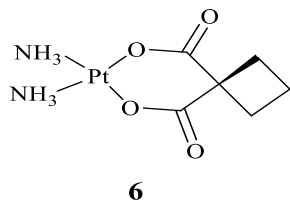
In 2012, 14 million new cases of cancer are reported annually all over the world with 8.2 million deaths registered; 8.8 million deaths registered in 2015. The deaths are projected to 13 million by 2030 as a result of population growth, lack of exercise, poor lifestyle as well as increase in the rate of infection (Atieno *et al.*, 2018).

Most of the existing anticancer drugs such as *cisplatin* face the challenge of multidrug resistance (MRD). MRD on chemotherapeutically potent drugs are associated with numerous mechanisms that include; increased drug efflux, decreased uptake of drug, activated DNA repair mechanism, activation of detoxifying systems, and drug induced apoptosis evasion among many more. Most of palladium thiosemicarbazone complexes are hydrophobic and insoluble in most organic solvents other than DMF and DMSO. This reason limits the biological applications of the ligands and complexes (Hosseini-Yazdi *et al.*, 2017).

In this work various thiosemicarbazone ligands and their palladium complexes have been synthesized, characterized and their anticancer activities in various cell lines investigated. This work focuses on synthesis of stable thiosemicarbazone ligands and their palladium(II) complexes.

1.5 Statement of the problem

For a very long time, *cisplatin* has been the most potent metal-based drug towards tumor cells; lung, ovarian, neck, bladder and brain cancers. Other platinum based drugs that are active towards cancer cells include carboplatin (**6**) and oxaliplatin (**7**) (Prajapati & Patel, 2019).



Cisplatin and other existing cancer drugs have shortcomings including multidrug resistance and severe side effects like nephrotoxicity, nausea, neurotoxicity and ototoxicity. Non-selectivity is also a major shortcoming of the available cancer drugs since they kill non-cancerous cells too (Prajapati & Patel, 2019).

The chemistry of thiosemicarbazones and their transition metal complexes are of interest due to their modes of coordination and numerous biological activities such as anti-tumor, anti-microbial, anti-malarial and antibacterial activities. Thiosemicarbazone complexes of palladium are active towards tumor cells however, activity problem arising from instability is a challenge in drug development, for this reason research on new biologically active metal complexes with bulky ligands, which enhance stability is necessary (Matsinha *et al.*, 2015).

1.6 Objectives

1.6.1 General Objective

Synthesize and determine the anticancer activities of thiosemicarbazones and their palladium complexes.

1.6.2 Specific Objectives

1. Synthesize thiosemicarbazone ligands.
2. Synthesize palladium (II) thiosemicarbazone complexes.
3. Determine the anticancer activities of the thiosemicarbazone ligands and palladium(II) complexes.

1.7 Justification of the study

Stability of palladium complexes is a challenge in biological application despite their anticancer activities. Palladium complexes have been reported to be cytotoxic towards breast and colorectal cancer cells by Munikumari *et al.*, (2019). Palladium(II) complexes are square planar complexes

where planarity is necessary for interaction with DNA and inhibition of replication. Therefore synthesis of thiosemicarbazone complexes of palladium(II), which are five-membered bulky chelates will improve the stability to act on pharmacological target without being structurally compromised (Munikumari *et al.*, 2019). Palladium(II) complexes have also been reported to have anticancer activities same as those of *cisplatin* with reduced side effects like nephrotoxicity, neurotoxicity and ototoxicity (Qin *et al.*, 2018).

Thiosemicarbazones derivatives of thiophene moiety are interesting owing to the structural and pharmacological activities such as anti-malarial, antifungal, antibacterial and antitumor (Munikumari *et al.*, 2019). Nyawade *et al.*(2021) established that thiophene based thiosemicarbazones had effective anticancer activities towards cervical cancer cell lines (HeLa), human colon carcinoma cell lines (Caco-2), human colorectal adenocarcinoma cells (HT-29) and non-cancerous immortalized human cells (KMST). The anticancer activities of the ligands were enhanced after coordination with palladium(II).The presence of thiophene ring in the structure increases the flexibility of denticity due to presence of sulfur (donor atom). In this research work new thiophene based thiosemicarbazone ligands and palladium complexes were prepared and anticancer activities determined.

This research is aimed at reducing the cancer burdens all over the world by synthesizing anticancer palladium(II) complexes which are stable with bulky ligands. The prepared compounds will also be useful in pharmaceutical industries and manufacturing industries to enhance efficiency of production, contribution to the Kenya's big four agenda (Universal Health Care and manufacturing) and realization of the good health and well-being, one of Sustainable Development Goals (SDG) of vision 2030.

CHAPTER TWO

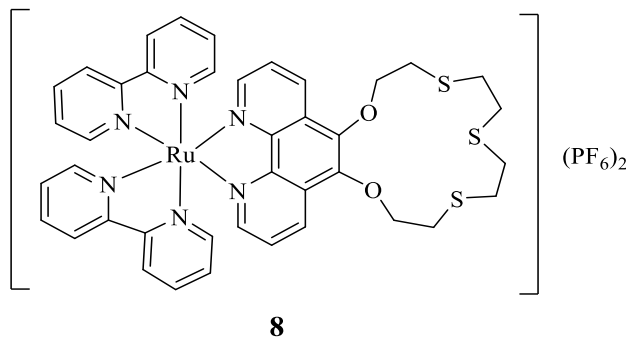
LITERATURE REVIEW

2.0 Transition metal complexes

Transition elements are elements with incompletely filled d-orbitals, elements between the s- and the p-block elements. This rationale disqualifies an element like Zn, a d^{10} from being a transition metal. The presence of incompletely filled *d*-orbitals in these metals make them distinct from other metals in the periodic table. They can easily exist in a number of stable oxidation states at room temperature depending on their electronic structure. For instance, vanadium can exist as V^{2+} , V^{3+} and V^{5+} and manganese as Mn^{+} , Mn^{2+} , Mn^{3+} , Mn^{4+} , Mn^{5+} , Mn^{6+} and Mn^{7+} , the highest oxidation states d-orbitals are engaged in bonding. These metal ions form coordination compounds with other molecules in which the interaction is covalent (Prajapati *et al.*, 2019).

The coordination chemistry of transition complexes has aided researchers to solve environmental pollutions resulting from human activities more so industrialization. Industrialization has led to melting of ice caps due to emission of greenhouse gases, contamination of fresh water and air. Presence of high levels heavy metals in waste water in most of the industries is alarming. Heavy metals accumulate in water bodies over a long period and end up in the biological system when contaminated water is consumed without proper purification. They have adverse effect to human health including damage of organs (kidney and brain), miscarriage, irritation of stomach and death (Mahurpawar 2015). The main source of heavy metal is industrial sludge from battery manufacturing companies. Most of such industries apply the knowledge of coordination chemistry to clean the sludge to minimize environmental contamination. The industries mostly use biodegradable chelating tetrasodium N,N-bis(carboxymethyl) glutamic acid to extract lead, zinc and copper from sludge (Wu *et al.*, 2015). Heavy metals such as Pb^{2+} , Cd^{2+} and Hg^{2+} are considered to be soft electron acceptors. To remove these metals from the environment, Odhiambo and coworkers (2018) synthesized crown ether based chemosensors of $[Ru(bpy)_2]^{2+}$ moiety which were made selective by varying the cavity of the crown ethers depending on the radius of the metal ions. They used $[Ru(bpy)_2]^{2+}$ moiety because its strong Metal-Ligand Charge Transfer (MLCT) produces suitable signaling unit and well defined photophysical, spectroscopic

and electrochemical characteristics sensitive to variations from external inputs. One of the crown ether complexes they synthesized showed visible color change upon interaction with Hg^{2+} ions. One of the complexes that they synthesized is shown in **(8)** below.



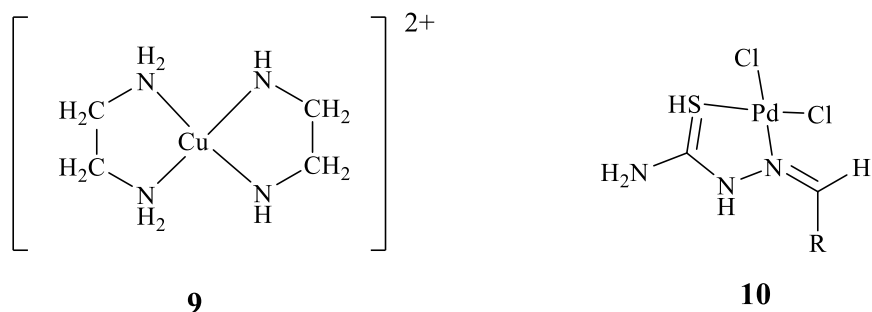
2.1 Stability of transition complexes

The stability of the transition complexes is dependent on various factors such as the crystal field stabilization energy (CFSE), the attainment of effective atomic number and the chelation/denticity of the ligands. The CFSE is the difference in energy gap between the e_g and the t_{2g} orbitals. The octahedral complexes are more stable than tetrahedral complexes because they are surrounded by six ligands causing more electronic repulsion hence high splitting energy. As the CFSE increases, the thermodynamic stability especially of the octahedral complexes increases. The ligand also determines the magnitude of the energy (Britz *et al.*, 2019).

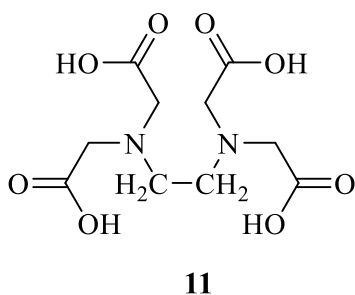
When ligands coordinate to the central metal ion, they donate lone pair of electrons to the vacant d -orbitals forming dative bonds. However, the metal will accept the electrons till it attains the noble gas electron configuration, the effective atomic number (EAN). Consider Potassium hexaammineferrate(II) $\text{K}_2[\text{Fe}(\text{NH}_3)_6]$. The Fe^{2+} ions have 24 electrons plus the 12 electrons donated by the six amino ligands adding to 36 which is a noble gas configuration for Krypton.

Denticity of the ligand also determines the stability of the complexes. Some of the ligands coordinate through more than one donor atoms. Such kind of ligand is called multidentate. The complexes of multidentate ligands are more stable than those formed by unidentate ligands. Ethylenediamine is one of the ligands that coordinate at two atoms (bidentate)(Britz *et al.*, 2019). They complex with various transition metal ions forming ring structures called chelates. The chelates formed by ethylenediamine **(9)** and thiosemicarbazones **(10)** are more stable than the

complexes with unidentate ligands because for more energy is required to break two bonds in chelates (Britz *et al.*, 2019).



The more the chelating, the more stable the compound is. Chelating agents with 3,4,5,6 donor atoms are referred to as tridentate, tetradentate, pentadentate and hexadentate ligands respectively. A good example of hexadentate ligand is ethylenediamine tetraacetic acid (EDTA) (**11**) shown below.

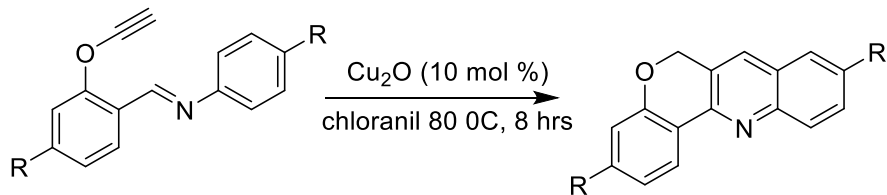


Chelates of biological importance include hemoglobin in the blood, magnesium-porphyrin complex in the chlorophyll and vitamin B₁₂ which is a complex of cobalt and enzyme cytochrome oxidase (Liu *et al.*, 2019).

2.2 Transition metal complexes in catalysis

Transition metals and their complexes are considered good catalysts because they can exist in multiple oxidation states. They can act either as Lewis acid or Lewis base enabling them to form intermediate complexes with reagents. Coordination complexes play special role in most organic synthesis reactions. Catalysts perform three major roles in reactions; reduction of activation energy, provision of alternative reaction route and provision of reaction surface area. Partially filled d-orbitals in transition metals enable metals to form reactive intermediates. Catalysis of

transition metal complexes are mostly influenced by the type of ligand in the complex. For instance in Cu catalyzed Diels-Alder reaction as shown in Equation 1, use of chelating ligands decreases catalytic efficiency by reducing equilibrium constants of reactions (Yu *et al.*, 2016).

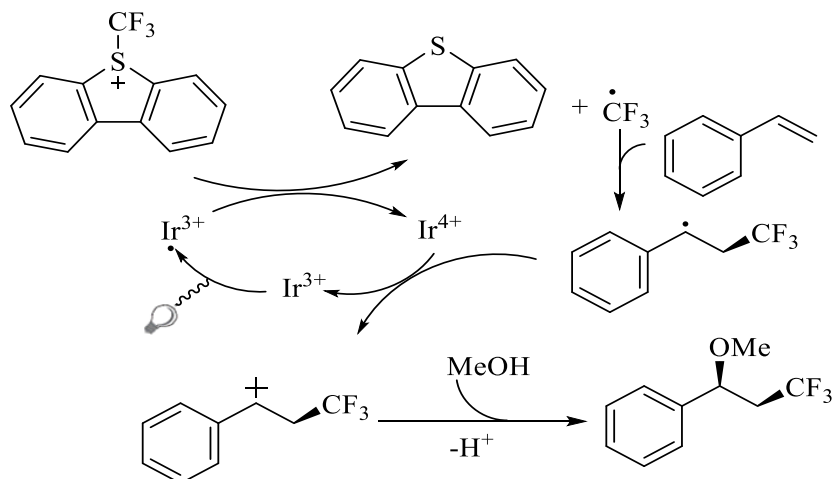


Scheme 2.1: Diels alder catalysis using copper (I) oxide

This happens because chelating ligands tend to block coordinating sites of metal ions. Various metal complexes have been used to catalyze different types of reaction (Jiang *et al.*, 2018).

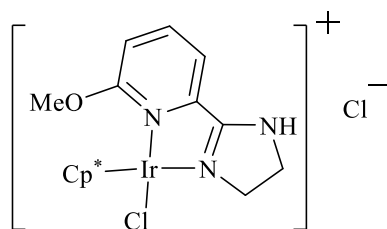
2.2.1 Iridium complexes

Iridium complexes are considered good catalyst in industrial application because they are resistant to corrosion, they can be used in both acidic and basic medium. Besides these, iridium complexes are used as industrial green catalyst because they are not environmental pollutants (Singh, 2016). Other catalytic applications include hydrogenation of benzene, amination of primary alcohols and 1,3-dipolar cycloaddition (Bayram *et al.*, 2010). Photoredox catalysis of styrene methoxytrifluoromethylation is an important reaction catalyzed by iridium aided by light. Iridium ion is coordinated to more conjugated ligands that decrease the High Occupied Molecular Orbital (HOMO)-Low Unoccupied Molecular Orbital (LUMO) gap and increasing the ligand field stabilization energy (LFSE). For these reasons they are capable of using visible light in photoredox catalysis. Triscyclometalated iridium(III)-2-(1-naphthyl)pyridine is one of the iridium complexes catalyzing such a reaction. The visible light is used to eject electron from Ir³⁺ ion forming a radical. The electron deficient metal ion catalyzes methoxytrifluoromethylation of styrene molecule. Scheme 2.2 below shows methoxytrifluoromethylation of styrene using triscyclometalated iridium(III)-2-(1-naphthyl)pyridine (Njogu *et al.*, 2019).



Scheme 2.2: Methoxytrifluoromethylation of styrene

Most alkylation processes of organic compounds including amines are done using alkyl halides however such reactions are usually slow. Besides slow nature of reaction, alkyl halides are toxic and accumulate in the environment. Researchers have established an alternative way of *N*-alkylation of amines using alcohols aided by nickel, copper, manganese and cobalt catalyst (Zhang *et al.*, 2015). The challenges with these catalysts high amount of loading and inefficiency in aqueous media. Tang's catalyst (**12**), cyclometalated pyridyl 4,5-dihydro-1*H*-imidazole iridium(II) complex is used to catalyze *N*-alkylation of amines using alcohol via borrowing hydrogen in aqueous media.

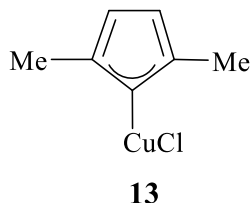


12

The advantage of Tang's catalyst over other metal complexes in catalysis is that reaction is faster, low temperature is required, less catalyst dosage and it is efficient in aqueous medium. Use of pyridyl 4,5-dihydro-1*H*-imidazole as electron donating ligand plays a role to realize high yield (Luo *et al.*, 2020).

2.2.2 Copper complexes

Copper complexes have been used in catalysis in organic reactions. *N*-heterocyclic carbene complexes of copper (**13**) are used in hydrosilylation of carbonyls.

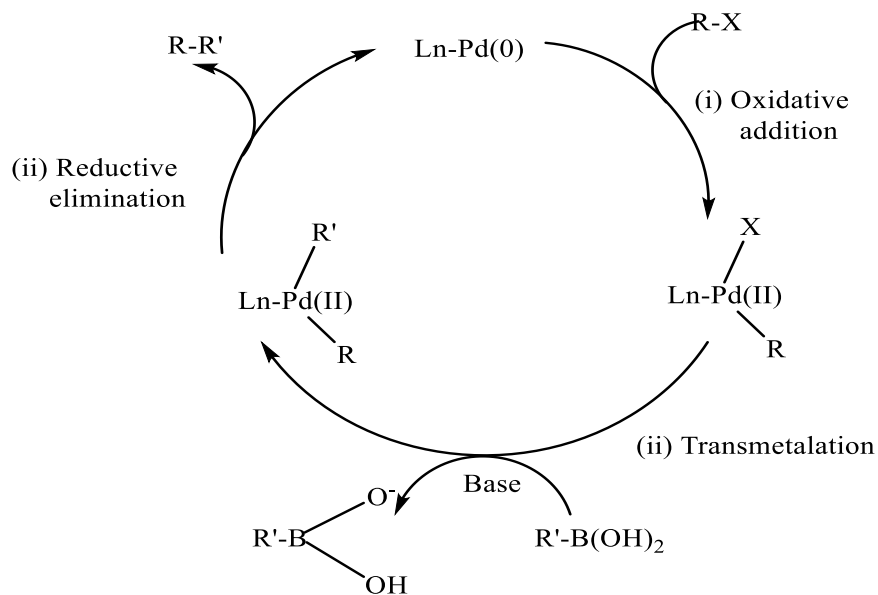


Hydrosilylation is an important reaction in industrial production of silylethers, mostly used as protecting groups. During this process, silicon-hydrogen bond is added across unsaturated carbon-carbon bond. The most important intermediate reaction is silicon-hydrogen bond cleavage to form silicon-oxygen bond (Egbert *et al.*, 2013). Bipyridine copper complexes are used as catalyst in addition of halogenated methane to olefins to produce polymer. Catalysis in production of polymeric compounds takes place via atom transfer radical addition (ATRA) mechanism. When copper complex is used in such a reaction, it is reported that the polymeric product formed has desirable architecture, functionalities and composition (Pintauer and Matyjaszewski, 2008). Copper complexes containing N,O and N,N donor ligands in conjunction with 2,2,6,6-tetramethyl-piperidinyloxy radical are used as catalyst in oxidation of alcohols to carbonyl compounds (Ma *et al.*, 2019). In industrial manufacture of urea based fertilizer, tetraammineaquacopper(II) sulphate complex, $[\text{Cu}(\text{NH}_3)_4(\text{H}_2\text{O})]\text{SO}_4$, is used in production of urea from ammonium carbamate. The first step of this process involves reaction of ammonia with CO_2 gas forming ammonium carbamate. Formation of carbamate is an exothermic process and does not involve catalyst. The second step is conversion of ammonium carbamate to urea which is a slow endothermic process. Due to thermodynamic obstacles in the second step, copper(II) catalyst is used in the reaction. The reaction is performed in high pressure steel reactor in a closed system (Hanson *et al.*, 2021).

2.2.3 Palladium complexes

One of the most important organic reactions catalyzed by palladium(II) complex is Suzuki-Miyaura coupling. This type of reaction involves formation of C-C bond which is not viable without catalyst due to electronic constraints. Suzuki coupling has been applied industrially to

form polymer of conjugated systems such as polystyrene, polyvinyls and polyalkenes. The process involves the use of organoborane and alkyl halide (Lennox and Lloyd-Jones, 2014). Suzuki coupling involves three main steps; The first step is oxidative addition of alkyl halide to Pd(0) complex to form first intermediate Pd(II). The second step is transmetalation where organoborane reacts with palladium(II) intermediate to form second intermediate of Pd(II) coordinated both alkyl from organoborane and alkylhalide. The last step of this catalysis is reductive elimination where alkyl halides bond together via C-C bond while Pd(II) is reduced back to Pd(0) (regeneration of catalyst). Suzuki coupling can be compared with Stille cross coupling where organotin instead of organoboron. However challenges associated with tin include lower tolerance to functional groups, high level of toxicity and high cost of tin (Levashov *et al.*, 2017). Mechanism of Suzuki coupling is shown in Scheme 2.2 below.



Scheme 2.3: Mechanism of Suzuki coupling

Palladium is also involved in catalysis of Wacker process where olefins are oxidized to alcohols and further to aldehydes using palladium(II) chloride (Hu *et al.*, 2018).

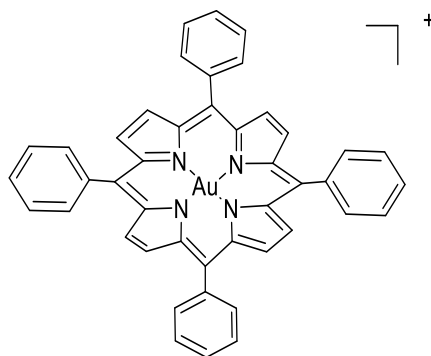
2.3 Metal complexes in medicine

In many of the complexes used as metal-based drugs, DNA is the main targets for effective therapeutic activities, whereby they bind with the DNA interfering with its transcription and replication. In the recent research, the biological activity of these drugs is due to enzyme inhibition, which occurs through ligand substitution mechanism. This reaction happens when central metal coordinates with donor atoms from protein residues like histidine, selenocystein, and cystein in biological system making them pharmacologically active (Che & Siu, 2010). Examples of the metal complexes used in treatment are discussed below:

2.3.1 Gold complexes

In more recent practice in chrysotherapy, gold based drugs have been used to treat rheumatoid arthritis. Rheumatoid arthritis is an inflammatory condition in the body support system leading to erosion of the cartilage lining of bones interfaces in joints. The first inflammation takes place in the synovial membrane then proceeds to synovial cavity between the bones. Gold based drugs are effective to approximately 70% of patients undergoing chrysotherapy, some do not benefit while others encounter mild side effects like skin rushes. However small percentage of those undergoing chrysotherapy encounter severe side effects like inhibition of formation of leukocytes and erythrocytes from the bone marrow (Mjos & Orvig, 2014).

One of the gold complexes used in medicine is auranofin (**14**) which is used in treating arthritis.



14

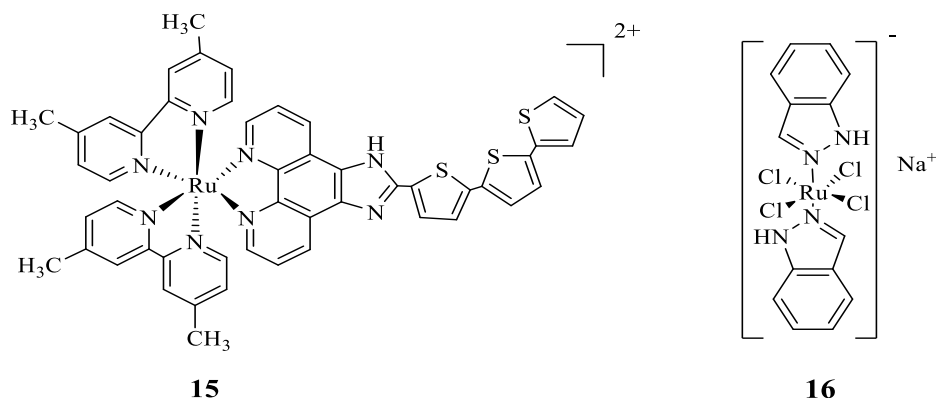
The therapeutic effect of this gold complex originates from enzyme inhibition through ligand exchange mechanism. The porphyrin, which is a ligand in the complex, is replaced by a seleno protein. The complex, auranofin, can also be used to treat cancer since it inhibits enzymatic

activities responsible for growth of tumor cells thereby active towards tumor cells. *In vivo* studies show that the therapeutic activity of auranofin is limited by its affinity towards protein thiols. Research on auranofin shows potential in antiproliferation activities when coordinated with naphthalimide ligands. The injectable gold(I) thiolates are more active towards inflammatory conditions than auranofins (Nakaya *et al.*, 2011).

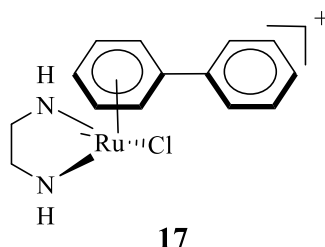
2.3.2 Ruthenium complexes

Ruthenium exists in three major oxidation states and mostly forms octahedral complexes. Ru⁴⁺ complexes are kinetically and thermodynamically stable, this property making them suitable for biological applications. Ru⁴⁺ complexes are used as pro-drugs on biological circumstances of acidic pH, hypoxia and high glutathione, indicating anticancer effects by being reduced to the corresponding Ru²⁺. Ru²⁺ is very cytotoxic towards tumor cells, it kills solid tumor via multiple mechanisms. Ru²⁺ complexes also have appreciable chemical and photophysical properties together with ligand exchange kinetics, they are more kinetically and thermodynamically stable compared to their corresponding Ru³⁺ complexes due to their low oxidation states. Ru²⁺ complexes show good biological activities especially anticancer activities. The major challenge they face during their application is their inability to dissolve in water. [Ru(C₄₉H₃₈N₈S₃)]²⁺ and [Ru(C₁₄H₁₂Cl₄N₄)]⁻ are examples of ruthenium based drugs that are approved for chemotherapeutic administration (Lin *et al.*, 2018).

Mechanisms of ruthenium complexes towards anticancer cells include; action on DNA telomere, interference with DNA replication and transcription and inhibition of enzymes. They also act by blocking cell cycles via formation of photo-crosslinking products of DNA hence preventing ribonucleic acid (RNA) polymerization enzymes from binding with the DNA thereby causing the apoptosis of the tumor cells (Lin *et al.*, 2018). Structures tris(bipyridine)ruthenium(II) (**15**) and dibenzimidazolerothene(III) tetrachloride (**16**) are examples of approved ruthenium based anticancer drugs.



[Ru(biphenyl)Cl(en)]⁺(**17**) was one of the first ruthenium complexes that was synthesized and investigated for antitumor activities.



It comprises of monodentate ligand (Cl), bidentate (diamine) and arene (biphenyl) ligands. The complex has “piano stool” geometry. The essence of synthesizing this complex was target DNA without activation via cellular reduction taking advantage of its low oxidation state; Ru²⁺. The biphenyl ligands provide hydrophobic site thereby allowing the complex to diffuse in the cell through plasma membrane. Immediately it enters the cell, it gets activated through ligand exchange mechanism on the Cl⁻ site since halogens are good leaving groups. The arene site of the complex enhances hydrophobic interaction between DNA and the complex. The single bond between the biphenyls gives room for freedom of rotation hence minimizing steric repulsion; as a result the binding affinity of the complex to DNA is increased (Nazarov *et al.*, 2014).

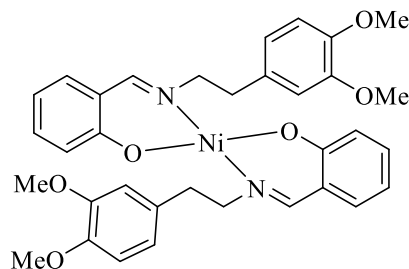
2.3.3 Nickel complexes

Nickel for a very long time has been regarded as an element without biological significance. In most cases nickel complexes are applied in the field of catalysis. For instance in organic synthesis, NiCl₂(PPh₃)₂ is used as catalyst in preparation of six membered heterocyclics from five membered (Kaur, 2019). However just like platinum, gold and any other transition metal

complexes, nickel complexes are applied in the medical field. They are either used to make medical equipment or drugs because nickel containing equipment are regarded to be safe, hygienic and easy to clean. Due to these reasons, they are used to make hospital equipment, operation instruments and pharmaceuticals supply. For instance alloy of nickel and titanium (Nitinol) is used in elevation of cardiovascular conditions; Nickel-chromium alloy is applied in dentistry because of good aesthetic properties (Radev, 2012).

Nickel being a cofactor in many bacterial enzymes (superoxide dismutase, urease, acireductone and dioxygenase), it is used to combat the deadly enterobacteriaceae. Enterobacteriaceae illnesses are caused by *Salmonella*, *Klebisella* and *Escherichia* bacteria species. These illnesses are costly and causes death as a result diarrheal illness. Though many metal chelators are being used, they face challenge of multi-drug resistance therefore nickel chelators are the best to use. Dimethylglyoxime chelate on Ni(II) is used as antibiotic because of its inhibitory activity on a number of bacteria (Benoit *et al.*, 2019).

Nickel complexes have also proved to be biologically active (Totta *et al.*, 2017) found that combination of nickel and naproxen (anti-inflammatory drug) had antioxidant properties. This was observed through inhibition of soybean lipoxygenase enzyme. Naproxen-nickel complex are also free radical scavengers Nickel(II) Salicylhydroxamic acid complex has irreversible microbial urase inhibition property with little side effects compared to existing antimicrobial drugs (Adegoke *et al.*, 2019). 2-hydroxybenzaldehyde 2-(3,4-dimethoxyphenyl) ethanamine Ni(II) (**18**) complex is used as antifungal and antimicrobial drug. The pharmacological use is as a result of research done on *S. aureus* bacteria and *C. albicans* fungi (Satheeshet *et al.*, 2016).

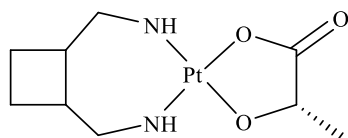


18

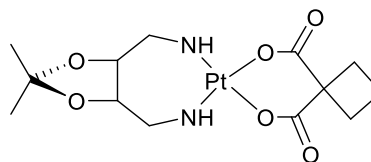
2.4 Metals complexes in cancer treatment

Metals are essential for processes in the cell. These metals are evaluated and selected to improve the cellular biochemical processes. Remarkable features of the metals especially transition metals include their modes of coordination in a complex, redox activity and reactions with organic substrate hence regulating their intercellular availability. These metal compounds are potential anticancer agents. However, ions of these metals beyond or below specific concentration are accompanied with variety of pathological disorders including cancer (Florea & Büsselberg, 2011).

Cisplatin has been used as an anticancer drug for treating various cancers such as soft tissue cancer, sarcoma cancers, bone cancers and cancer of blood vessels. *Cisplatin* and its derivatives have been effective towards cancerous tissues but its use is limited due to adverse effects in the normal cells. Despite platinum compounds proving to be clinically successful few of these compounds have been clinically approved, for example carboplatin (**6**) and oxaplatin (**7**) are not yet approved while others like lobaplatin (**19**) heptaplatine (**20**) have very limited approval towards clinical use.



19



20

This is because most of these compounds tend to offer little substantial clinical advantages (Florea & Büsselberg, 2011).

Despite all these significant moves in treatment of cancer, multi drug resistance and toxicity has been a bottleneck in chemotherapy. For instance, ototoxicity, vomiting, neurotoxicity, nausea and nephrotoxicity have been major challenges in the use of *cisplatin* in chemotherapy. Ototoxicity for instance is caused by effects of *cisplatin* on key cells in the cochlea which are involved in the sound transduction hence affecting the hearing of the patient. The cochlea has outer hair cells (OHC) which are highly vulnerable target cells upon induction of *cisplatin*. The loss of the outer hair cells leads to less sensitivity to sounds especially of low intensity and decreases ability to hear sounds of different frequencies (Bielefeld *et al.*, 2013).

2.5 Schiff base ligands

Schiff base group of compounds was discovered by Hugo Schiff in 1864. Schiff base ligands are ligands derived from a condensation reaction of primary amines and carbonyl compounds majorly aldehydes/ ketones. This group of compounds is also known as azomethines or anils. They are π donors unsaturated compounds with O, N, S and P donors showing high potentiality in biological applications (Warad *et al.*, 2020). They have made remarkable advancements in the modern inorganic and coordination chemistry owing to their chemical and thermal stabilities. The stability of Schiff base compounds is associated with the versatility in coordination in that they can form chelates with bivalent, trivalent and tetravalent metal ions. For this reason they use gadolinium (III) complex derived from tetrapodal Schiff base ligands are used as a Magnetic Resonance Imaging (MRI) contrast agent in therapeutic and diagnostic practices (Dutta *et al.*, 2010). Their ease of synthesis has made it easy for researchers to fine-tune their structural design on the basis of application. Multidenticity of this group of ligands to metal ions displays high performance as far as electronic soft tuning and steric characteristics are concerned. They have applications in the field of catalysis, optical materials and inorganic biochemistry (Buldurun *et al.*, 2020). Schiff base metal complexes have high catalytic activities. Complexes with chiral Schiff base ligands display high selectivity to a number of organic reactions like epoxidation, aldol condensation, oxidation, hydroxylation and Suzuki Miyaura coupling due to versatility in chelation with the metal center in a complex. For instance Fe(II) and Co(II) pyridine bis-(imine) and pyridyl bis(imide) are applied in catalysis of propylene and ethylene polymerization. The effectiveness of this group of catalysts are more enhanced at high temperature and humid environments (Gupta & Sutar, 2008).

Schiff base ligands have provided efficient and relatively cheap alternative in sensing toxic environmental pollutants. The methods being used currently such as X-ray fluorescence spectrometry, flame atomic absorption spectroscopy, stripping voltammetry and plasma mass spectrometry are tedious, interms of sample preparation, time consuming and costly (Bansod, 2017). Environmental contaminants such as Co(II) in water bodies have been sensed using (*E*)-benzyl-2-((7-(diethylamino)-2-oxo-2H-chromen-3-yl)methylene)hydrazine where the color change from yellow to red is witnessed. This is based in the ligand to metal charge transfer (LMCT) between cobalt and the ligand. Others include 4-((2, 4-dichlorophenyl) diazenyl)-2-(3-hydroxypropylimino)methylphenol in calorimetric detection of phosphates (Berhanu *et al.*,

2019). Strontium sensor PVC membrane was developed based salicylaldehyde thiosemicarbazone affinity towards citations. The sensor was highly selective at a pH range 2.8-10.4 (Zamani, 2008).

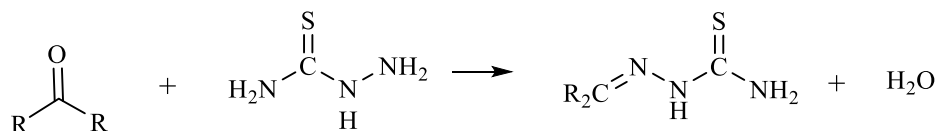
Schiff bases have been widely studied in the medicinal field owing their biological activities including anticancer and anti-HIV (Rao *et al.*, 2020). Schiff base ligands have high anticancer activities than *cisplatin* especially when coordinated to transition metal ions. Palladium Schiff base complexes are more selective and have milder side effects compared to *cisplatin*. Benzathiol Schiff bases, thiosemicarbazones, isatin derived imines, N-(5-nitro-salicylidene)-Schiff bases among many have antitumor activities against lung ovarian, neck and cervical cancers (Özdemir *et al.*, 2020).

2.5. 1 Thiosemicarbazones

Coordination chemistry of thiosemicarbazones has received an interest because of their biological activities. This is evident mostly when thiosemicarbazone form chelates with transition metals. Thiosemicarbazone derivatives such as N-methylisatin-8-thiosemicarbazone and 3-aminopyridine-2-carboxyaldehyde thiosemicarbazone are used in medical practices. One of the challenges these compounds face is hydrophobicity and insolubility in various organic solvents causing difficulties in biological applications. When the compound is highly hydrophilic, there is no use of solubilizers giving a room for high intravenous administration during the development of the candidate drug (Hosseini-Yazdi *et al.*, 2017).

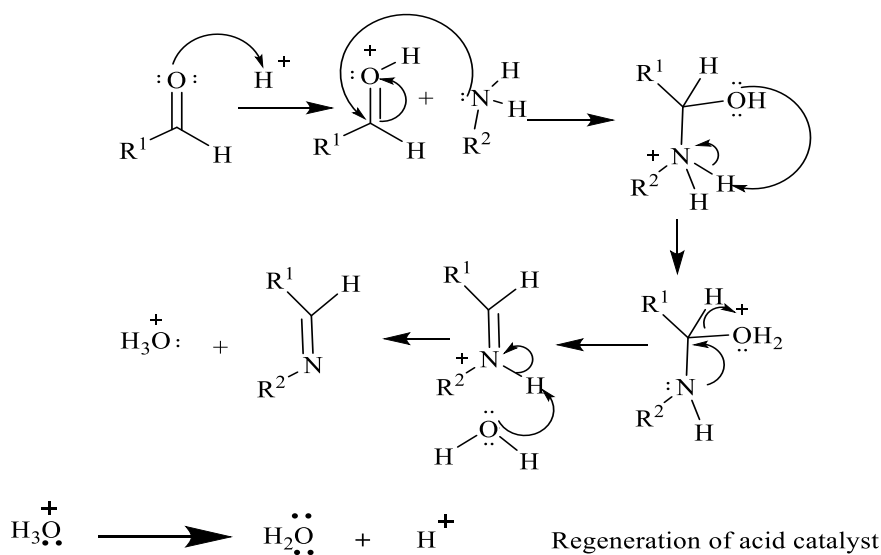
The chemistry of thiosemicarbazones and other Schiff base ligands with their platinum group metal complexes is that they meet planarity criteria to interact with DNA. These compounds form complexes which are planar, which enables them to form non-covalent bonds with DNA therefore becoming more effective. The metal complexes of thiosemicarbazone have enhanced biological activities compared to the thiosemicarbazone ligands. They mostly undergo complexation through deprotonation of ^1N (Lobana *et al.*, 2009).

Thiosemicarbazones are organic molecules (amines) derived from a condensation reaction between an aldehyde/ketone with a thiosemicarbazide. The reaction is also referred to as reductive amination where amine(semicarbazide) reduces a carbonyl to imine.



Scheme 2.4: Reaction in thiosemicarbazone synthesis

Thiosemicarbazones are mainly synthesized by condensation reaction of thiosemicarbazide (amine) with an aldehyde or ketone in alcoholic solvent media, catalyzed by an acid as shown in Scheme 2.3 (Sukhorukov, 2020).



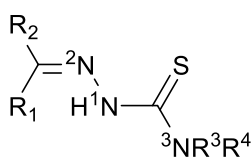
Scheme 2.5: Reaction mechanism for aldehyde and primary amines

The reaction is usually a one-step reaction except in cases where a specific substituent is required on the thiosemicarbazide. Thiosemicarbazide is synthesized in a one pot reaction by reacting amines with CS_2 , $\text{ClCH}_2\text{COONa}$ and hydrazine. This method gives room for modifications in terms of redox potential, structural complex stability and biological activities. Availability of lone pairs on electrons in S and azomethinic N allow for formation of five-membered with transition metal ions. During metallation, deprotonation of hydrazinic nitrogen may occur causing an increase in C-S bond length. The negative charge on sulfur after deprotonation improves its coordination ability (Paterson & Donnelly, 2011). Palladium complexes of

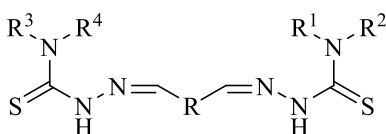
thiosemicarbazones are synthesized by reacting PdCl₂ with thiosemicarbazone in acetonitrile. However direct reaction with PdCl₂ results to lower yield of 50-60% and problems *in vacuo* drying due to high boiling point of acetonitrile (82 °C) (Munikumari *et al.*, 2019). Therefore, palladium(II) thiosemicarbazone complexes are synthesized in two steps; the first step is synthesis of precursors PdCl₂(PPh₃)₂ or Pd(cod)Cl₂ then reacting with thiosemicarbazide at room temperature for 24-48 hours (Motswainyana *et al.*, 2012).

Structures of both ligands and complexes are confirmed using FTIR, UV-Vis, NMR, single X-ray crystallography, elemental analysis and mass spectrometry techniques. Successful synthesis of thiosemicarbazone is usually achieved by confirmation of C=N characteristic peak on FT-IR which is normally observed between 1520- 1700 cm⁻¹ with a shift to higher or lower frequency after complex formation. The metal also coordinate via thiocarbonyl sulfur thereby shifting the stretching frequency of thiocarbonyl bond to lower frequency which is usually observed between 1000cm⁻¹ to-1280 cm⁻¹ (Trotsko *et al.*, 2020). The ¹H NMR peaks for azomethine protons are observed as singlet between 7.5 to 9.0 ppm with either downfield or upfield chemical shift after complex formation since azomethine-N is involved in bonding, downfield shift experience in most cases after complex formation (Haribabu *et al.*, 2020).

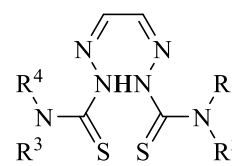
Thiosemicarbazones exist in thione in solid state however in solution they tautomerise into thiol tautomer. The complexation of this group of compounds is achieved through the dissociation of an acidic proton making it to form chelate ring which is five membered. Thiosemicarbazones exist as mono-thiosemicarbazones and bis-thiosemicarbazones and even in rare cases tris-thiosemicarbazones. Mono-thiosemicarbazones (**21**) are bidentate while bis-thiosemicarbazones have two arms connected via a ring (**22**) or via a C-C bond (**23**) (Pal *et al.*, 2002). Thiosemicarbazones are multidentate ligands that form stable complexes with transition metals. If the substituent on C¹ is a donor atom in a mono-thiosemicarbazone, then the ligand can be tridentate (Pal *et al.*, 2002).



21



22



23

Thiosemicarbazone compounds coordinate with the metal centers in various modes. For a neutral ligand it coordinates through S(I), S-bridging(II), N²S chelation(III), N²S chelation S bridging(IV), tridentate if the group attached to C¹ is a donor atom X(V), tridentate S bridging(VI) and tridentate X bridging(VII) as shown in the Figure 2.1.

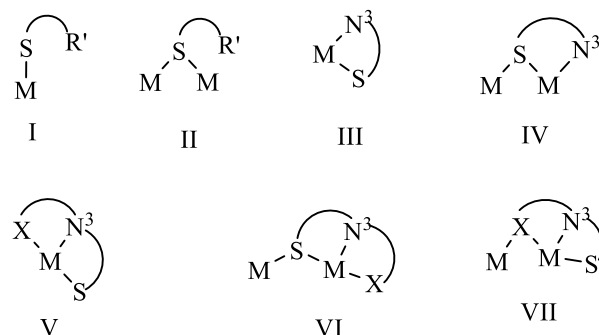


Figure 2.1: Bonding modes of thiosemicarbazone

The same bonding modes are also experienced in ionic form only that in the ionic form N³ also participates in bonding. Bis-thiosemicarbazone is a tetradentate ligand in both ionic and neutral (Lobana *et al.*, 2009)

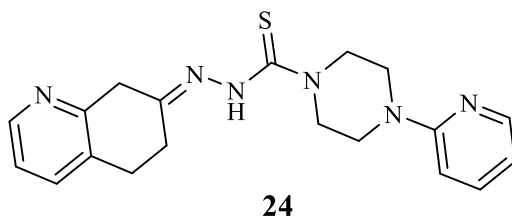
2.5.2 Heterocyclic thiosemicarbazones

In 1940's, thioacetazone (pacetamidobenzaldehyde thiosemicarbazone), was the first thiosemicarbazone-based drug to be clinically approved to treat tuberculosis. Methisazone (N-methylisatin thiosemicarbazone) was the second to undergo clinical developments in the treatment of small pox. However, the developments were short-lived with the discovery of the small-pox vaccine therefore there was preference in immunization as opposed to curative measures (Heffeter *et al.*, 2019).

The anticancer research has been mainly focused on the S-heterocyclic and N-heterocyclic thiosemicarbazones. In most of the researches, heterocyclic derivatives of thiosemicarbazones have displayed potency towards cancer cells especially when chelated with metals. Triapine (3-Aminopyridine-2-carboxaldehyde thiosemicarbazone) (**4**) is one of the TSCs undergoing clinical trials against myeloid leukaemia, cervical and breast cancer. Currently, patients are being recruited for phase III clinical trial to monitor the effectiveness of combination of *cis*platin with

3-Aminopyridine-2-carboxaldehyde thiosemicarbazone in advanced stages of vaginal and cervical cancers (Enyedy *et al.*, 2020).

From previous studies on thiosemicarbazones, variations in chalcogens ranging from O-S Se-Te have resulted to effective changes in both biological activities, physical and chemical properties. The changes in substituents may result in increased stability in solution, lipophilicity, permeability in membrane, *in vivo* and *in vitro* antitumor activities of metal-TSC complexes (Park *et al.*, 2016). For instance, studies have shown that there is increased cytotoxicity 1000 times by methylation of N adjacent to imine-N. Dimethylation of either or both terminal and pyridine-NH₂ also results to increased stability and the ability of the complexed to be reduced (Kowol *et al.*, 2007). (E)-N²-(5,8-dihydroquinolon-7(6H-ylidene)-4-(pyridine-2-yl)piperazine-1-carbothiohydrazine (**24**), commercially known as Coti-2 is a thiosemicarbazone derivative which is very cytotoxic towards a number of cancer cells at very low concentrations in comparison to 3-aminopyridine-2-carboxaldehyde thiosemicarbazone (Parsa *et al.*, 2020)



It is having very milder side effects and exhibits nanomolar IC₅₀. Currently this compound is on clinical trial against advanced head and neck squamous cell cancer whose victims have 25% survival rate (Lindemann *et al.*, 2019).

It has been established that thiosemicarbazone hybrid ligands when coordinated with metal ions are very effective towards cancer cells. Palladium complexes with chiral thiosemicarbazone derivatives of camphor (L), (-) carvone and monoterpenoids (+) have proved to be active towards advanced stages of human laryngeal carcinoma. This suggests that monoterpenoids and other natural products can be manipulated to form thiosemicarbazone derivatives with very effective activities (Kokina *et al.*, 2019).

2.5.3 Thiophene substituted thiosemicarbazones

Thiophenes are five-membered heterocyclics with a general formula C_4H_4S . Thiophenes are aromatic and planar just as benzene. However their aromaticity is significant because the lone pair of electrons are delocalized in the π -system hence the degree of aromaticity is not as much as that of benzene ring (Valencia *et al.*, 2012). They are liquid at room temperature with quiet pleasant odor. Polythiophenes like phenylthiophenes and bithiophenes are obtained from polymerization of respective π -systems using electrochemical methods. The rings can also be fused together or with other cyclic pi-systems to form substituted thiophenes. Thiophene forms complexes with transition metals despite exhibiting little sulfide character. They coordinate as pi-ligands in piano stool complexes like $Cr(\eta^5-C_4H_4S)(CO)_3$ (Heinz and Makuch, 2010). Thiophenes are naturally available in species like *Calderillaacidophila* as secondary metabolites from biosynthesis. These group of heterocyclics are less hazardous to the environment because they can be microbially degraded either by sulfur oxidizing or sulfate reducing bacteria (Gogoi and Bezbaruah, 2002).

Wide research on thiophene substituted thiosemicarbazones of N,S donor atoms together with their transition metals complexes have been of concern for the last 20 years due to structure and bonding modes. These group of thiosemicarbazones can also coordinate in N, S, S tridentate fashion depending on the group and the position of the group on thiophene ring. Their interest is also as a result of ease of condensation with different carbonyls and structural manipulation. Thiophene substituted thiosemicarbazones formed from aldehydes coordinate with nickel to form trans square planar complexes while little is still known on those formed from ketones.

Thiophene derivatives of thiosemicarbazones have been studied to have anticancer activities. One of the derivatives found to be active on more than nine cancer cell lines even at very low concentrations is 2-thiophene thiosemicarbazones. However this depends on the alkyl or halide position on thiophene. When a group is attached at position 3, the activity of the ligand and the complex is decreased due to decreased coordination ability. When thiophene is substituted to 4-bromo-phenyl it was found to be active towards human kidney cancer (de Oliveira *et al.*, 2015) Marques *et al.* (2019) found that 5-nitro-thiophene thiosemicarbazone displays appreciable antitumor activities against human chronic myelocytic leukemia, acute lymphoblastic leukemia, human breast and human lung cancers. When the compound was substituted further with groups

such as phenyl groups, the activities decreased as opposed to unsubstituted nitrothiophene thiosemicarbazones with IC_{50} values ranging from 0.5-1.9 $\mu\text{g mL}^{-1}$.

Şenet *et al.* (2019) synthesized 2,5-disubstituted thiophene thiosemicarbazone; (2-acetyl-5-chloro-thiophenethiosemicarbazone with complexes and determined their activity on colorectal adenocarcinoma tumor cells. Palladium(II), Nickel(II) and Cobalt(II) complexes were found to be soluble in DMF and DMSO only. Among the complexes prepared *Cis*-[dichloro(2-acetyl-5-chloro-thiophenethiosemicarbazonato)] palladium(II) complex had the highest activity against adenocarcinoma cells. Palladium complex was synthesized via $\text{Pd}(\text{DMSO})_2\text{Cl}_2$ precursor.

2.6 Anticancer activities of palladium complexes

Clinical and pharmacological research on antitumor coordination complexes yielded anticancer agents like *cisplatin* (2), carboplatin (6) and oxaliplatin (7).

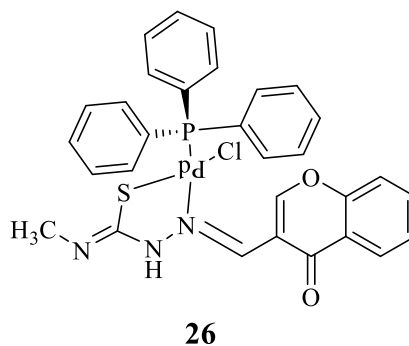
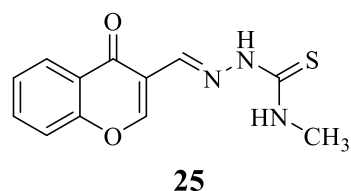
Analog complexes have been developed since the discovery of *cisplatin*. Rules of structure-activities have been broken with the establishment of platinum complexes bearing no NH groups like multinuclear complexes, *trans*-platinum complexes. This resulted to the discovery of several classes of other metal complexes including Pd^{2+} complexes. There exists common characteristics in coordination chemistry of Pt^{2+} and Pd^{2+} complexes and this has made the researchers to show interest on the study of palladium complexes as anticancer drugs. Palladium complexes are useful because of their ligand exchange kinetics. Hydrolysis of these complexes is 10^5 times faster compared to the platinum analogs. Palladium complexes dissociate very fast in solutions making them not able to reach most of the pharmacological targets (Abu-Surrah *et al.*, 2008).

For this reason the corresponding complexes like *cispalladiumcis*{ $\text{Pd}(\text{NH}_3)_2\text{Cl}_2$ } compared to *CISPLATIN* do not exhibit any anticancer activity. This is because of faster ligand exchange kinetics that compromises the structure before reaching pharmacological target. However, there are a good number of palladium complexes exhibiting the anticancer properties other than their corresponding platinum analogues towards the cancer cell lines. As a way to stabilize most of palladium complexes, bidentate ligands have been used instead of monodentate, one to solve the nightmare of not reaching the pharmacological target through rapid dissociation in solutions and two to avoid the *cis-trans* isomerism. *Trans*-palladium complexes are prepared using very large monodentate ligands for steric reasons to minimize possibility of *cis-trans* isomerism for ease of

separation of desired *trans* isomer. Most *trans* isomer shows better antitumor activities compared to the *cis* isomer and to some extent they show these activities equal to their platinum analogues. Pd²⁺ complexes especially with donor ligands (with N, S, O) have proven to be more active than the ones without these substituents or these atoms on the ligands. The more the donor atoms on the ligands the more active the complex is. For example palladium(II) dihalide complexes having diethyl-2-quinolmethylphosphonate is more active on cancerous cells than monoethyl-2-quinolmethylphosphonate. Palladium(II) dihalide complexes with bidentate nitrogen ligands such as spermidine and spermine have interesting biological activities because of their involvement in proliferation and cells differentiation in the replication of DNA and stabilization of cell membrane (Abu-Surrah *et al.*, 2008).

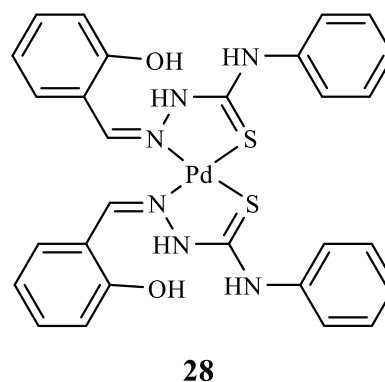
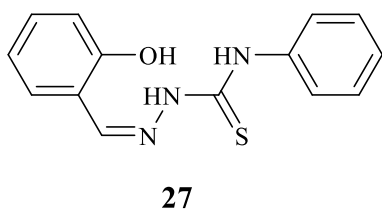
Thiosemicarbazones metal complexes have various biological activities. For this reason, it has been used in treatment of various diseases for many decades such as leprosy, small pox and tuberculosis and cell tumor. Their antitumor activities depend on the topology of the cancerous cells and it is well differentiated. For this reason, these classes of complexes are of interest because of selectivity. The presence of metal ions in thiocarbazono compounds improves their activity though it is still challenge because their activities target more than one cell. Currently the main effects in relation to their antitumor activities includes: reactive oxygen species production, ribonucleotide reductase inhibition, mitochondria disrupt, topoisomerase II inhibition and multi drug resistance (MDR) protein inhibition. Researchers have found that the anticancer activities of these complexes is derived from their ability of inhibiting ribonucleotide reductase enzyme which is necessary for the synthesis of DNA (Pelosi, 2010).

As a result of cyclometallation process during complexation of thiosemicarbazones with Pd²⁺ metal ion, palladium-thiosemicarbazone complexes have anticancer activities making it suitable for use as anticancer drug (Quiroga & Ranninger, 2004). For example (*E*)-*N*-methyl-2-((*H*-chromen-3-yl)methylene)hydrazine-carbothioamide (**25**) and its palladium complex (**26**) were synthesized by Haribabu *et al.* (2020).



The anticancer activities were determined against cervical cancer. It was established that cytotoxic activity of ligand (**25**) was enhanced after complex (**26**) formation with palladium. Single x-ray crystallography revealed that ligand existed in thionetautomer in *E*-conformation whereas the complex was found to be in square planar geometry.

Thiosemicarbazones and their palladium complexes have good anticancer activities. The cytotoxicity activities are enhanced after coordination with palladium(II) metal ion. The substituents on thiosemicarbazone ligands also play a role in enhancement of cytotoxicity. For instance ligand (**27**) and complex (**28**) synthesized by Kokina *et al.* (2019) were active towards human breast cancer cell line (MCF-7).



The complex had enhanced cytotoxic activities compared to free ligand. The substituent -OH had an influence on cytotoxicity of ligand and the complex which is associated with intra-molecular H-bonding limiting delocalization of electrons in the molecule.

The main challenge of thiosemicarbazone complexes of palladium (II) is ability to dissolve in water and alcoholic solvents. In most cases the complexes dissolve in dimethylsulfoxide (DMSO) and dimethyl formamide (DMF). This challenge makes it difficult to undertake some characterization techniques. For instance growing crystals high boiling point solvents like DMF and DMSO is tedious, making it difficult to obtain X-ray crystallography data (Pahontu *et al.*, 2013). Other than characterization, inability to dissolve in solvents including water is also a challenge during biological applications (Barani *et al.*, 2020; Khanye *et al.*, 2011).

CHAPTER THREE

MATERIALS AND METHODS

3.0 instrumentation

Perkin-Elmer Spectrum 100 series FTIR instrument available at University of the Western Cape (UWC) was used to record FTIR spectra at a range of 4000-400 cm^{-1} using KBr pellets. UV-Vis spectroscopy was performed at UWC using Nicolet evolution100 spectrophotometer from Thermo Electron Corporation at 200-800 nm range, with DMSO used as solvent for complexes and DCM for ligands. Origin software was used for analysis UV-Vis and FTIR data.

Both ^1H and ^{13}C NMR spectroscopy were done using Bruker 400 MHz spectrometer available at UWC. Series 1112 Elemental Analyzer accessible at Stellenbosch University was used to carry out C,H,N,S elemental analysis. Single crystal X-ray crystallography was done in Rutgers University, USA, using Bruker Smart CCD APEXII area detector diffractometer.

3.1 Chemicals

All the reagents used were of analytical grade purchased from Sigma Aldrich Company in South Africa. The reagents purchased other than the solvents were not subjected to purification. Chemicals used were; 4,4-dimethyl-3-thiosemicarbazide (98%), 5-(5-methylthiophen-2-yl)-thiophene-2-carboxaldehyde (97%), glacial acetic acid (100%), 5-phenyl-2-thiophencarboxaldehyde (97%), 4-ethyl-3-thiosemicarbazide (97%), 4-phenyl thiosemicarbazide (98%), 1,5-cyclooctadien (99%) and palladium(II) chloride (99%). Solvents used in the reactions were dried using respective standard drying agents through reflux in nitrogen atmosphere using standard drying agents. Solvents used were ethanol, dichloromethane, dimethylsulfoxide, methanol, *n*-hexane, acetonitrile, acetone and *N,N*-dimethyl-formamide. Deuterated acetone, chloroform and dichloromethane were used in Nuclear Magnetic Resonance (NMR) analysis. The reactions took place under inert nitrogen atmosphere using Schlenk technique. Reagents which are not commercially available were prepared using established literature methods with modifications. Synthesis in the inert environment was followed by characterization; FT-IR, UV-

Vis, ¹H NMR, ¹³C NMR, elemental analysis, and single crystal X-ray crystallography for ligand L2.

3.2 Synthesis of ligands

3.2.1 (*E*)-*N,N'*-dimethyl-2-((5'-methyl-[2,2'-bithiophen]-5-yl)methylene)hydrazine-1-carbothioamide (L1)

A mass of 0.0850 g (0.6951 mmol) of 4,4-dimethyl-3-thiosemicarbazide was added to a 20 mL ethanolic solution of equimolar 5-(5-methylthiophen-2-yl)-thiophene-2-carboxaldehyde in Schlenk tube. Three drops of glacial acetic acid were then added to the mixture to catalyze condensation reaction. The mixture was refluxed at 60 °C for 6 hours while stirring using magnetic stirrer bar forming orange solution. The orange product was allowed to cool and dried under reduced pressure in Schlenk line. Recrystallization was done by dissolving the dried product by minimum amount of dry dichloromethane and slightly more amount of dry *n*-hexane; dipped in liquid nitrogen for 3 seconds, allowed to settle for 1 hour undisturbed, decanted then further dried.

3.2.2 (*E*)-*N*-ethyl-2-((5-phenylthiophen-2-yl)methylene)hydrazine-1-carbothioamide (L2)

A mass of 0.2 g (1.041 mmol) of 5-phenyl-2-thiophencarboxaldehyde was added to a Schlenk tube filled with 10 mL dry ethanol under nitrogen atmosphere and stirred for 3 minutes. An equimolar solution of 4-ethyl-3-thiosemicarbazide was added to the aldehyde drop-wise while stirring. Three drops of acetic acid were then added to the mixture to catalyze condensation reaction. The mixture was refluxed at 60 °C for 6 hours, allowed to cool then dried under reduced pressure using Schlenk line. The yellow solid formed was purified through recrystallization. This was done by dissolving it in minimum amount of dichloromethane and adding a little more *n*-hexane. The content was cooled in liquid nitrogen for 5 seconds. It was allowed to settle for one hour, mother liquor decanted then further dried.

3.2.3 (*E*)-2-((5'-methyl)-[2,2'-bithiophen]-5-yl)methylene)-*N*-phenylhydrazine-1-carbothioamide (L3)

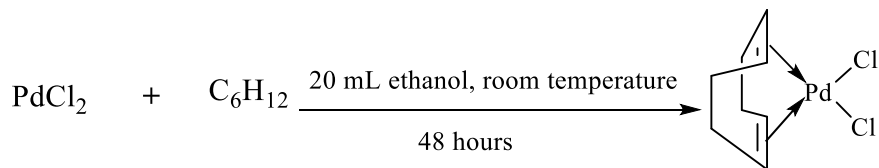
A mass of 0.1573 g (0.9313 mmol) of 4-phenyl thiosemicarbazide was added to an equimolar 20 mL ethanolic solution of 5-(5-methylthiophen-2-yl)thiophene-2-carboxaldehyde. Three drops of acetic acid were added to the mixture to catalyze the reaction. The mixture refluxed at 60 °C for

6 hours, while stirring with magnetic stirrer bar, allowed to cool then dried under reduced pressure using Schlenk line. The product formed was a yellow solid which was purified through recrystallization by dissolving it in the minimum amount of dichloromethane and adding a little more *n*-hexane, cooled in liquid nitrogen for 5 seconds; allowed to settle for one hour, mother liquor decanted from the solid then further dried.

3.3 Synthesis of thiosemicarbazone complexes of palladium

3.3.1 Synthesis of *cis*-cyclooctadienepalladium(II) chloride precursor

Synthesis of complexes was done in a two steps reaction. A precursor Pd(cod)Cl₂, was prepared by treating a suspension of 1.00g (5.6392 mmol) PdCl₂ in 30 mL methanol with 2.1 mL 1,5-cyclooctadien. The mixture was then refluxed for 48 hours at room temperature under inert nitrogen atmosphere using Schlenk technique as shown in Scheme 3.1.



Scheme 3.1: Synthesis of Pd(cod)Cl₂

Solid was formed, filtered and washed with 20 mL dry *n*-hexane then dried under reduced pressure. FTIR of the compound was verified with Pd(cod)Cl₂ from authentic source.

3.3.2 Synthesis of (*E*)-*N,N'*-dimethyl-2-((5'-methyl-[2,2'-bithiophen]-5-yl)methylene)hydrazine-1-carbothioamide palladium(II)chloride (C1)

A solution of 0.1228 g (0.3968 mmol) of **L1** in 10 mL dry dichloromethane was added to a Schlenk tube containing a suspension of 0.15g (0.4009 mmol) Pd(cod)Cl₂ in 20 mL 1:1 dichloromethane/Et₂O solvent mixture. The content was stirred for at room temperature for 12 hours under inert nitrogen atmosphere. Orange precipitate was formed immediately. The orange solid was filtered, washed with 20 mL dry *n*-hexane then purified by recrystallization using dichloromethane/*n*-hexane system. The product was further dried under reduced pressure using Schlenk line.

3.3.3 Synthesis of (*E*)-*N*-ethyl-2-((5-phenylthiophen-2-yl)methylene)hydrazine-1-carbothioamide palladium(II)chloride (C2)

A solution of 0.1148 g (0.3968 mmol) of **L2** in 10 mL dry dichloromethane was added to a Schlenk tube containing a suspension of 0.15 g (0.4009 mmol) Pd(cod)Cl₂ in 1:1 dichloromethane/Et₂O mixture. The content was stirred for at room temperature for 12 hours. Orange precipitate was formed immediately. The orange solid was filtered, washed with 20 mL dry hexane then purified by recrystallization using dichloromethane/*n*-hexane system. The product was further dried under reduced pressure using Schlenk line.

3.3.4 Synthesis of (*E*)-2-((5'-methyl)-[2,2'-bithiophen]-5-yl)methylene)-*N*-phenylhydrazine-1-carbothioamide palladium(II)chloride (C3)

A solution of 0.1419 g (0.3968 mmol) of **L3** in 10 mL dry dichloromethane was added to a Schlenk tube containing a suspension of 0.15 g (0.4009 mmol) Pd(cod)Cl₂ in 1:1 dichloromethane/Et₂O mixture. The content was stirred for at room temperature for 12 hours. Orange precipitate was formed immediately. The orange solid was filtered, washed with 20 mL dry *n*-hexane then purified by recrystallization using dichloromethane/*n*-hexane system. The product was further dried under reduced pressure using Schlenk line.

The % yield of ligands and complexes were determined using the formula below;

$$\% \text{ yield} = \frac{\text{moles of the product}}{\text{moles of the starting material}} \times 100\%$$

3.4 Characterization of ligands and complexes

3.4.1 Melting point

Melting points of both ligands and complexes were carried SMP SMP-10 melting point apparatus using glass capillaries at University of the Western Cape.

3.4.2 Fourier Transform Infrared spectroscopy

PerkinElmer Spectrum 100 Series FTIR instrument was used to run FTIR spectra between 4000–400 cm⁻¹ range using KBr pellets. The blank scan was first obtained by running FTIR of KBr pellets without samples. The equipment used was available at University of the Western Cape.

3.4.3 UV-Visible spectroscopy

UV-Vis spectroscopy was carried out at an absorption range of 200-800 nm. Blank DCM solvent was first scanned to calibrate the instrument. All complexes were dissolved in (DMSO) while ligands were dissolved in dichloromethane to obtain a concentration of $1.0 \times 10^{-3} \text{M}$. Absorption wavelength of the compounds were observed in UV-Vis spectra generated using Nicolet evolution 100 spectrophotometer available at University of the Western Cape. Interpretation of data was done using Origin software.

3.4.4 Nuclear Magnetic Resonance

Both ^1H and ^{13}C NMR of the compounds were obtained by running them on Bruker 400 MHz using Tetramethylsilane (TMS) as a reference. Bruker 400 MHz instrument was available at University of the Western Cape. ^1H and ^{13}C NMR of Ligand **L1** was done using deuterated chloroform (CDCl_3) while Ligands **L2** and **L3** were done using deuterated acetone (acetone- d_6). Deuterated DMSO (DMSO- d_6) was used as NMR solvent for all the complexes. The NMR data obtained were analyzed using MestreNova software.

3.4.5 Elemental analysis

Elemental analysis was performed on Server 1112 series Elemental Analyzer available at Stellenbosch University, South Africa. The obtained C, H, N, and S % obtained were compared with the calculated % mass of the expected structure of ligands and complexes. The expected difference between the observed and calculated % mass was $\pm 1.0\%$ except for Sulfur atom which may have wide range due to allotropy.

3.4.6 Single X-ray crystallography

Crystal growth for ligands was done in slow diffusion of *n*-hexane in dichloromethane. The ligands were dissolved in minimum amount of dichloromethane enough to dissolve it then three times volume of *n*-hexane was added. The mixture was put in the refrigerator for three weeks for the crystals to grow. Among the ligands, there was a successful growth in **L2** which was then subjected to X-ray crystallography at The State University of Rutgers- USA. The selected crystals were glued on glass fibers tip. The tip was then mounted in a cold nitrogen stream at 100K and put at the center of X-ray beam by use of a video camera. Bruker SMART CCD Apex-II area-detector was used to perform the single X-ray crystallography for the ligand. Refining

and resolution of the crystal structure were done using SHELXS method(Zhao *et al.*, 2016). Mercury software was further used to analyze the CIF data.

3.5 Determination of stability

Stability test for ligands and complexes were conducted using ¹H NMR. The ¹H peaks were observed at an interval of 6 hours within a period of 3 days.

3.6 Determination of anticancer activities

Anticancer activities of the compounds were determined on HT-29 (colorectal adenocarcinoma), Hela (cervical), KMST (non-cancer) and Caco-2(colon) human cell lines. Cell lines were cultured using respective medium for 24hours. The cell lines were incubated at 37°C under 5% humidified carbon (IV) oxide incubator. Confluency of the cell lines was checked. Seeding of density 1×10^5 cells/mL in 96-well plate was conducted. The cell lines were incubated for 24 hours at a temperature of 37 °C. The cell lines were treated with varying concentrations; 12.5, 25, 50 and 100 µg/mL in DMSO. After treating the cells with the compound, MTT assay was conducted by adding to each plate 10 µL of 5µg/mL of MTT (Sigma, USA). MTT reduction was read using POLARstar omega plate reader at a wavelength of 580 nm.

The IC₅₀ on each of the cell lines were determined with the help of GraphPad Prism software version 5 (GraphPad Software, California, USA). The equationbelow was used to determine the viability of the cell lines as far as MTT assay is concerned.

$$\% \text{ cell viability} = \frac{\text{average absorbance of treated cells}}{\text{average absorbance of control}} \times 100\%$$

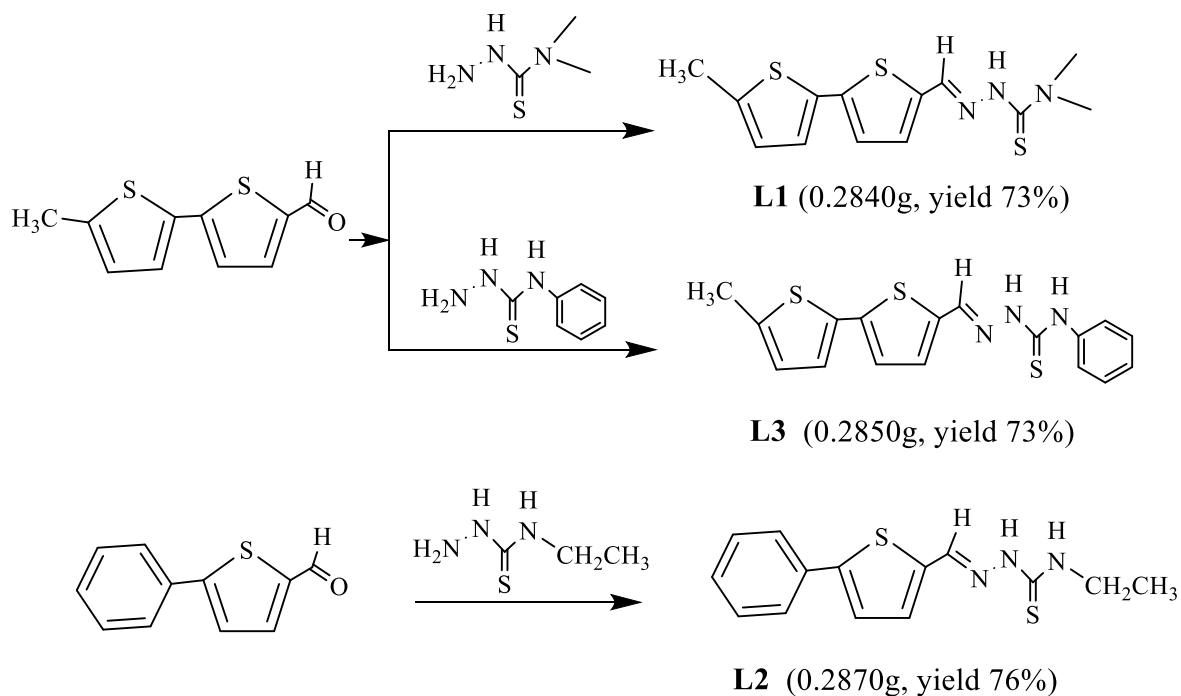
Morphological changes of the cells were observed under microscope (EVOS XL Core microscope; Thermo Fisher Scientific, Germany) at a magnification of 10X.

CHAPTER FOUR

RESULTS AND DISCUSSION

4.0 Thiosemicarbazones ligands

Ligands **L1**, **L2** and **L3** in Scheme 4.1 were synthesized and the yields were between 73-76%.



Scheme 4.1: Synthesis of thiosemicarbazone ligands

Ligands were then subjected to characterization using Fourier Transform infrared (FTIR), UV-Visible, CHNS elemental analysis, single crystal X-ray crystallography, ^1H and ^{13}C Nuclear Magnetic Resonance (NMR) to confirm the structures. Crystals for the ligands were grown under reduced temperature with slow diffusion of hexane in dichloromethane. **L2** was the only ligand whose crystal grew successfully for single X-ray crystallography studies.

4.2 Physical properties for ligand L1

Ligand **L1** was an orange solid (0.2840 g, yield 73%) with a melting point of 185-188°C. It dissolved in dichloromethane, dimethylsulfoxide (DMSO), dimethylformamide (DMF), acetone,

acetonitrile and ethanol (on heating). No change on ^1H NMR spectra over 72 hours when the ligand was subjected to stability test, conclusion that the ligand was stable in DMSO within 72 hours hence was subjected to anticancer investigation.

4.3 Characterization and structural confirmation of ligand L1

FTIR spectroscopy studies were carried on **L1** to confirm the successful formation of azomethine bond, a characteristic feature of thiosemicarbazones. The appearance of sharp peak at 1543 cm^{-1} showed the successful formation of imine. No peak was observed at 1700 cm^{-1} , this indicated the absence aldehyde used in the reaction. The C=S peak was observed at 924 cm^{-1} while the N-H 3143 cm^{-1} . These results is in agreement (Lavericket *al.*, 2021) where stretching frequency for imine was observed at $1539\text{-}1591\text{ cm}^{-1}$. FTIR spectra for **L1** is shown if Figure 4.1.

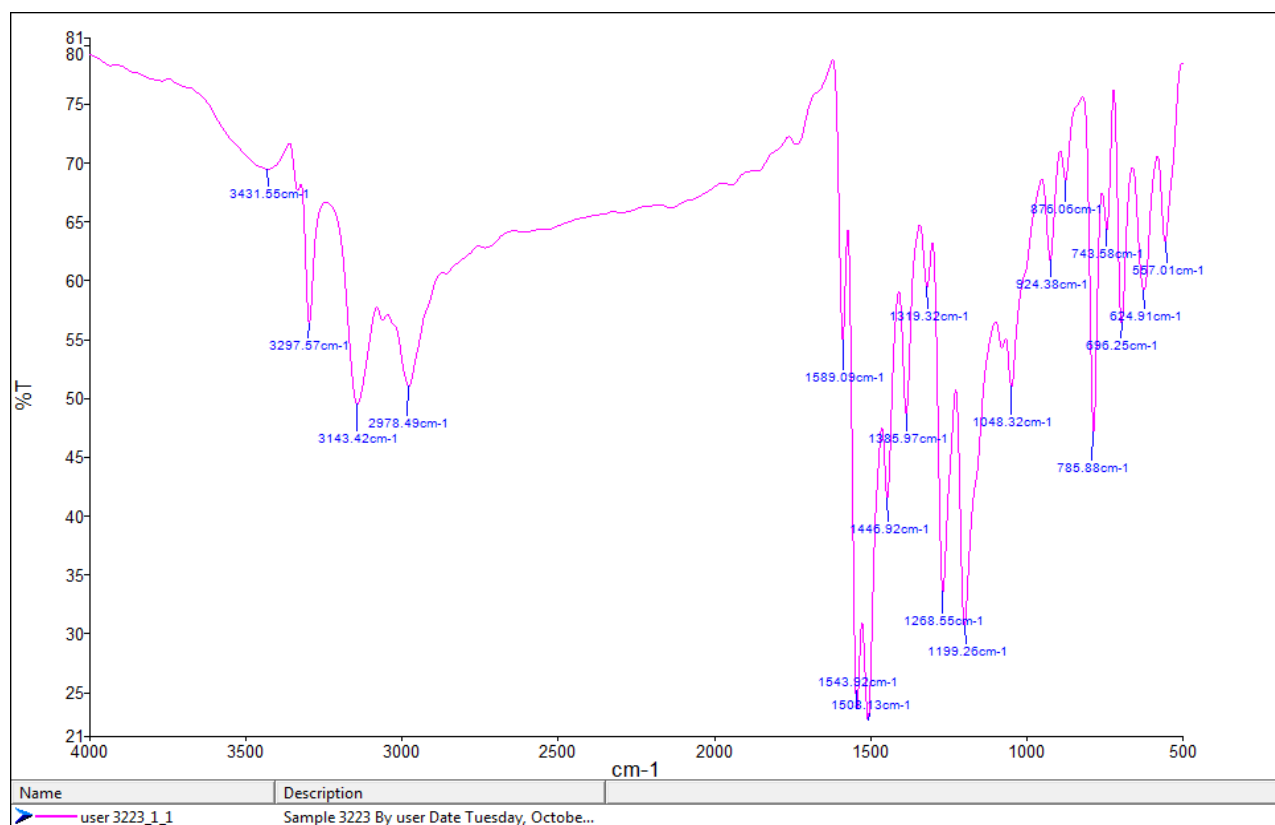


Figure 4.1: FT-IR spectrum for **L1**

UV-Vis absorption spectra for the ligands were obtained in DCM solvents using 1cm micro-cuvettes between 200-80 nm range at room temperature. All the ligands were soluble in DCM therefore it was the best choice for use in UV-Vis due to its characteristic solvent cutoff wavelength (230 nm). This meant minimal interference with UV-Vis spectra of the ligands. Three absorption wavelengths were observed in ligand **L1**. These were 300 nm which was as a result of $\pi \rightarrow \pi^*$ transitions, 381 nm $n \rightarrow \pi^*$ and 452 nm which was attributed to intra-ligand charge transfer. Lambda maximum was observed at 452 nm. Similar observations were made by (Nyawade *et al.*, 2021). UV-Vis spectrum is shown in Figure 4.2.

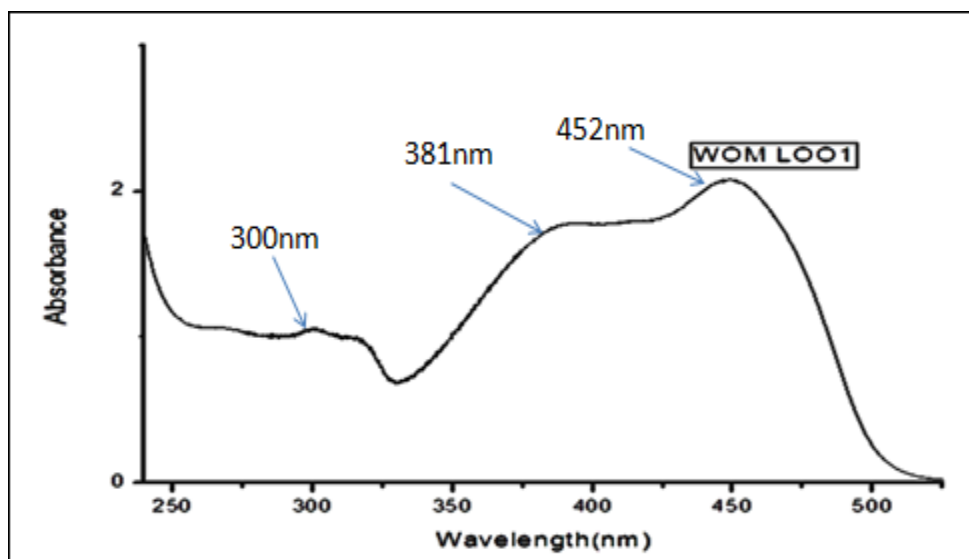


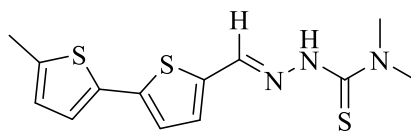
Figure 4.2: UV-Vis spectrum for **L1**

Broad peaks were due to unresolved rotational and vibration energies accompanying electronic excitation energy, between High Occupied Molecular Orbital (HOMO) to Low Unoccupied Molecular Orbital (LUMO) in smaller molecules (Kose *et al.*, 2018)

NMR for ligand **L1** was carried out using deuterated chloroform (CDCl_3). Peak was observed at δ 9.8 ppm in ^1H NMR, this was the chemical shift of N-H proton. No peak was observed around δ 9.0-9.5 ppm indicating the absence of aldehydic proton. Iminic proton was observed at δ 8.38 ppm. Peaks observed at δ 6.79 ppm (d), 7.16 ppm (d), 7.36 ppm (d) and 7.38 ppm (d) were due to bithiophene protons. Thiosemicarbazide methyl protons were observed at δ 2.2 ppm while those for bithiophene were observed at δ 2.50 ppm. This ^1H NMR data agrees with the literature

data reported by (Sibuh *et al.*, 2021) and (Islam *et al.*, 2021). The upfield frequency shift is as a result of less electronegativity effect of N compared to O in the aldehyde. ^{13}C NMR displayed no peak at δ 190-200 ppm. This is an indication that there was no aldehyde carbon present in the product. The highest shift was observed at δ 183.0 ppm which was as a result of C=S. The imine carbon was observed at δ 148.0 ppm. Bithiophen carbons were seen at δ 132.0, 124.7, 125.2, 126.7, 140.5, 134.4, 140.2 and 136.9 ppm. Similar results were reported by (El-Atawy *et al.*, 2019). Correlations between proton and carbon atoms were established by two-dimension NMR; Distortionless enhancement by polarization transfer (DEPT), homonuclear correlation spectroscopy (COSY) and Heteronuclear Multiple Bond Correlation (HMBC). NMR spectra are available in the appendices section.

The structure **L1** of the ligand was further confirmed by elemental analysis. The observe data was in agreement with the calculated ones within acceptable margin. Elemental analysis gave: N, 13.81%; C, 51.27%; H, 4.18%; S, 31.14% while calculated was: N, 13.58%; C, 50.46%; H, 4.89%; S, 31.08%. Elemental analysis result also indicated that the prepared ligand was pure.



L1

4.4 Physical properties for ligand L2

Ligand **L2** was a yellow solid, (0.2850 g, yield 73%), with a melting point of 176-178°C. It was soluble in DCM, DMSO, DMF, acetone and acetonitrile. No change on ^1H NMR spectra over 72 hours when the ligand was subjected to stability test, conclusion that the ligand was stable in DMSO within 72 hours hence was subjected to anticancer investigation.

4.5 Characterization Structural confirmation of ligand L2

FTIR study was conducted for ligand **L2** to confirmed successful completion of condensation reaction. This was also conducted to ascertain successful synthesis of Schiff base ligand through formation of imine and disappearance of aldehyde stretching frequency band. No peak was observed around 1700 cm^{-1} suggesting that aldehyde was consumed in the reaction. Imine stretching frequency was seen at 1534 cm^{-1} . N-H bands were observed between $3360\text{-}3130\text{ cm}^{-1}$

¹and C=S at 1087 cm⁻¹. These stretching frequency values agree with literature according to (Islam *et al.*, 2021). FTIR spectrum for ligand **L2** is available in the appendices section.

UV-Visible spectra for ligand **L2** displayed two absorption peaks. Peaks at 268 nm and 375 nm were as a result of $\pi \rightarrow \pi^*$ and $n \rightarrow \pi^*$ electronic transitions with Lambda maximum observed at 375nm. This is in agreement as per Mbugua *et al.* (2020).

Both ¹H and ¹³C NMR for ligand **L2** were conducted using deuterated acetone (acetone-d₆). Imine proton was observed at δ 7.94 ppm while N-NH proton at 9.53 ppm. There was no peak around δ 9.0-9.2 ppm suggesting the absence of starter aldehyde in the product. Aromatic peaks were observed at δ 7.33 ppm (t), 7.40 ppm (t) and 7.62 ppm (d). Thiophene protons were observed at δ 7.22 ppm (d) and 7.26 ppm (d). Methylene and methyl proton peaks were seen at δ 3.76 ppm (m) and 1.32 ppm (t) respectively as shown in Figure 4.3.

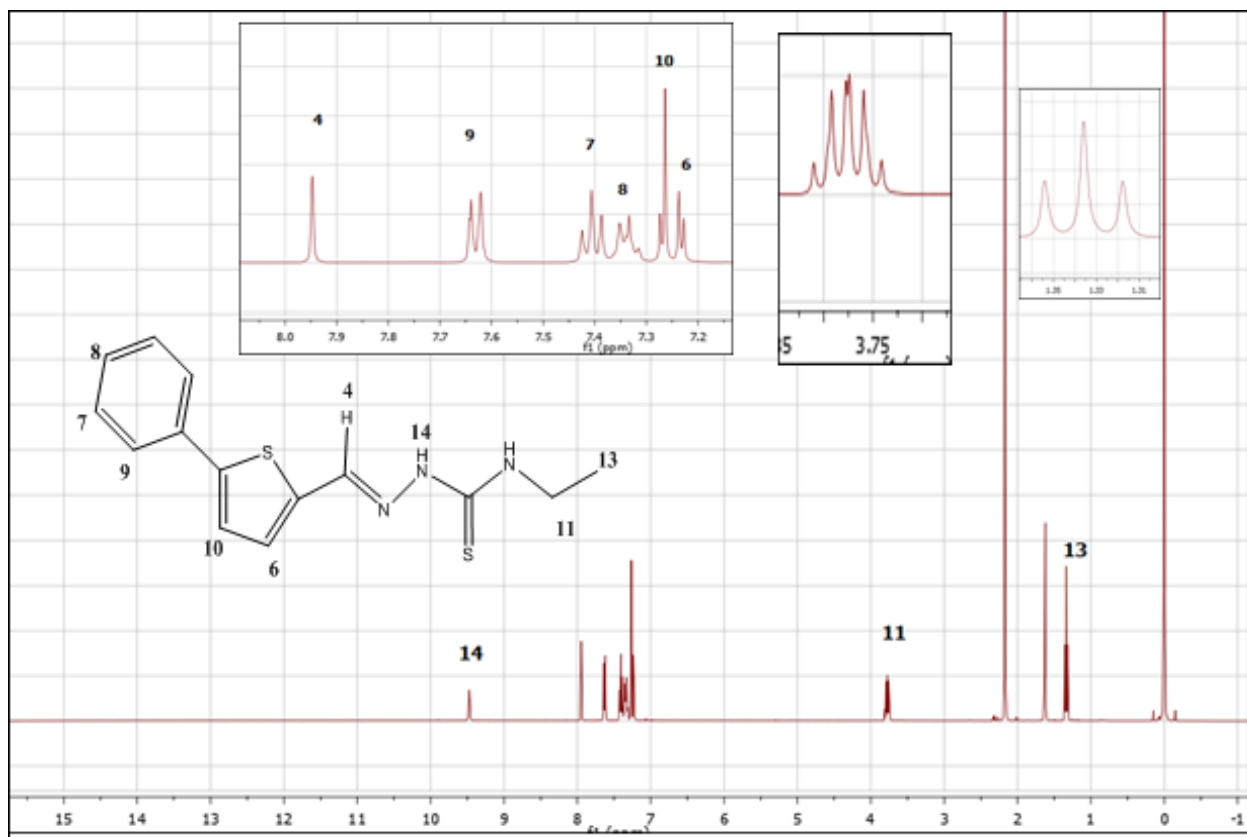


Figure 4.3: ¹H NMR spectra for **L2**

^{13}C NMR displayed a peak at δ 207.0 ppm, this was the deuterated acetone carbon peak. Imine carbon was observed at δ 136.7 ppm while $\text{C}=\text{S}$ was seen at δ 176.8 ppm. Aromatic carbon peaks were seen at δ 126.0 ppm, 128.5 ppm, 129.1 ppm and 133.6 ppm. Thiophene carbon peaks were seen at δ 123.6 ppm, 131.8 ppm, 137.0 ppm and 147.3 ppm. Methyl and methylene carbon peaks were seen at δ 39.5 ppm and 15.0 ppm respectively. ^{13}C NMR spectra for ligand **L2** is shown in the Figure 4.4 below.

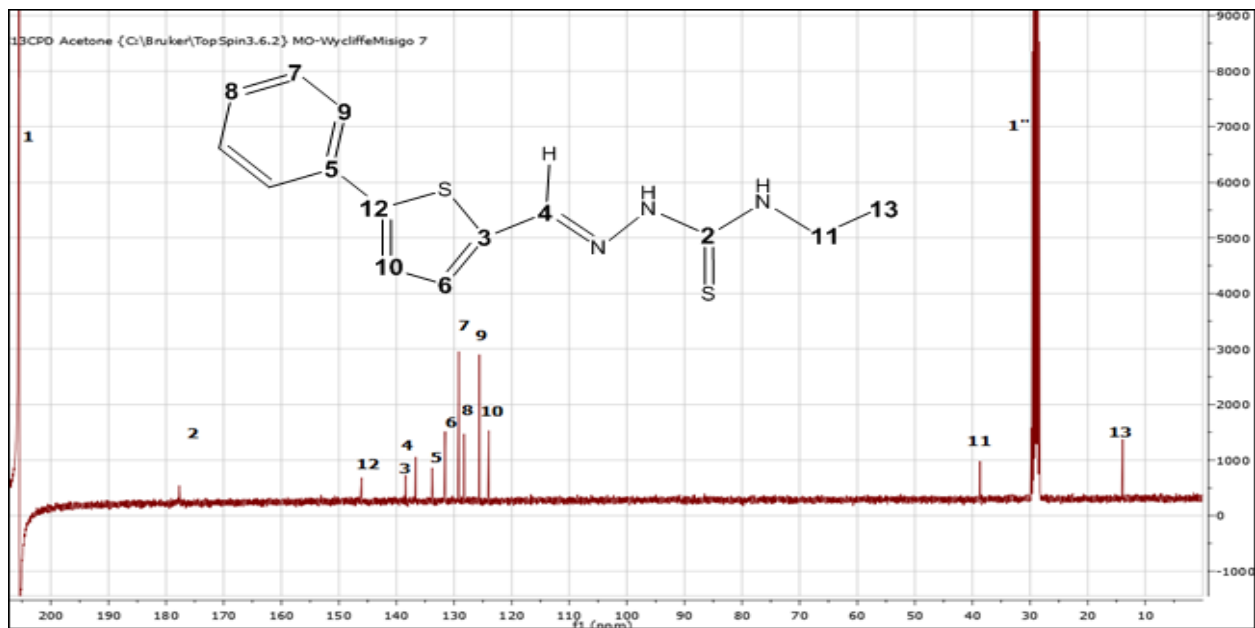


Figure 4.4: ^{13}C NMR spectrum for ligand **L2**

DEPT spectra in Figure 4.5 also revealed that only one $-\text{CH}_2$ was present further confirming the structure of the ligand.

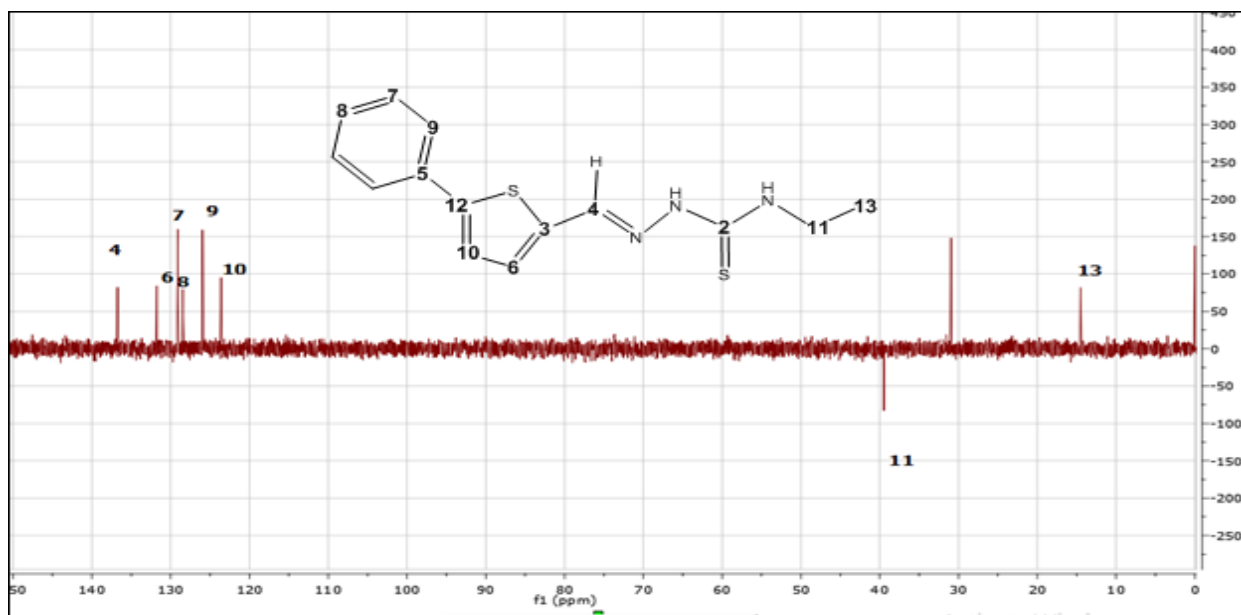


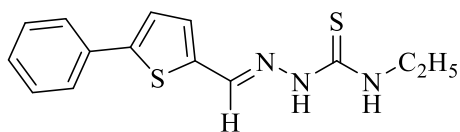
Figure 4.5: DEPT spectra for **L2**

Data from 2D NMR assisted in confirming the structure. The data obtained showed the correlation of protons to carbons as shown in Table 4.1.

Table 4. 1: 1D and 2D NMR data for **L2**

Position	¹³ C	DEPT-135	Proton	COSY	HMBC
1	207	C(Solvent)			
2	176.8	C			
3	137	C			
4	136.7	CH	7.94		6,4,3
5	133.6	C			
6	131.8	CH	7.22		10,3,4, 12
7	129.1	CH	7.4	9	9,7,5
8	128.5	CH	7.33		9
9	126	CH	7.62	7	9,8,12
10	123.6	CH	7.26		6,3,12
11	39.5	CH ₂	3.76	13	13,2
12	147.3	C			
13	15	CH ₃	1.32	11	11
14			9.46		4,2

The structural purity of **L2** was confirmed by elemental analysis data between the observed and the calculated. There was minimum discrepancy between the calculated and the observed values confirming was the write structure. Elemental analysis gave; N, 14.47; C, 57.91; H, 5.16; S, 21.63; while calculated was; N, 14.52; C, 58.10; H, 5.22; S, 22.16. Structure was the confirmed structure for ligand **L2**.



L2

Among the ligands, **L2** was successfully grown in slow diffusion of hexane in DCM under reduced temperatures. From the single X-ray crystallography, ligand **L2** belongs to monoclinic crystal class and a P 21/c space group. There are four molecules in a unit cell with dimensions and angles as shown in Table 2.

Table 4.2: Single-Crystal Data and Structure Refinement Parameters for **L2**

Compound	L2
Formula	C ₁₄ H ₁₅ N ₃ S ₂
Space group	P21/c
Cell lengths	a=7.9785(4), b=5.6579(3), c=31.3640(14)
Cell angles	α =90, β = 92.380(3), γ =90
Cell volume	141,46
Z,Z'	Z=4, Z'=0
Temperature	100K

The four molecules are held up together with various interactions network. These are intermolecular hydrogen bonding; N(2)-H(2) S(2); Van de Waals forces C(14)-H(14B) S(2), C(13)-H(13B) C12 and C(10)-H(10) C3 and N(2) S(2); and π hydrogen interactions C(10)-H(10) C2. All these interactions lead to a formation of three-dimension lattice as shown in Figure 4.6.

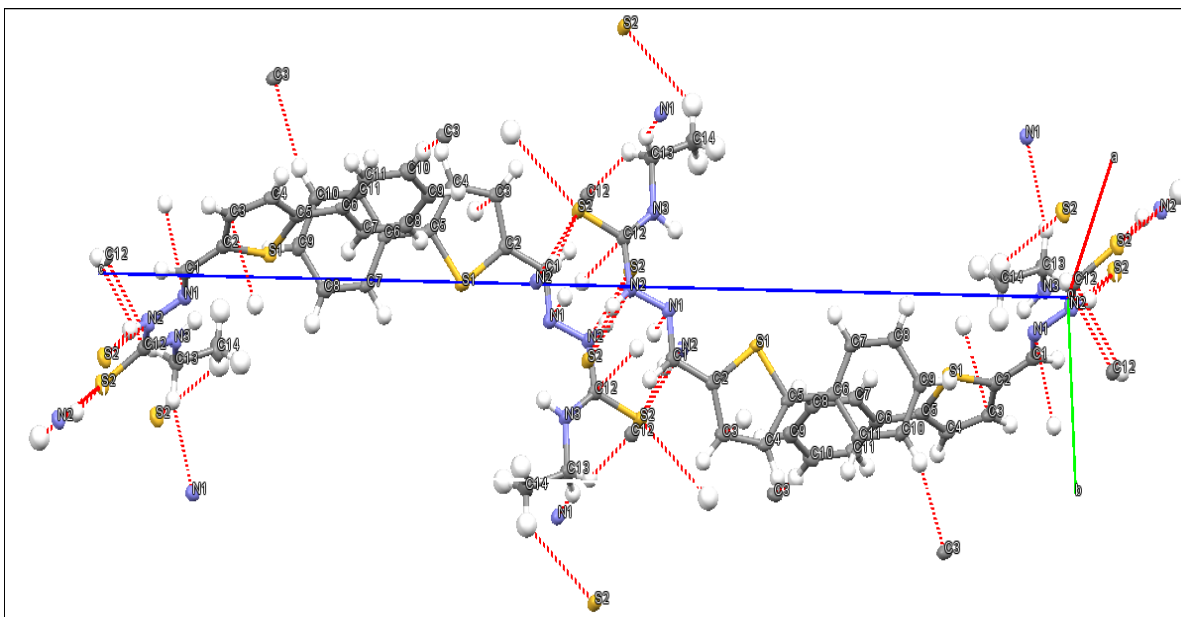


Figure 4.6: Crystal structure for **L2**

The values of torsion angles of thiosemicarbazone fragments 173.5(1) and 176.7 (1) for S(2)-C(12)-N(2)-N(1) and N(2)-N(1)-C(1)-C(2) respectively suggests that there is likelihood of intramolecular hydrogen bonding in N(3)-H(3) N(1) though not observed in the crystal structure.

Thiophene fragment of the ligand has torsion angles of 0.1(2) and 0.5(2) for S(1)-C(5)-C(4) and S(1)-C(2)-C(3)-C(4) respectively. The torsion of the planes confirms the planarity of the thiophene ring. This is shown in Figure 4.7below.

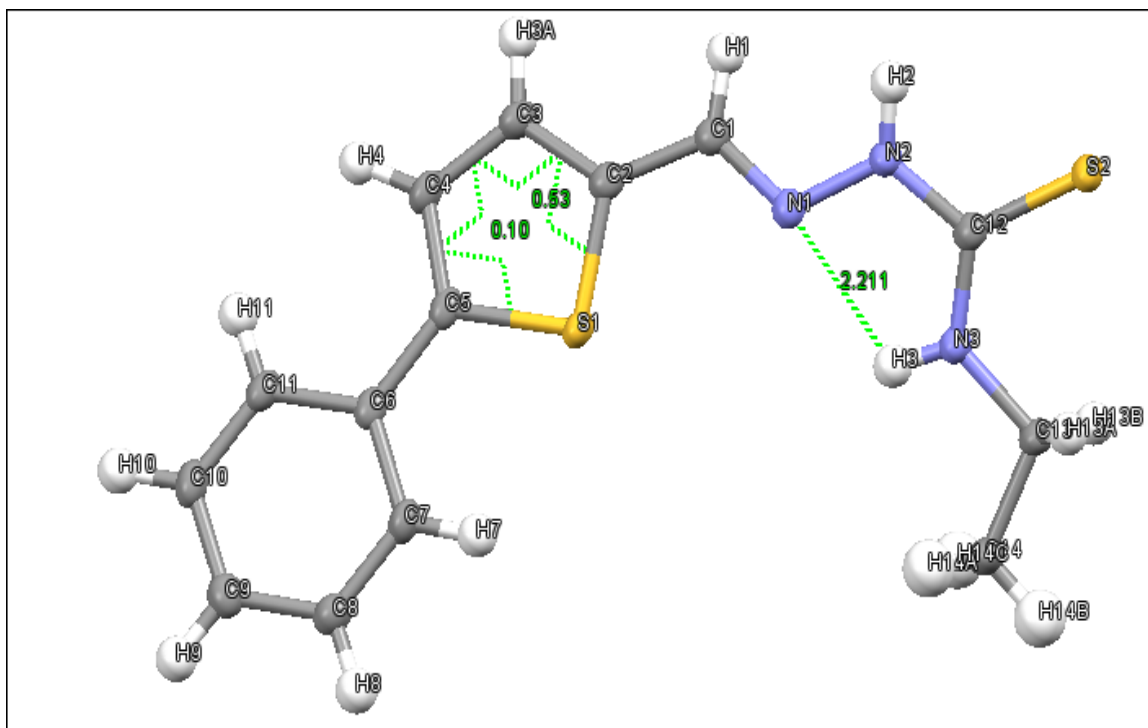


Figure 4.7: Tortion angles in thiophene and intramolecular H-bonding

Tortion angles of benzene ring fall between -0.58 to 0.8° . This confirms the planarity of benzene ring. Bond angle for N(1)-N(2)-H(2) was found to be 120.24° suggesting that N(2) and N(1) are sp^2 hybridized, hence successful formation of imine. The clear indication on the existence of the imine bond is also evident in the difference in C(1)-N(1) and C(2)-N(12) bond length which are 1.291\AA and 1.363\AA respectively. From the crystal structure, the ligand possesses an *E*-configuration in reference to the C=N bond. The C=S bond length (1.691\AA) suggests that the ligand exists in thioamido form as reported in literature (Mathews *et al.*, 2020). Measurements for the other bondlengths, bond angles and torsion angles are summarized in Table 4.3.

Table 4.1: Geometric parameters for ligand **L2**

Bond distances(Å)	Bond angles(degrees)
C(1)-N(1) 1.291	C(1)-N(1)-N(2) 116.13
N(1)-N(2) 1.375	N(1)-N(2)-C(12) 118.72
N(2)-C(12) 1.363	C(12)-N(3)-C(13) 125.20
C(12)-N(3) 1.321	N(2)-C(12)-N(3) 116.58
C(12)-S(2) 1.691	N(2)-C(12)-S(2) 119.61
N(3)-C(13) 1.462	N(3)-C(12)-S(2) 123.8
Tortons angle	(degrees)
C(1)-N(1)-N(2)-C(12)	176.67
N(1)-N(2)-C(12)-S(2)	173.53
N(1)-N(2)-C(12)-N(3)	7.57
N(2)-C(12)-N(3)-C(13)	178.34
S(1)-C(2)-C(3)-C(4)	0.53
S(1)-C(5)-C(4)-C(3)	0.1
N(2)-N(1)-C(1)-C(2)	-175.73
C(6)-C(7)-C(8)-C(9)	-0.3
C(6)-C(11)-C(10)-C(9)	0.7

4.6 Physical properties for ligand **L3**

Ligand **L3** was a yellow solid, (0.2870 g, yield 76%), with a melting point of 198-201°C. It was soluble in DCM, DMSO, DMF, acetone and acetonitrile. No change on ¹H NMR spectra over 72 hours when the ligand was subjected to stability test, conclusion that the ligand was stable in DMSO within 72 hours hence was subjected to anticancer investigation.

4.7 Characterization and structural confirmation of ligand **L3**

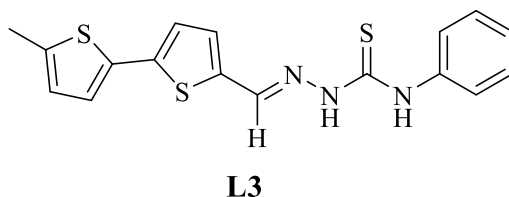
FTIR studies were conducted on **L3** proved that Schiff base was successfully synthesized. No peak was observed around 1700 cm⁻¹ suggesting that the starter aldehyde was not present in the end product. Imine peak was observed at 1579 cm⁻¹. N-H stretching frequency bands were seen at 3254 cm⁻¹ and 3384 cm⁻¹. C=S stretching frequency was observed at 997 cm⁻¹. These FTIR data agree with literature values according to Arshia *et al.* (2021). The FTIR spectra for ligand **L3** is available in appendices section.

UV-Vis spectrum for **L3** showed two bands at 277 nm, 307 and 398 nm due to $\pi \rightarrow \pi^*$, $n \rightarrow \pi^*$ and intraligand charge transfer transitions respectively with Lambda maximum of 398nm. Close

values have been reported by (Kumar & Nath, 2019). The UV-Vis spectrum is available in the appendices section.

Both ^1H and ^{13}C NMR for ligand **L3** were conducted using deuterated acetone (acetone- d_6). Imine proton was observed at δ 9.70 ppm. There was no peak around δ 9.00-9.20 ppm suggesting the absence of aldehyde. N-NH peak was seen at δ 10.70 ppm and C-NH seen at δ 8.38 ppm. Aromatic protons were observed at δ 7.19 ppm, 7.36 ppm and 7.75 ppm. Bithiophene protons were observed at δ 7.38 ppm, 7.37 ppm, 6.79 ppm and 7.16 ppm; Thiophene methyl group at 2.49 ppm. Spectrum from ^{13}C NMR showed imine carbon at δ 137.4 ppm. C=S carbon peak was observed at δ 176.4 ppm. Bithiophene carbons were seen at δ 132.0, 124.7, 125.2, 126.7, 140.5, 134.4, 140.2 and 136.9 ppm. Aromatic carbon peaks seen at δ 123.4 ppm, 124.4 ppm and 128.2 ppm; Thiophene methyl group at δ 14.4 ppm. These data agree with literature according to Garg *et al.* (2013). 2D NMR was also conducted to elucidate the structure of **L3**. It is observed that chemical shift for imine proton and imine carbon was more downfield in **L3** than **L1** and **L2**. The higher chemical shift is attributed to anisotropic effect by phenyl group of the amine end and electronegative effect of the bithiophene group. Resonance effect was negligible to chemical shift due to difference in the sizes of pi-orbitals of S and C in thiophene ring (Lee *et al.*, 2002). Both ^{13}C and ^1H NMR are available at the appendices section.

Elemental analysis data for **L3** was close to calculated. This was done to prove the structural purity of ligand **L3**. Elemental analysis gave; N, 11.42; C, 56.48; H, 4.24; S, 25.67%; while calculated was; N, 11.75; C, 57.11; H, 4.23; S, 26.90 %.



4.8. Palladium (II) thiosemicarbazone complexes

Preparation of palladium(II) complexes synthesized by first preparing precursor $\text{Pd}(\text{cod})\text{Cl}_2$; a yellow solid yield of 97.69% (1.5730 g) as shown in Scheme 3.1.

FT-IR spectra of the prepared yellow Pd(cod)Cl₂ was compared to a sample of Pd(cod)Cl₂ from the authentic source (Sigma-Aldrich) as shown in Figure 4.8 and Figure 4.9 respectively and there was similarity.

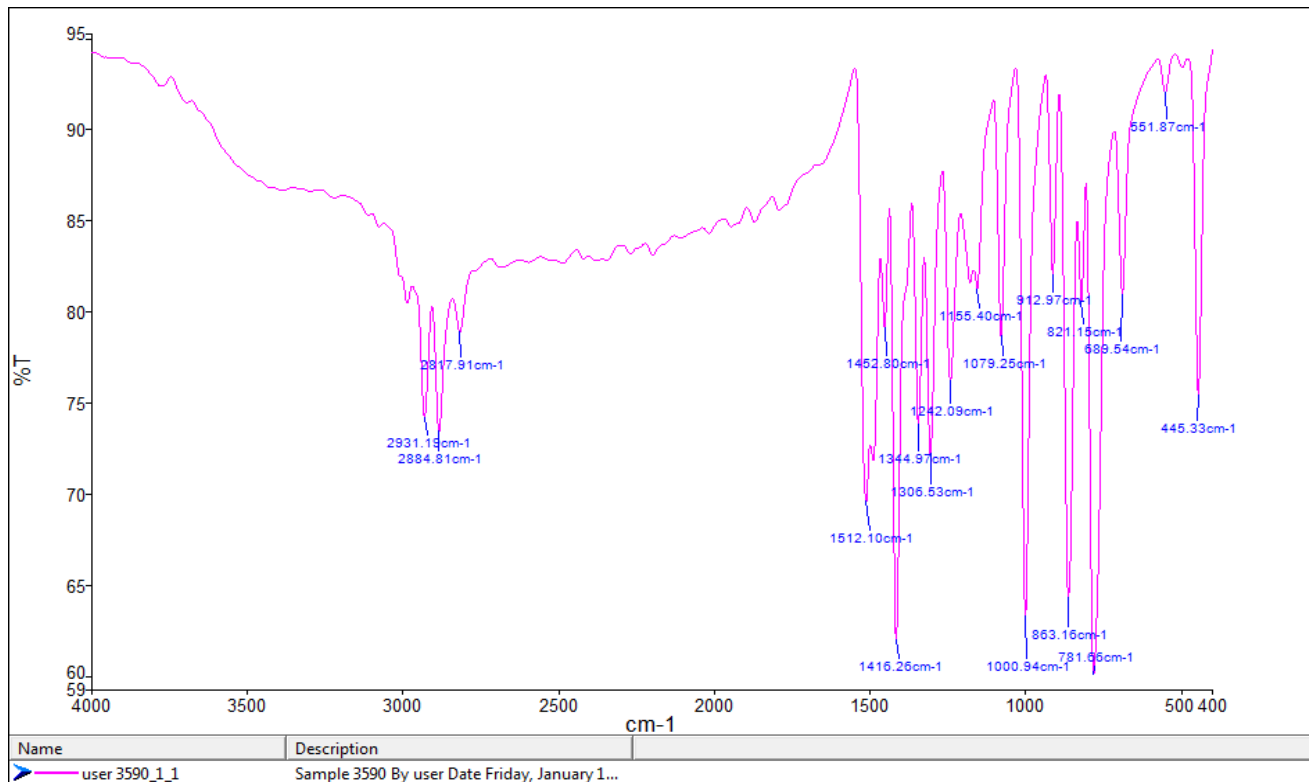


Figure 4.8: FTIR spectra of prepared Pd(cod)Cl₂

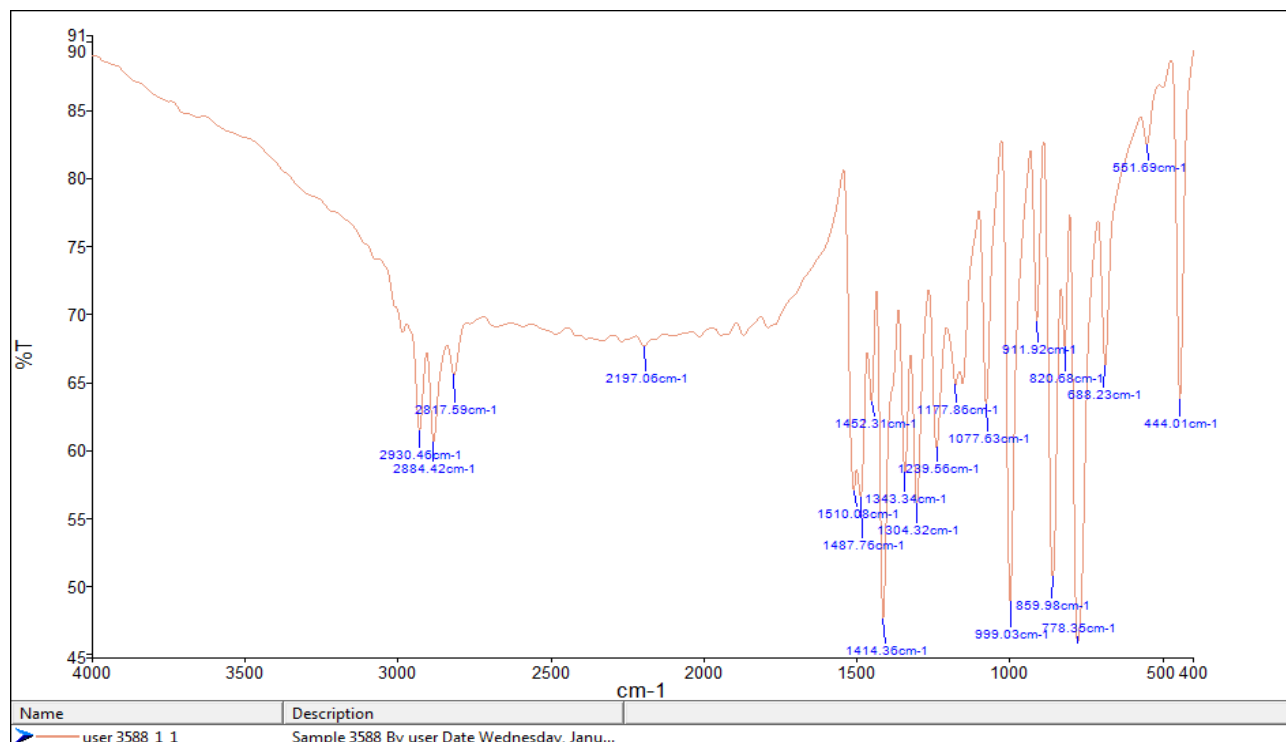
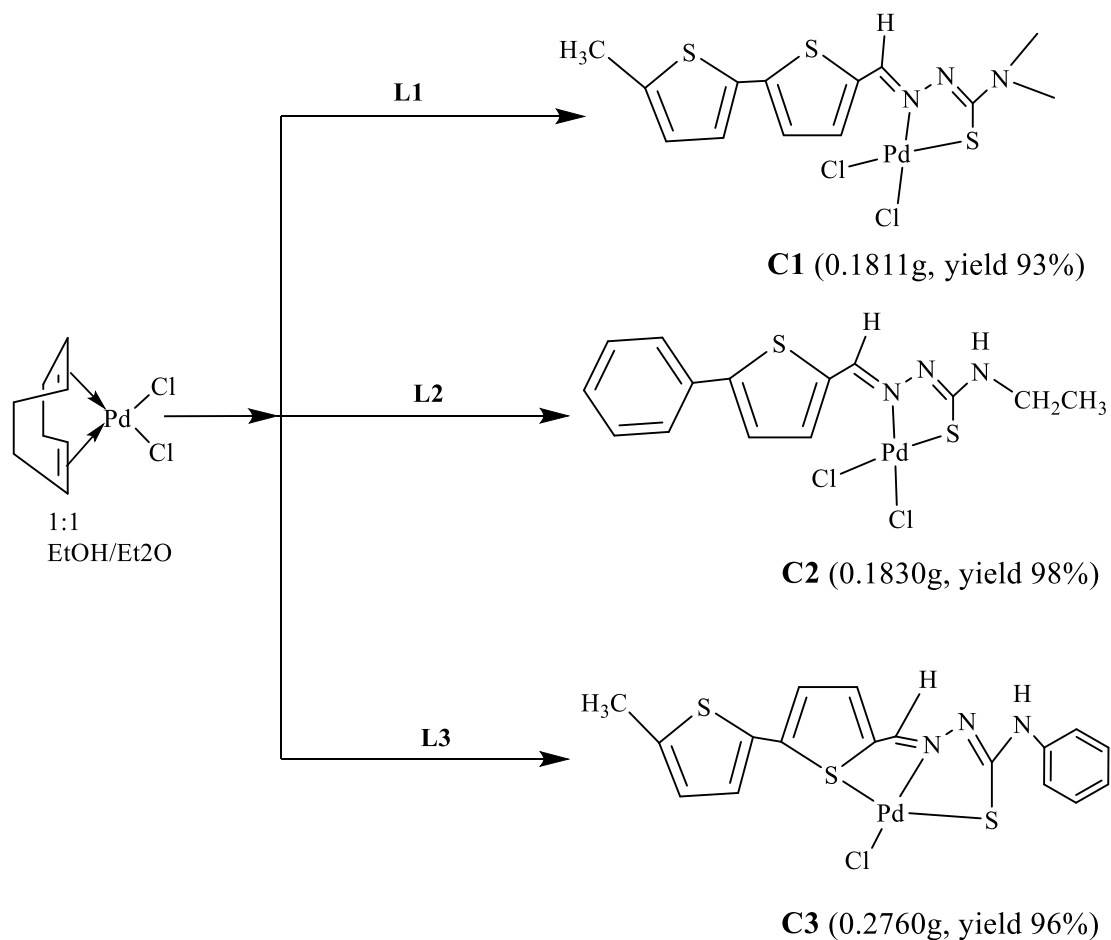


Figure 4.9: FTIR spectra of Pd(cod)Cl₂ from the authentic source.

Pd(cod)Cl₂ of 0.4009mmol was reacted with equimolar solutions of ligands **L1**, **L2** and **L3** in Schlenk tube for 24 hours at room temperature (Motswainyana *et al.*, 2012). The Scheme 4.1 for reaction is shown below for preparation of complex **C2**. Complexes **C1** and **C3** all prepared using the same procedure.



Scheme 4.2: Synthesis of the complexes

The complexes were all powder with high yields and orange in color. The orange color was observed immediately after solutions of the ligands in DCM were added to the suspension of Pd(cod)Cl₂ in DCM/Et₂O. They were soluble in DMSO and DMF. They were all characterized using UV-Vis, NMR, elemental analysis and FT-IR.

4.9 Physical properties for complex C1

Complex **C1** was an orange solid with a melting point of 271-273 °C. It was soluble in DMSO and DMF. No change on ¹H NMR spectra over 72 hours when the complex was subjected to stability test, conclusion that the ligand was stable in DMSO within 72 hours hence was subjected to anticancer investigation.

4.10 Characterization and structural confirmation of complex C1

Fourier Transform infrared spectroscopy studies were carried out using KBr pellets to confirm successful coordination of ligand **L1** to palladium metal. Significant change in C=N, N-H and C=S stretching frequencies were observed. Imine band for complex **C1** was observed 1517 cm^{-1} . This bathochromic from 1543 cm^{-1} of free ligand to 1517 cm^{-1} after coordination indicated the **L1** coordinated to Pd(II) metal via azomethine-nitrogen bathochromic shift was also witnessed in thiocarbonyl bond from 924 cm^{-1} of free ligand to 908 cm^{-1} of complex. This suggests that the ligand coordinated to the metal via thiocarbonyl sulfur as well. Decrease in bond frequency with the disappearance of N-H peak suggested that the ligand coordinated to the metal in thiolate form after deprotonation of N-H proton. Similar observations were made by (Prabhu&Ramesh, 2013). FTIR spectrum for **C1** is shown in Figure 4.10 below.

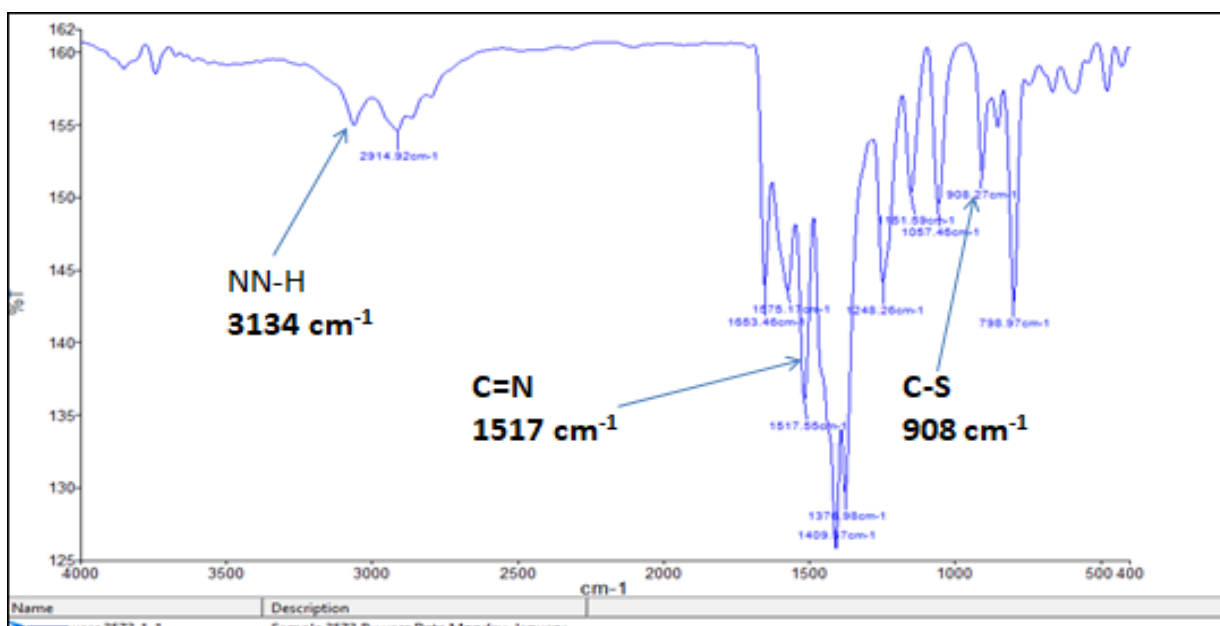


Figure 4.10: FTIR spectra for complex C1

UV-Vis for complexes **C1** was conducted in DMSO as a solvent at room temperature using 1cm quartz micro-cuvettes. The UV-Vis was scanned at a range of 200-800 nm. Complexes **C1** displayed one absorption band at 427 nm as shown in Figure 4.11. The absorption bands were due to ligand to metal charge transfer (LMCT), a confirmation of coordination through S→M

bond. The absorption energy is higher than that of free ligand due to the presence of metal's nuclear charge that draws electrons density from π system reducing the π - π^* energy gap for UV – Vis absorption energy (Dkharr *et al.*, 2020).

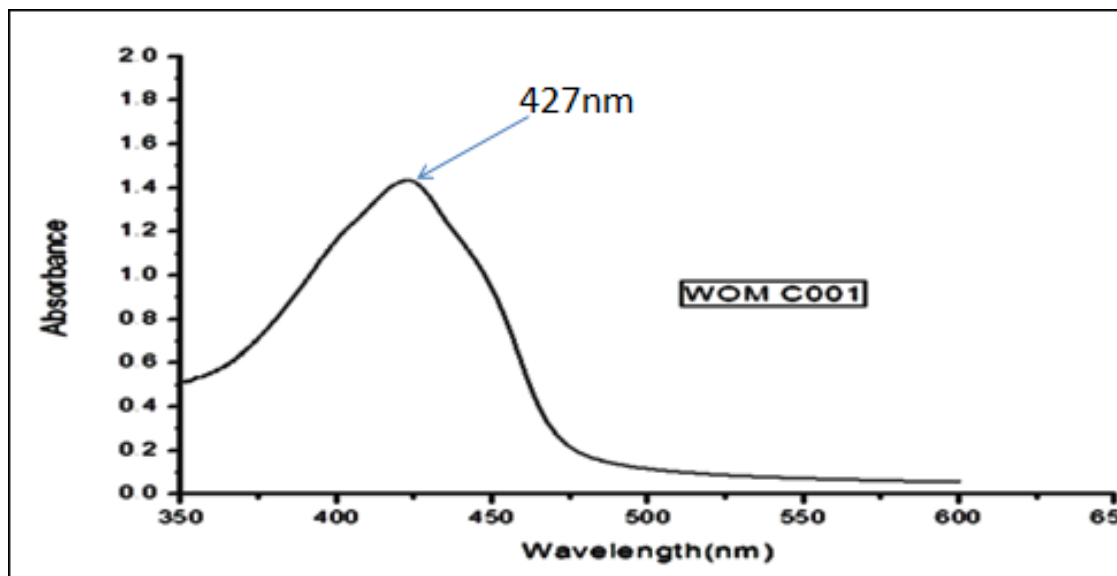


Figure 4.11: UV-Vis spectrum for complex C1

^1H NMR study of the complex was done to confirm their successful synthesis. The studies were compared with their respective ligands to establish any change in regard to chemical shift positions of the protons. NMR for prepared complex **C1** was done using deuterated dimethyl sulfoxide (DMSO-d_6) solvent at room temperature. Tetramethyl silane (TMS) was used as internal standard. Downfield shift was witnessed in aminic proton from δ 8.38ppm of free ligand **L1** to 8.53 ppm suggesting that the ligand coordinated via azomethine nitrogen. Downfield chemical shift is due to donation of π -electrons from azomethine to empty d -orbitals of the metal hence deshielding azomethine proton. N-H proton peak was conspicuously missing in complex **C1** NMR spectrum suggesting possible deprotonation hence the ligand coordinated in thiol form. Similar observation is also reported by (Haribabu *et al.*, 2020). Figure 4.12 shows ^1H NMR spectrum for **C1**.

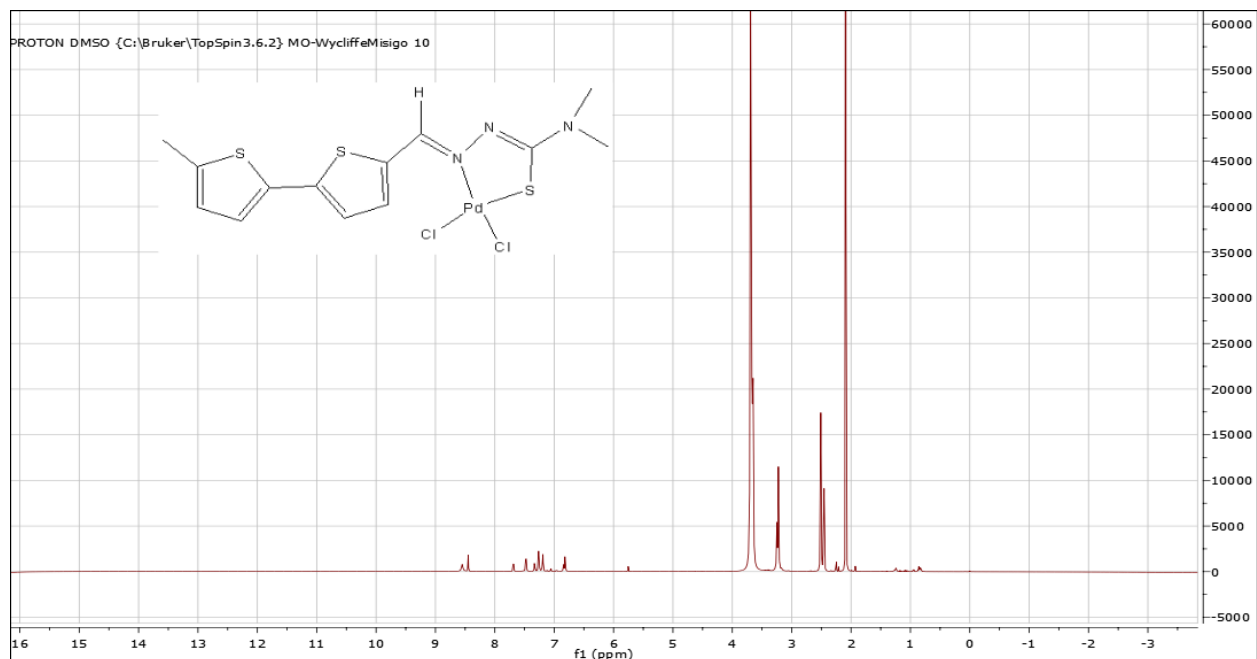
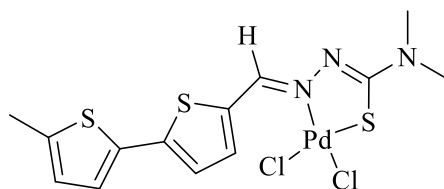


Figure 4.12: ^1H NMR spectrum for complex C1

C, H, N and S elemental analysis was conducted to ascertain the structure and purity of complex **C1**. There was very little discrepancy between the % weight of element observed and the calculated: Elemental analysis observed Elemental analysis observed; N, 8.50, C, 30.66; H, 2.93; S, 15.96; Calculated; N, 8.65; C, 32.14; H, 2.91; S, 19.80. Elemental analysis result also suggested that the ligand coordinated to the metal in a bidentate fashion.



C1

4.11 Physical properties for complex C2

Complex **C2** was an orange solid with a melting point of 260-263 °C. It was soluble in DMSO and DMF. No change on ^1H NMR spectra over 72 hours when the complex was subjected to stability test, conclusion that the ligand was stable in DMSO within 72 hours hence was subjected to anticancer investigation.

4.12 Characterization and structural confirmation of complex C2

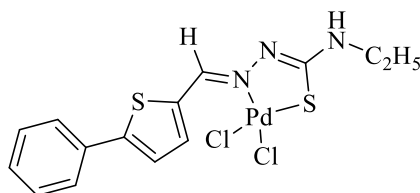
The FTIR stretching frequencies in **C2** was compared to the free ligand **L2** to establish how the ligand coordinated to palladium(II) metal. Hypsochromic shift was witnessed in azomethine stretching frequency from 1534 cm^{-1} of free ligand **L2** to 1581 cm^{-1} of **C2**. Stretching frequency of thiocarbonyl also decreased from 1087 cm^{-1} of free ligand to 1066 cm^{-1} of the complex. These indicate that ligand **L2** coordinated to the metal in N,S fashion. Thioamide N-H stretching peak missing in the FTIR spectra for the complex suggesting that **L2** coordinated to the metal in thiolate form after deprotonation. Similar results have been reported in literature by (Mbugua *et al.*, 2020; Muralisankar *et al.*, 2017;Rebolledo *et al.*, 2005). FTIR spectrum for complex **C2** is available in the appendices section.

Complex **C2** displayed one absorption peak 448nm in UV-Vis. This was as a result of ligand to metal charge transfer, a confirmation of coordination through thiocarbonyl sulfur ($\text{S}\rightarrow\text{M}$). The absorption energy is higher than that of free ligand due to the presence of metal's nuclear charge that draws electrons density from π system reducing the $\pi\text{-}\pi^*$ energy gap. The absorption bands were due to ligand to metal charge transfer (LMCT) as suggested in the literature by Dkhar r *et al.* (2020). UV-Vis spectrum for complex **C2** is available in the appendices section.

^1H NMR studies for the complex was done using deuterated DMSO (DMSO-d_6) at room temperature. Chemical shifts of protons of interest were compared with those of free ligand **L2** to confirm the mode of coordination. Downfield shift was witnessed in azomethine proton from $\delta 8.38\text{ppm}$ of free ligand **L2** to 8.49ppm in **C2** suggesting that coordination took place via azomethine N. According to Al- Fregi, (2015), the downfield shift is as a result to donation of π electrons from azomethine group to the metal's d -orbital. This transfer of electron electrons reduces the electron density of azomethine hence de-shielding azomethine proton. Thioamide N-H proton peak was missing in **C2** ^1H NMR peak suggesting possible deprotonation hence **L2** coordinated to the metal in thiolate form. Similar observation made by (Haribabu, Srividya, *et al.*, 2020). ^1H NMR NMR spectrum for **C2** is available in the appendices section.

C, H, N, S elemental analysis was carried out on **C2** to confirm the structure and purity. There was acceptable difference between the observed % weight values and calculated. Elemental analysis observed; N, 9.45; C, 39.67; H, 3.33; S, 12.18; Calculated; N, 9.02; C, 38.11; H, 3.03; S,

13.77. The elemental analysis results suggested that ligand coordinated to the metal in a bidentate fashion.



C2

4.13 Physical properties for complex C3

Complex **C3** was an orange solid with a melting point of 278-281°C. It was soluble in DMSO and DMF. No change on ^1H NMR spectra over 72 hours when the complex was subjected to stability test, conclusion that the ligand was stable in DMSO within 72 hours hence was subjected to anticancer investigation.

4.14 Characterization and structural confirmation of complex C3

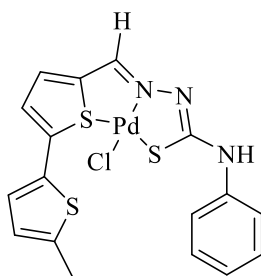
The FTIR frequency shift positions for **C3** were compared to those of free ligand **L3** ascertain successful complexation. Notable changes were observed in azomethine (C=N), thiocarbonyl (C=S) and azomethine frequencies. Bathochromic shift was noted in azomethine stretching frequency from 1579 cm^{-1} of free ligand to 1557 cm^{-1} of **C3** suggesting that coordination took place via azomethine-N. Bathochromic shift could to decrease HOMO→LUMO energy gap caused by the presence of the Pd (II) metal. Thiocarbonyl frequency shifted from 997 cm^{-1} of free ligand to 910 cm^{-1} . Disappearance of C=S band suggested coordination took place via thiocarbonyl S. Absence of thioamide N-H band in **C3** FTIR spectrum is a clear indication that **L3** coordinated to the metal in thiolate form after deprotonation. FTIR data indicates that the **L3** coordinated to Pd(II) in N,S fashion. Similar observations were made by (Arancibia *et al.*, 2015). FTIR spectrum for **C3** is available in the appendices section.

UV-Vis spectra of **C3** showed two absorption peaks at 312 nm and 425 nm. 312 nm was due to $\pi \rightarrow \pi^*$ while 425 nm due to ligand to metal charge transfer (LMCT) transitions with a λ_{max} maximum observed at 425 nm. LMCT transition is a confirmation of coordination through thiocarbonyl sulfur (S→M). The presence of the metal reduced the HOMO-LUMO energy gap

for transition of π -electrons hence increase in $\pi \rightarrow \pi^*$ transitions wavelength from 307 nm (**L3**) to 312 nm (**C3**). The observations were verified in literature according to (Bakir *et al.*, 2017).

^1H for complex **C3** was done using deuterated DMSO (DMSO-d_6). Tetramethyl silane (TMS) was used as internal standard. ^1H NMR was carried out at room temperature chemical shift positions of azomethine and thioamide protons were compared to those of free ligand **L3**. Azomethine proton was deshielded after complex formation resulting to a downfield shift from 9.70 ppm of **L3** to 9.82 ppm of **C3**. This suggests that coordination took place via imine-N. The donation of pi-electrons from the Schiff base deshielded the proton reduces the electron density around azomethine proton hence downfield shift. Disappearance of thioamide N-H proton peak after coordination in all the complexes was observed suggesting that the ligand coordinated with palladium metal in a monobasic manner after enolization process. The ^1H NMR data also proves that the ligand coordinated to the metal in N,S fashion. Similar observations were made by (Nyawade *et al.*, 2020). ^1H NMR spectrum for **C3** is available in the appendices section.

C, H, N and S elemental analysis studies were conducted to ascertain the structure and the purity of complex **C3**. The % mass observed had acceptable variations from calculated. Elemental analysis observed was N, 8.09; C, 40.68; H, 2.90; S, 17.40 %; while calculated; N, 8.07; C, 40.89; H, 2.83; S, 19.26 %. The data suggests that the complex was pure. From the data it was deduced that the ligand coordinated to the metal in a tridentate fashion. Thiophene-S donated π -electrons from the aromatic system displacing one chloro from the metal. Similar observations were made by (Nyawade *et al.*, 2021).



C3

4.15 Cytotoxicity studies

Anticancer activities of both the ligands and the corresponding palladium(II) complexes were screened against human Caco-2 (colorectal adenocarcinoma), HeLa (cervical), HT-29 (colon) and KMST (non-cancer) cell lines. *Cisplatin* was used as a positive control in the cytotoxicity studies to induce cell mortality. These cell lines were treated with range of concentrations of each compound (6.25, 12.5, 25, 50, 100 $\mu\text{g/mL}$) for a period of 24 hours. The viability of the cells was then examined via MTT assay and expressed as % cell viability. The degree of cytotoxicity of the compounds varied with the concentrations and type of the cell line. In many instances the compounds were more active at a concentration of 100 $\mu\text{g/mL}$.

All the cell lines showed high susceptibility to ligand **L1** compared to all the other compounds including *cisplatin*. Ligands **L2** and **L3** demonstrated low degree of toxicity to all cell lines since the viability of the cells were >47 in all the concentrations as shown in figure **14**. Anticancer activities of the ligands were enhanced after complexing with palladium(II). The complexes displayed higher toxicity compared to their respective ligands except for **L1** whose activity was higher than that of **C1**. The positive charge on the central metal increases the acidity of the coordinated ligand protons leading to formation of strong hydrogen bonds with DNA, preventing further replication. (El-Tabl *et al.*, 2015). For instance, **L1** vs **C1** in cell line were HeLa (0 vs 23%), Caco-2 (2 vs 13%), HT-29 (0 vs 23%) and KMST (12.4 vs 57%) at 100 $\mu\text{g/mL}$ concentrations as shown in figure 4.13.

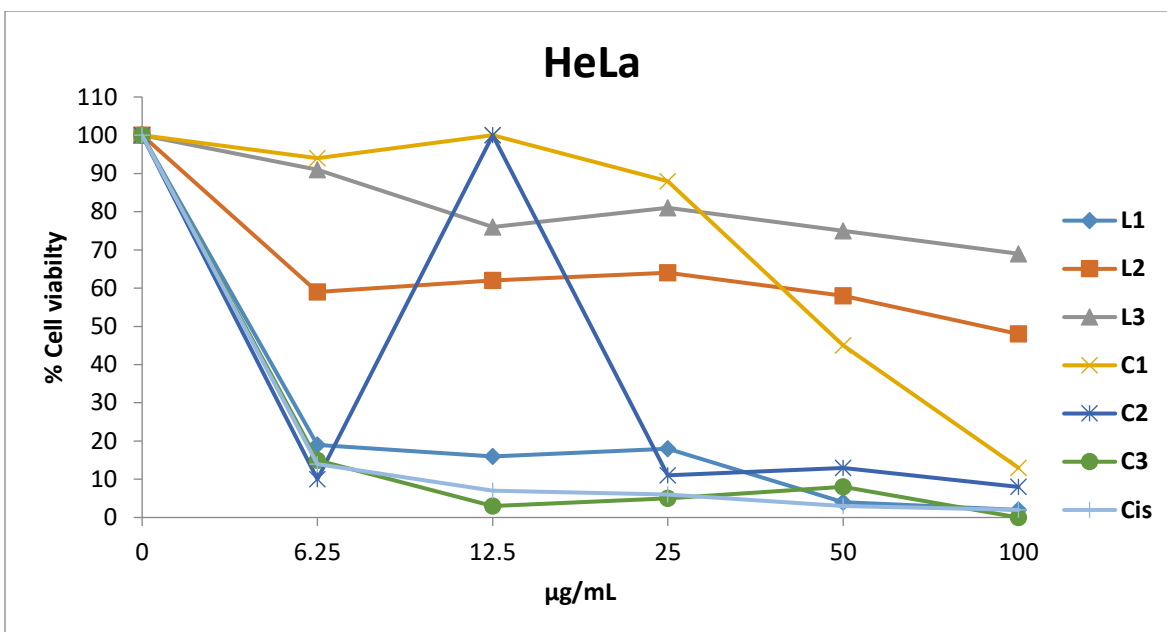


Figure 4.13: Viability of HeLa cell line to compounds

The complexes exhibited relatively high mortality in all the cell lines in comparison with *cisplatin*. **C3** showed impressive selectivity features since it was highly lethal to cancer cell lines and less lethal to non-cancer KMST cells ($IC_{50} > 100 \mu\text{g/mL}$). **C1** and **C2** were lethal to all cancer cell lines including KMST at $100 \mu\text{g/mL}$ as shown in Figure 4.14.

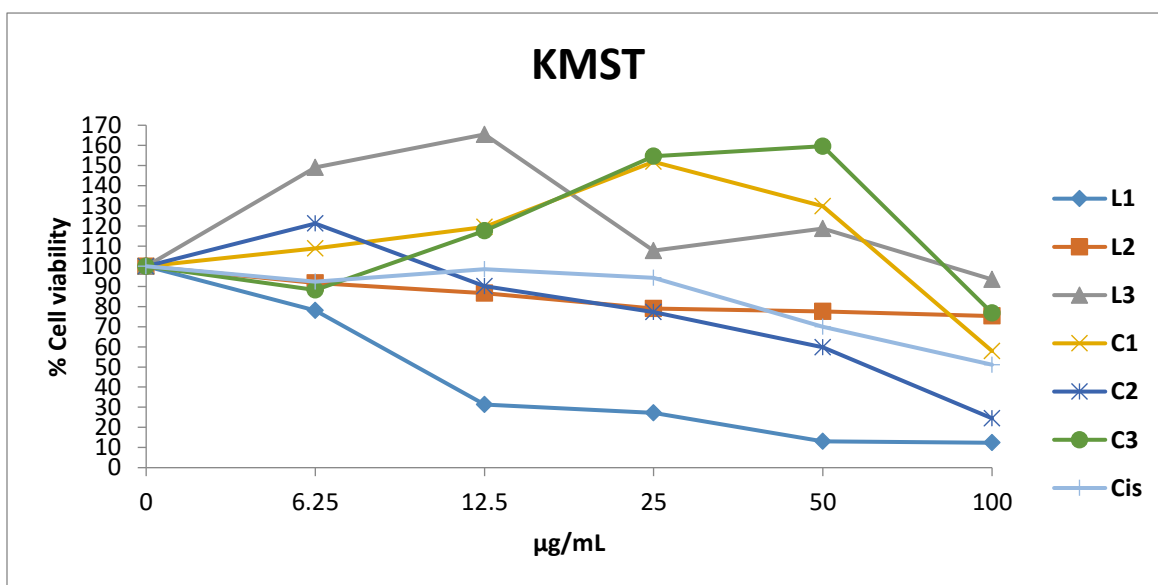


Figure 4.14: Response of KMST cell line to treatment

Colon cancer cells (HT-29) and colorectal adenocarcinoma cells (Caco-2) demonstrated high level of susceptibility to **C2** at 100 $\mu\text{g}/\text{mL}$ concentration than all the other compounds as shown in Figures 4.15 and 4.16 respectively. At 100 $\mu\text{g}/\text{mL}$, the viability of HT-29 cells was 8.8% while its corresponding ligand **L2** with the highest viability of 63.8%. High level of susceptibility was also witnessed in Caco-2 with cell viability of 16.1% and 75.1 upon treatment with 100 $\mu\text{g}/\text{mL}$ of **C2** and **L2** respectively.

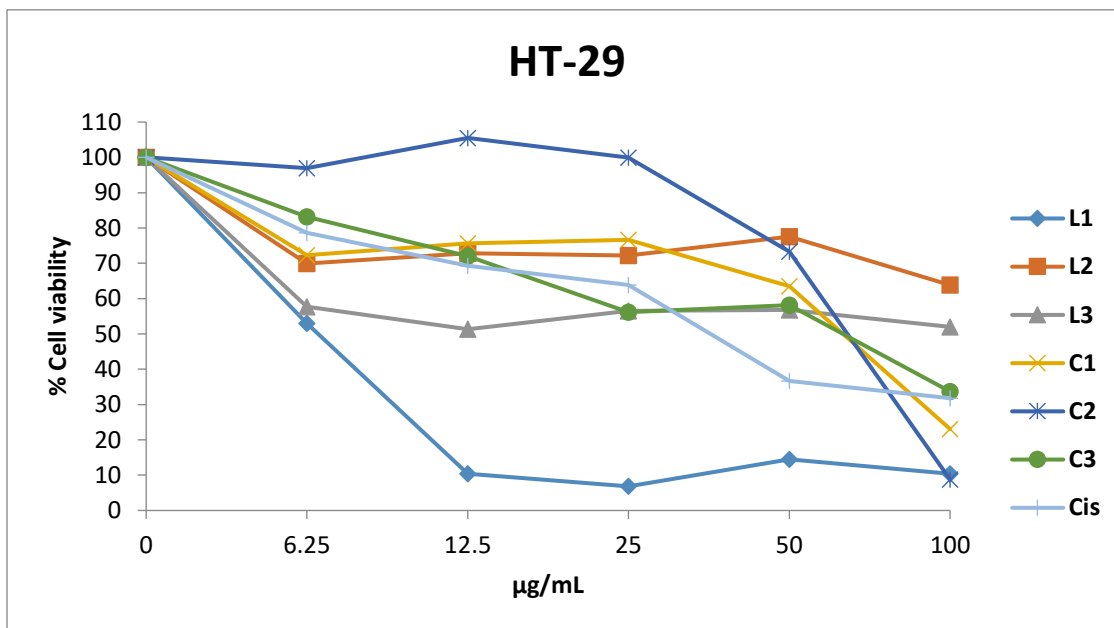


Figure 4.2: Response of colon cancer (HT-29) upon treatment

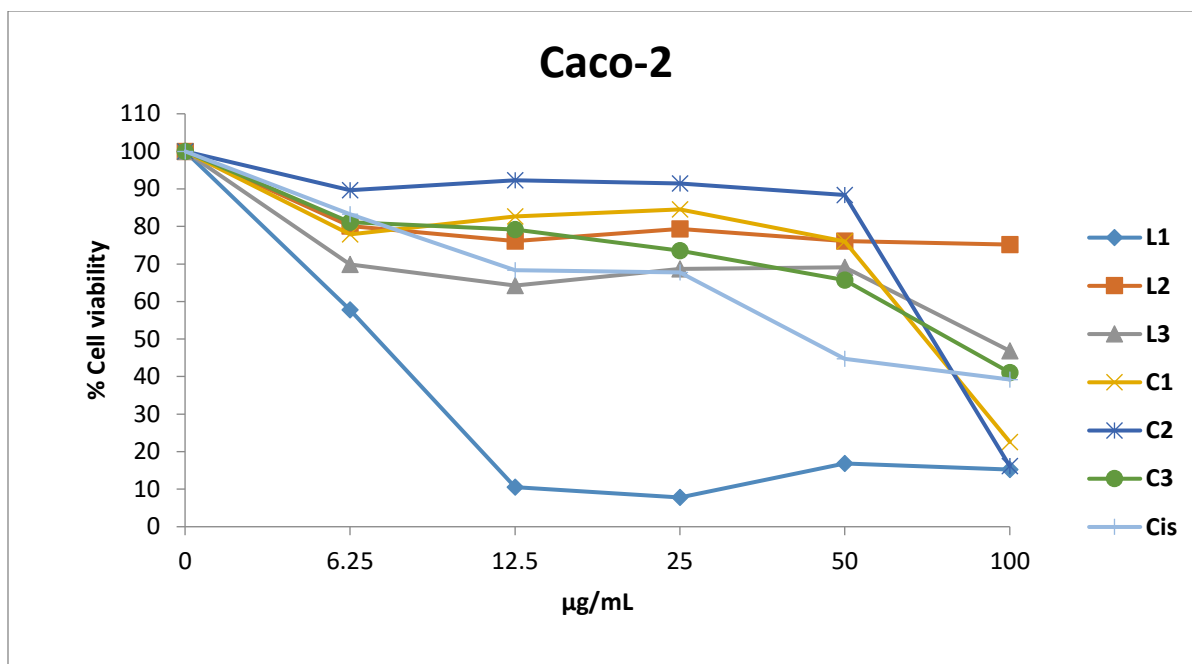


Figure 4.16: Response of Caco-2 upon treatment

50% cell proliferation inhibition concentration (IC_{50}) of all the compounds were estimated using Graph Pad prism version 5 software. IC_{50} of all the compounds are shown in Table 4.4.

Table 4.2: IC_{50} values ($\mu\text{g/mL}$) of compounds

	Caco-2	HT-29	HeLa	KMST
L1	6.814	6.449	0.2619	10.79
L2	>100	>100	0.10	>100
L3	>100	>100	>100	>100
C1	66.67	54.26	47.56	>100
C2	73.06	61.6	59.52	57
C3	84.32	49.1	0.73	>100
<i>Cisplatin</i>	48.83	35.5	0.11	100

The values revealed that more than 100µg/mL of **L3** was required to inhibit 50% cell proliferation of in all the cells. **L2** in all the cells except for HeLa cells whose IC₅₀ was estimated to be 0.10 µg/mL. **L1** showed high inhibition of cell proliferation in all the cells in the order of KMST < Caco-2 < HT-29 < HeLa.

HeLa cells displayed relatively high susceptibility upon treatment with all the prepared complexes in the order of **C3** > **C1** > **C2** with IC₅₀ of 0.73, 47.56 and 59.52 µg/mL respectively. All the complexes had selective cytotoxicity except for **L1** and **C2** which were had an effect on KMST cell line. It was noted the absence or the presence of one of the coordinated chlorides in tridentate and bidentate complex might or might have not had an influence on the cytotoxicity of complexes. **C1** and **C2** had two chloro ligands while **C3** had one chloro. **C3** had good inhibition and also selective (from IC₅₀ values) than **C2**, **C3** and *cisplatin*. Cell viability of KMST was 76.8% when treated with C3 and 51.1% when treated with *cisplatin* at 100 µg/mL. This further confirms **C3** was more selective than *cisplatin*. The difference in the inhibitory activities in **C1** and **C2** can be associated with the number of sulfur atoms in the compounds since **C1** has three sulfur atoms while **C2** has two (Sobiesiak *et al.*, 2014).

CHAPTER FIVE

CONCLUSION AND RECOMMENDATIONS

5.0 Conclusion

Research objectives of this work were met. A total of three new thiosemicarbazone ligands were synthesized. Structural confirmation of ligands was achieved using ^1H and ^{13}C NMR, UV-Vis, FTIR, single x-ray crystallography and elemental analysis. Infrared spectroscopy for ligands showed expected vibration peaks for N-H ($2900\text{-}3300\text{ cm}^{-1}$), C=S ($900\text{-}1100\text{ cm}^{-1}$) and C=N ($1500\text{-}1590\text{ cm}^{-1}$). 1D and 2D NMR were used to confirm the chemical shift position of carbons and protons and C-H correlation as well. Single x-ray crystallography confirmed that ligand **L2** had E conformation in thione form. Elemental analysis further confirmed the purity of synthesized ligands since there was minimum discrepancy between calculated and observed % weight values.

Palladium(II) complexes of ligands **L1**, **L2** and **L3** were successfully synthesized under inert nitrogen atmosphere. Complexes were characterized by FTIR confirming successful coordination of ligands to palladium(II) metal through the bathochromic and hypsochromic shifts of N-H and C=N, confirming coordination took place through azomethine-N and thiocarbonyl-S. Absence of thioamide N-H vibration band was a clear indication of coordination after deprotonation in thiolate form. UV-Vis results showed successful coordination of ligands to metal by displaying ligand to metal charge transfer transition (LMCT) around 400nm. The ^1H and ^{13}C NMR data were used to confirm structure of ligands and coordination of ligands to metals. Downfield chemical shift of azomethine proton after coordination indicated successful bonding to metal. Disappearance of thioamide N-H proton in ^1H NMR spectra confirmed that the ligand coordinated in thiolate tautomer. Molecular structure of **L2** was confirmed by single-crystal X-ray crystallography which showed that the ligand had *E* conformation. The synthesized ligands were did not dissolve in water and alcoholic organic solvents Pd(II) complexes with bulky ligands were stabile during their biological application.. Data from elemental analysis confirmed that complexes were pure. The data was also used to established that ligands **L1** and

L2 coordinated to palladium metal in a bidentate fashion, (N S fashion) while **L3** coordinated in a SNS tridentate fashion.

Other than **L1** and inhibition of **L2** in HeLa cells ($IC_{50}=0.1\mu\text{g/mL}$), the ligands did not inhibit the cells compared to their corresponding complexes. Caco-2 cell lines displayed high inhibition to the compounds except **L1** (based on IC_{50} values). All the cell lines showed high susceptibility to **L1** than any other prepared compound. However **L1** was not selective since it inhibited the growth of KMST cells. *Cisplatin* and **C1** had had best anticancer activities but with poor selectivity. **C3** was selective compared to *cisplatin*. KMST cell viabilities were 76.8% and 51.1% upon treatment with *cisplatin* and **C3** ($100\mu\text{g/mL}$). Activity of **C3** is associated bulky bithiophene and phenyl rings attached on the ligand. The IC_{50} values also confirm that **C3** was selective compared to *cisplatin* and other complexes.

5.1 Recommendations

Thiosemicarbazone ligands and their respective palladium(II) complexes were successfully synthesized and characterized using analytical and spectroscopic techniques. Their anticancer activities were determined in four cell lines. However, the following recommendations were made:

- 1) More research should be carried out on other Platinum Group Metals (PGM) complexes of the newly synthesized ligands. Their biological activities especially anticancer activities should be carried out.
- 2) Anticancer activities of the prepared novel ligands and their palladium (II) complexes should be investigated on other cancer cell lines.
- 3) Further research on *in vivo* activities should be conducted on the synthesized ligands and complexes.

REFERENCES

- Abu-Surrah, A. S., Al-Sa'doni, H. H., & Abdalla, M.Y. (2008). Palladium-based chemotherapeutic agents: routes toward complexes with good antitumor activity. *Cancer therapy*, 6, 1-10.
- Adegoke, A. V., Aliyu, D. H., Akefe, I. O., & Nyan, S. E. (2019). A Review on the Metal Complex of Nickel (II) Salicylhydroxamic Acid and its Aniline Adduct. *J Transl Sci Res*, 2(006) 1435-1447.
- Al-Fregi, A. A. (2015). Synthesis, Characterization And Molar Conductivity Study Of Some New Palladium (II) And Platinum (II) Complexes Containing Heterocyclic Tellurium-Dicarboxylato Ligands. *Int. J*, 3, 637-647.
- Ali, A. Q., Teoh, S. G., Eltayeb, N. E., Khadeer Ahamed, M. B., Abdul Majid, A. M. S., & Almutaleb, A. A. (2017). Synthesis, structure and in vitro anticancer, DNA binding and cleavage activity of palladium (II) complexes based on isatin thiosemicarbazone derivatives. *Applied Organometallic Chemistry*, 31(12), 3813-3823.
- Arafa, W. A., & Badry, M. G. (2016). Facile synthesis of bis-thiosemicarbazone derivatives as key precursors for the preparation of functionalised bis-thiazoles. *Journal of Chemical Research*, 40(7), 385-392.
- Arancibia, R., Quintana, C., Biot, C., Medina, M. E., Carrere-Kremer, S., Kremer, L., & Klahn, A. H. (2015). Palladium (II) and platinum (II) complexes containing organometallic thiosemicarbazone ligands: Synthesis, characterization, X-ray structures and antitubercular evaluation. *Inorganic Chemistry Communications*, 55, 139-142.
- Arshia, Fayyaz, S., Shaikh, M., Khan, K. M., & Choudhary, M. I. (2021). Anti-glycemic potential of benzophenone thio/semicarbazone derivatives: synthesis, enzyme inhibition and ligand docking studies. *Journal of Biomolecular Structure and Dynamics*, 40 (22) 1-12.
- Ashok, V., Yadav, A., & Naik, V. K. (2019). Fault Detection and Classification of Multi-location and Evolving Faults in Double-Circuit Transmission Line Using ANN. In *Soft Computing in Data Analytics* (pp. 307-317). Springer, Singapore.

- Atieno, O. M., Opanga, S., Martin, A., Kurdi, A., & Godman, B. (2018). Pilot study assessing the direct medical cost of treating patients with cancer in Kenya; findings and implications for the future. *Journal of medical economics*, 21(9), 878-887.
- Bakir, M., Lawrence, M. A., Ferhat, M., & Conry, R. R. (2017). Spectroscopic, electrochemical and X-ray crystallographic properties of a novel palladium (II) complex of thioamide deprotonated di-2-pyridyl ketone thiosemicarbazone (dpktsc-H)⁻. *Journal of Coordination Chemistry*, 70(17), 3048-3064.
- Bal, T. R., Anand, B., Yogeeswari, P., & Sriram, D. (2005). Synthesis and evaluation of anti-HIV activity of isatin β -thiosemicarbazone derivatives. *Bioorganic & medicinal chemistry letters*, 15(20), 4451-4455.
- Bansod, B., Kumar, T., Thakur, R., Rana, S., & Singh, I. (2017). A review on various electrochemical techniques for heavy metal ions detection with different sensing platforms. *Biosensors and Bioelectronics*, 94, 443-455.
- Baruah, J., Gogoi, R., Gogoi, N., & Borah, G. (2017). A thiosemicarbazone–palladium (II)–imidazole complex as an efficient pre-catalyst for Suzuki–Miyaura cross-coupling reactions at room temperature in aqueous media. *Transition Metal Chemistry*, 42(8), 683-692.
- Bayram, E., Zahmakıran, M., Ozkar, S., & Finke, R. G. (2010). In situ formed “weakly ligated/labile ligand” iridium (0) nanoparticles and aggregates as catalysts for the complete hydrogenation of neat benzene at room temperature and mild pressures. *Langmuir*, 26(14), 12455-12464.
- Benoit, S. L., Schmalstig, A. A., Glushka, J., Maier, S. E., Edison, A. S., & Maier, R. J. (2019). Nickel chelation therapy as an approach to combat multi-drug resistant enteric pathogens. *Scientific reports*, 9(1), 1-10.
- Berhanu, A. L., Mohiuddin, I., Malik, A. K., Aulakh, J. S., Kumar, V., & Kim, K. H. (2019). A review of the applications of Schiff bases as optical chemical sensors. *TrAC Trends in Analytical Chemistry*, 116, 74-91.

- Bermejo, A., Ros, A., Fernández, R., & Lassaletta, J. M. (2008). C 2-Symmetric Bis-Hydrazones as Ligands in the Asymmetric Suzuki– Miyaura Cross-Coupling. *Journal of the American Chemical Society*, 130(47), 15798-15799.
- Bielefeld, E. C., Tanaka, C., Coling, D., Li, M., Henderson, D., & Fetoni, A. R. (2013). An Src-protein tyrosine kinase inhibitor to reduce *cisplatin* ototoxicity while preserving its antitumor effect. *Anti-cancer drugs*, 24(1), 43-51.
- Bormio Nunes, J. H., Hager, S., Mathuber, M., Pósa, V., Roller, A., Enyedy, E. A., ...& Kowol, C. R. (2020). Cancer Cell Resistance Against the Clinically Investigated Thiosemicarbazone COTI-2 Is Based on Formation of Intracellular Copper Complex Glutathione Adducts and ABCC1-Mediated Efflux. *Journal of medicinal chemistry*, 63, 13719–13732
- Bray, F., Ferlay, J., Soerjomataram, I., Siegel, R. L., Torre, L. A., & Jemal, A. (2018). Global cancer statistics 2018: GLOBOCAN estimates of incidence and mortality worldwide for 36 cancers in 185 countries. *CA: a cancer journal for clinicians*, 68(6), 394-424.
- Brigger, I., Dubernet, C., & Couvreur, P. (2012). Nanoparticles in cancer therapy and diagnosis. *Advanced drug delivery reviews*, 64, 24-36.
- Britz, A., Gawelda, W., Assefa, T. A., Jamula, L. L., Yarranton, J. T., Galler, A., ...& March, A. M. (2019). Using ultrafast X-ray spectroscopy to address questions in ligand-field theory: The excited state spin and structure of [Fe (dcpp) 2] 2+. *Inorganic chemistry*, 58 (14), 9341-9350.
- Buldurun, K. (2020). Synthesis, Characterization, Thermal Study and Optical Property Evaluation of Co (II), Pd (II) Complexes Containing Schiff Bases of Thiophene-3-Carboxylate Ligand. *Journal of Electronic Materials*, 49(3), 1935-1943.
- Buldurun, K., Turan, N., Bursal, E., Aras, A., Mantarcı, A., Çolak, N., ...& Gülçin, İ. (2020). Synthesis, characterization, powder X-ray diffraction analysis, thermal stability, antioxidant properties and enzyme inhibitions of M (II)-Schiff base ligand complexes. *Journal of Biomolecular Structure and Dynamics*, 102, 1-8.

- Che, C. M., & Siu, F. M. (2010). Metal complexes in medicine with a focus on enzyme inhibition. *Current opinion in chemical biology*, *14*(2), 255-261.
- Cowley, A. R., Dilworth, J. R., Donnelly, P. S., Labisbal, E., & Sousa, A. (2002). An unusual dimeric structure of a Cu (I) bis (thiosemicarbazone) complex: implications for the mechanism of hypoxic selectivity of the Cu (II) derivatives. *Journal of the American Chemical Society*, *124*(19), 5270-5271.
- de Oliveira, J. F., da Silva, A. L., Vendramini-Costa, D. B., da Cruz Amorim, C. A., Campos, J. F., Ribeiro, A. G., ... & de Lima, M. D. C. A. (2015). Synthesis of thiophene-thiosemicarbazone derivatives and evaluation of their in vitro and in vivo antitumor activities. *European journal of medicinal chemistry*, *104*, 148-156.
- Dkhar, L., Banothu, V., Poluri, K. M., Kaminsky, W., & Kollipara, M. R. (2020). Platinum group complexes containing salicylaldehyde based thiosemicarbazone ligands: Their synthesis, characterization, bonding modes, antibacterial and antioxidant studies. *Journal of Organometallic Chemistry*, 121298.
- Dutta, S., Biswas, P., Flörke, U., & Nag, K. (2010). Structure, stereochemistry, and physico-chemical properties of trinuclear and dinuclear metal (II) complexes of a phenol-based tetrapodal Schiff base ligand. *Inorganic chemistry*, *49*(16), 7382-7400.
- Egbert, J. D., Cazin, C. S., & Nolan, S. P. (2013). Copper N-heterocyclic carbene complexes in catalysis. *Catalysis Science & Technology*, *3*(4), 912-926.
- El-Atawy, M. A., Omar, A. Z., Hagar, M., & Shashira, E. M. (2019). Transalkylation reaction: green, catalyst-free synthesis of thiosemicarbazones and solving the NMR conflict between their acyclic structure and intramolecular cycloaddition products. *Green Chemistry Letters and Reviews*, *12*(3), 364-376.
- El-Sawaf, A. K., El-Essawy, F., Nassar, A. A., & El-Samanody, E. S. A. (2018). Synthesis, spectral, thermal and antimicrobial studies on cobalt (II), nickel (II), copper (II), zinc (II) and palladium (II) complexes containing thiosemicarbazone ligand. *Journal of Molecular Structure*, *1157*, 381-394.

- El-Tabl, A. S., Mohamed Abd El-Waheed, M., Wahba, M. A., & Abou El-Fadl, A. E. H. (2015). Synthesis, characterization, and anticancer activity of new metal complexes derived from 2-hydroxy-3-(hydroxyimino)-4-oxopentan-2-ylidene benzohydrazide. *Bioinorganic chemistry and applications*, 2015(43), 1458-1473.
- Enyedy, É. A., May, N. V., Pape, V. F., Heffeter, P., Szakács, G., Keppler, B. K., & Kowol, C. R. (2020). Complex formation and cytotoxicity of Triapine derivatives: a comparative solution study on the effect of the chalcogen atom and NH-methylation. *Dalton Transactions*.
- Fabra, D., Matesanz, A. I., Herrero, J. M., Alvarez, C., Balsa, L. M., Leon, I. E., & Quiroga, A. G. (2021). Two different thiosemicarbazone tauto-conformers coordinate to Palladium (II). Stability and biological studies of the final complexes. *European Journal of Inorganic Chemistry*, 2021(11), 1041-1049.
- Favoriti, P., Carbone, G., Greco, M., Pirozzi, F., Pirozzi, R. E. M., & Corcione, F. (2016). Worldwide burden of colorectal cancer: a review. *Updates in surgery*, 68(1), 7-11.
- Florea, A. M., & Büsselberg, D. (2011). Cisplatin as an anti-tumor drug: cellular mechanisms of activity, drug resistance and induced side effects. *Cancers*, 3(1), 1351-1371.
- Garg, R., Kumari, A., Joshi, S. C., & Fahmi, N. (2013). Manganese (II) and Dioxomolybdenum (VI) Complexes with Monobasic Bidentate Schiff Bases: Synthesis, Characterization and Biological Investigation. *Bulletin of the Korean Chemical Society*, 34(8), 2381-2386.
- Ghani, N. T. A., & Mansour, A. M. (2012). Novel palladium (II) and platinum (II) complexes with 1H-benzimidazol-2-ylmethyl-N-(4-bromo-phenyl)-amine: Structural studies and anticancer activity. *European journal of medicinal chemistry*, 47, 399-411.
- Gillet, J. P., & Gottesman, M. M. (2010). Mechanisms of multidrug resistance in cancer. In *Multi-drug resistance in cancer* (Vol. 22, pp. 47-76). Humana Press.
- Gogoi, B. K., & Bezbaruah, R. L. (2002). Microbial degradation of sulfur compounds present in coal and petroleum. In *Progress in Industrial Microbiology* (Vol. 36, pp. 427-456). Elsevier.

- Gupta, I. K., & Sutar, A. K. (2008). Catalytic activities of Schiff base transition metal complexes. *Coordination Chemistry Reviews*, 252(12-14), 1420-1450.
- Guven, A., Rusakova, I. A., Lewis, M. T., & Wilson, L. J. (2012). Cisplatin@ US-tube carbon nanocapsules for enhanced chemotherapeutic delivery. *Biomaterials*, 33(5), 1455-1461.
- Hanson, D. S., Wang, Y., Zhou, X., Washburn, E., Ekmekci, M. B., Dennis, D., ...& Zhou, M. (2021). Catalytic Urea Synthesis from Ammonium Carbamate Using a Copper (II) Complex: A Combined Experimental and Theoretical Study. *Inorganic Chemistry*, 60(8), 5573-5589
- Haribabu, J., Balachandran, C., Tamizh, M. M., Arun, Y., Bhuvanesh, N. S., Aoki, S., & Karvembu, R. (2020). Unprecedented formation of palladium (II)-pyrazole based thiourea from chromone thiosemicarbazone and [PdCl₂ (PPh₃)₂]: Interaction with biomolecules and apoptosis through mitochondrial signaling pathway. *Journal of inorganic biochemistry*, 205(21), 110988-110101.
- Haribabu, J., Srividya, S., Mahendiran, D., Gayathri, D., Venkatramu, V., Bhuvanesh, N., & Karvembu, R. (2020). Synthesis of Palladium (II) Complexes via Michael Addition: Antiproliferative Effects through ROS-Mediated Mitochondrial Apoptosis and Docking with SARS-CoV-2. *Inorganic chemistry*, 59(23), 17109-17122.
- Heffeter, P., Pape, V. F., Enyedy, É. A., Keppler, B. K., Szakacs, G., & Kowol, C. R. (2019). Anticancer thiosemicarbazones: chemical properties, interaction with iron metabolism, and resistance development. *Antioxidants & redox signaling*, 30(8), 1062-1082.
- Heinz, J., & Schulze-Makuch, D. (2020). Thiophenes on Mars: Biotic or Abiotic Origin?. *Astrobiology*, 20(4), 552-561.
- Helland, R., Bjørkeng, E. K., Rothweiler, U., Sydnes, M. O., & Pampanin, D. M. (2019). The crystal structure of haemoglobin from Atlantic cod. *Acta Crystallographica Section F: Structural Biology Communications*, 75(8), 537-542.
- Hernández, W., Carrasco, F., Vaisberg, A., Spodine, E., Manzur, J., Icker, M., ...& Beyer, L. (2020). Synthesis, Spectroscopic Characterization, Structural Studies, and In Vitro

Antitumor Activities of Pyridine-3-carbaldehyde Thiosemicarbazone Derivatives. *Journal of Chemistry*, 2020,1-12

Hieringer, W., Flechtner, K., Kretschmann, A., Seufert, K., Auwärter, W., Barth, J. V., ...& Gottfried, J. M. (2011). The surface trans effect: influence of axial ligands on the surface chemical bonds of adsorbed metalloporphyrins. *Journal of the American Chemical Society*, 133(16), 6206-6222.

Hosseini-Yazdi, S. A., Mirzaahmadi, A., Khandar, A. A., Mahdavi, M., Rahimian, A., Eigner, V., ...&Zarrini, G. (2017). Copper, nickel and zinc complexes of a new water-soluble thiosemicarbazone ligand: Synthesis, characterization, stability and biological evaluation. *Journal of Molecular Liquids*, 248, 658-667.

Hu, K. F., Ning, X. S., Qu, J. P., & Kang, Y. B. (2018). Tuning regioselectivity of Wacker oxidation in one catalytic system: Small change makes big step. *The Journal of organic chemistry*, 83(18), 11327-11332.

Islam, M., Khan, A., Shehzad, M. T., Khiat, M., Halim, S. A., Hameed, A., ...& Shafiq, Z. (2021). Therapeutic potential of N4-substituted thiosemicarbazones as new urease inhibitors: Biochemical and in silico approach. *Bioorganic Chemistry*, 109, 104691.

Jain, V. K., & Chauhan, R. S. (2016). New vistas in the chemistry of platinum group metals with tellurium ligands. *Coordination Chemistry Reviews*, 306, 270-301.

Jemal, A., Bray, F., Center, M. M., Ferlay, J., Ward, E., & Forman, D. (2011). Global cancer statistics. *CA: a cancer journal for clinicians*, 61(2), 69-90.

Jiang, B., Liang, Q. J., Han, Y., Zhao, M., Xu, Y. H., &Loh, T. P. (2018). Copper-Catalyzed Dehydrogenative Diels–Alder Reaction. *Organic letters*, 20(11), 3215-3219.

Kapdi, A. R., & Fairlamb, I. J. (2014). Anti-cancer palladium complexes: a focus on PdX₂L₂, palladacycles and related complexes. *Chemical Society Reviews*, 43(13), 4751-4777.

Kaur, N. (2019). Nickel catalysis: six membered heterocycle syntheses. *Synthetic Communications*, 49(9), 1103-1133.

- Kohli, E., Arora, R., & Kakkar, R. (2014). Theoretical study of the stability of tautomers and conformers of isatin-3-thiosemicarbazone (IBT). *Can Chem Trans*, 2, 327-42.
- Kokina, T. E., Glinskaya, L. A., Sheludyakova, L. A., Eremina, Y. A., Klyushova, L. S., Komarov, V. Y., ... & Larionov, S. V. (2019). Synthesis, structure, and cytotoxicity of complexes of zinc (II), palladium (II), and copper (I) chlorides with (-)-camphor thiosemicarbazone. *Polyhedron*, 163, 121-130.
- Kose, E., Atac, A., & Bardak, F. (2018). The structural and spectroscopic investigation of 2-chloro-3-methylquinoline by DFT method and UV-Vis, NMR and vibrational spectral techniques combined with molecular docking analysis. *Journal of Molecular Structure*, 1163, 147-160.
- Kowol, C. R., Eichinger, R., Jakupec, M. A., Galanski, M., Arion, V. B., & Keppler, B. K. (2007). Effect of metal ion complexation and chalcogen donor identity on the antiproliferative activity of 2-acetylpyridine N, N-dimethyl (chalcogen) semicarbazones. *Journal of inorganic biochemistry*, 101(11-12), 1946-1957.
- Kumar, L. V., & Nath, G. R. (2019). Synthesis, characterization and biological studies of cobalt (II), nickel (II), copper (II) and zinc (II) complexes of vanillin-4-methyl-4-phenyl-3-thiosemicarbazone. *Journal of Chemical Sciences*, 131(8), 1-13.
- Laszlo, P. (1986). Catalysis of organic reactions by inorganic solids. *Accounts of Chemical Research*, 19(4), 121-127.
- Laverick, R. J., Zhang, N., Reid, E., Kim, J., Kilpin, K. J., & Kitchen, J. A. (2021). Solution processible Co (III) quinoline-thiosemicarbazone complexes: synthesis, structure extension, and Langmuir-Blodgett deposition studies. *Journal of Coordination Chemistry*, 74(1-3), 321-340.
- Lee, C. K., Yu, J. S., & Ji, Y. R. (2002). Determination of aromaticity indices of thiophene and furan by nuclear magnetic resonance spectroscopic analysis of their anilides. *Journal of heterocyclic chemistry*, 39(6), 1219-1227.

- Lennox, A. J., & Lloyd-Jones, G. C. (2014). Selection of boron reagents for Suzuki–Miyaura coupling. *Chemical Society Reviews*, *43*(1), 412-443.
- Levashov, A. S., Buryi, D. S., Goncharova, O. V., Konshin, V. V., Dotsenko, V. V., & Andreev, A. A. (2017). Tetraalkynylstannanes in the Stille cross coupling reaction: a new effective approach to arylalkynes. *New Journal of Chemistry*, *41*(8), 2910-2918.
- Li, C., Cai, J., Geng, J., Li, Y., Wang, Z., & Li, R. (2012). Purification, characterization and anticancer activity of a polysaccharide from *Panax ginseng*. *International journal of biological macromolecules*, *51*(5), 968-973.
- Lin, K., Zhao, Z., Bo, H., Hao, X., & Wang, J. (2018). Applications of Ruthenium Complex in Tumor Diagnosis and Therapy. *Frontiers in pharmacology*, *9*, 1323-1333.
- Lindemann, A., Patel, A. A., Silver, N. L., Tang, L., Liu, Z., Wang, L., ...& Zhao, M. (2019). COTI-2, a novel thiosemicarbazone derivative, exhibits antitumor activity in HNSCC through p53-dependent and-independent mechanisms. *Clinical Cancer Research*, *25*(18), 5650-5662.
- Liu, D. S., Qiu, Z. J., Xiao, Y. L., Shen, Y. J., Zhou, Q., Chen, W. T., & Sui, Y. (2019). A novel tetranuclear Pb²⁺ compound based on ethylenediaminetetraacetate and azide mixed-ligands: Synthesis, structure and properties. *Journal of Solid State Chemistry*, *279*(9), 1-6.
- Liu, D. S., Qiu, Z. J., Xiao, Y. L., Shen, Y. J., Zhou, Q., Chen, W. T., & Sui, Y. (2019). A novel tetranuclear Pb²⁺ compound based on ethylenediaminetetraacetate and azide mixed-ligands: Synthesis, structure and properties. *Journal of Solid State Chemistry*, *279*(9), 1-6.
- Lobana, T. S., Sharma, R., Bawa, G., & Khanna, S. (2009). Bonding and structure trends of thiosemicarbazone derivatives of metals—an overview. *Coordination Chemistry Reviews*, *253*(7-8), 977-1055.
- Luo, N., Zhong, Y., Wen, H., & Luo, R. (2020). Cyclometalated Iridium Complex-Catalyzed N-Alkylation of Amines with Alcohols via Borrowing Hydrogen in Aqueous Media. *ACS omega*, *5*(42), 27723-27732.

- Ma, Z., Wang, Q., CBA Alegria, E., C Guedes da Silva, M. F., MDRS Martins, L., Telo, J. P., ... & JL Pombeiro, A. (2019). Synthesis and structure of copper complexes of a N6O4 macrocyclic ligand and catalytic application in alcohol oxidation. *Catalysts*, 9(5), 424.
- Mathews, N. A., Jacob, J. M., Begum, P. S., & Kurup, M. P. (2020). Cu (II) and Zn (II) complexes from a thiosemicarbazone derivative: Investigating the intermolecular interactions, crystal structures and cytotoxicity. *Journal of Molecular Structure*, 1202, 127319-127341.
- Matsinha, L. C., Mao, J., Mapolie, S. F., & Smith, G. S. (2015). Water-Soluble Palladium (II) Sulfonated Thiosemicarbazone Complexes: Facile Synthesis and Preliminary Catalytic Studies in the Suzuki–Miyaura Cross-Coupling Reaction in Water. *European Journal of Inorganic Chemistry*, 2015(24), 4088-4094.
- Mbugua, S. N., Njenga, L. W., Odhiambo, R. A., Wandiga, S. O., Meyer, M., Sibuyi, N., ... & Onani, M. O. (2020). Synthesis, Characterization, and DNA-Binding Kinetics of New Pd (II) and Pt (II) Thiosemicarbazone Complexes: Spectral, Structural, and Anticancer Evaluation. *Journal of Chemistry*, 2020(33), 12367-12381.
- Mbugua, S. N., Sibuyi, N. R., Njenga, L. W., Odhiambo, R. A., Wandiga, S. O., Meyer, M., ... & Onani, M. O. (2020). New palladium (II) and platinum (II) complexes based on pyrrole Schiff bases: synthesis, characterization, X-ray structure, and anticancer activity. *ACS omega*, 5(25), 14942-14954.
- McHenry, M. E., & Laughlin, D. E. (2014). Magnetic properties of metals and alloys. In *Physical Metallurgy* (pp. 1881-2008). Elsevier.
- Mjos, K. D., & Orvig, C. (2014). Metallodrugs in medicinal inorganic chemistry. *Chemical reviews*, 114(8), 4540-4563.
- Moradi-Shoeili, Z., Boghaei, D. M., Amini, M., Bagherzadeh, M., & Notash, B. (2013). New molybdenum (VI) complex with ONS-donor thiosemicarbazone ligand: preparation, structural characterization, and catalytic applications in olefin epoxidation. *Inorganic Chemistry Communications*, 27, 26-30.

- Motswainyana, W. M., Onani, M. O., & Madiehe, A. M. (2012). Bis (ferrocenylimine) palladium (II) and platinum (II) complexes: Synthesis, molecular structures and evaluation as antitumor agents. *Polyhedron*, *41*(1), 44-51.
- Munikumari, G., Konakanchi, R., Nishtala, V. B., Ramesh, G., Kotha, L. R., Chandrasekhar, K. B., & Ramachandraiah, C. (2019). Palladium (II) complexes of 5-substituted isatin thiosemicarbazones: Synthesis, spectroscopic characterization, biological evaluation and in silico docking studies. *Synthetic Communications*, *49*(1), 146-158.
- Munín, P., Lucio-Martínez, F., Reigosa, F., Fernandez-Figueiras, A., Vila, J. M., Pereira, M. T., & Ortigueira, J. M. (2017, November). Preparation and characterization of thiosemicarbazone ligands and study of their iron and palladium derivatives. In *Presented at the 21st International Electronic Conference on Synthetic Organic Chemistry* (Vol. 1, p. 30).
- Muralisankar, M., Basheer, S. M., Haribabu, J., Bhuvanesh, N. S., Karvembu, R., & Sreekanth, A. (2017). An investigation on the DNA/protein binding, DNA cleavage and in vitro anticancer properties of SNO pincer type palladium (II) complexes with N-substituted isatin thiosemicarbazone ligands. *Inorganica Chimica Acta*, *466*, 61-70.
- Nagendiran, A., Verho, O., Haller, C., Johnston, E. V., & Backvall, J. E. (2014). Cycloisomerization of Acetylenic Acids to γ -Alkylidene Lactones using a Palladium (II) Catalyst Supported on Amino-Functionalized Siliceous Mesocellular Foam. *The Journal of organic chemistry*, *79*(3), 1399-1405.
- Nakaya, A., Sagawa, M., Muto, A., Uchida, H., Ikeda, Y., & Kizaki, M. (2011). The gold compound auranofin induces apoptosis of human multiple myeloma cells through both down-regulation of STAT3 and inhibition of NF- κ B activity. *Leukemia research*, *35*(2), 243-249.
- Nassau, K. (1978). The origins of color in minerals. *American mineralogist*, *63*(3-4), 219-229.
- Nazarov, A. A., Hartinger, C. G., & Dyson, P. J. (2014). Opening the lid on piano-stool complexes: an account of ruthenium (II)-arene complexes with medicinal applications. *Journal of Organometallic Chemistry*, *751*, 251-260.

- Nazarov, Alexey A., Christian G. Hartinger, and Paul J. Dyson. "Opening the lid on piano-stool complexes: an account of ruthenium (II)–arene complexes with medicinal applications." *Journal of Organometallic Chemistry* 751 (2014), 251-260.
- Nguyen, M. H., Nguyen, H. H., Phung, Q. M., & Dinh, T. H. (2019). Emissive Pd (II) thiosemicarbazones bearing anthracene: New complexes with unusual coordination mode. *Inorganic Chemistry Communications*, 102, 120-125.
- Nirmala, M., Manikandan, R., Prakash, G., & Viswanathamurthi, P. (2014). Ruthenium (II) complexes of hybrid 8-hydroxyquinoline–thiosemicarbazone ligands: synthesis, characterization and catalytic applications. *Applied Organometallic Chemistry*, 28(1), 18-26.
- Niu, Z., Peng, Q., Zhuang, Z., He, W., & Li, Y. (2012). Evidence of an Oxidative-Addition-Promoted Pd-Leaching Mechanism in the Suzuki Reaction by Using a Pd-Nanostructure Design. *Chemistry–A European Journal*, 18(32), 9813-9817.
- Njogu, R. E., Fodran, P., Tian, Y., Njenga, L. W., Kariuki, D. K., Yusuf, A. O., ... & Wallentin, C. J. (2019). Electronically Divergent Triscyclometalated Iridium (III) 2-(1-naphthyl) pyridine Complexes and Their Application in Three-Component Methoxytrifluoromethylation of Styrene. *Synlett*, 30(07), 792-798.
- Nyawade, E. A., Sibuyi, N. R., Meyer, M., Lalancette, R., & Onani, M. O. (2020). Synthesis, characterization and anticancer activity of new 2-acetyl-5-methyl thiophene and cinnamaldehyde thiosemicarbazones and their palladium (II) complexes. *Inorganica Chimica Acta*, 515, 120036.
- Nyawade, E. A., Sibuyi, N. R., Meyer, M., Lalancette, R., & Onani, M. O. (2021). Synthesis, characterization and anticancer activity of new 2-acetyl-5-methyl thiophene and cinnamaldehyde thiosemicarbazones and their palladium (II) complexes. *Inorganica Chimica Acta*, 515, 120036.
- Odhiambo, R. A., Aluoch, A. O., Njenga, L. W., Kagwanja, S. M., Wandiga, S. O., & Wendt, O. F. (2018). Synthesis, characterisation and ion-binding properties of oxathiacrown ethers

- appended to [Ru (bpy) ₂] ²⁺. Selectivity towards Hg ²⁺, Cd ²⁺ and Pb ²⁺. *RSC advances*, 8(7), 3663-3672.
- Oliveira, C. G., Romero-Canelón, I., Coverdale, J. P., Maia, P. I. S., Clarkson, G. J., Deflon, V. M., & Sadler, P. J. (2020). Novel tetranuclear Pd II and Pt II anticancer complexes derived from pyrene thiosemicarbazones. *Dalton Transactions*, 49(28), 9595-9604.
- Özdemir, Ö., Gürkan, P., Demir, Y. D. Ş., & Ark, M. (2020). Novel palladium (II) complexes of N-(5-nitro-salicylidene)-Schiff bases: Synthesis, spectroscopic characterization and cytotoxicity investigation. *Journal of Molecular Structure*, 1207, 127852-127864.
- Pahontu, E., Julea, F., Rosu, T., Purcarea, V., Chumakov, Y., Petrenco, P., & Gulea, A. (2015). Antibacterial, antifungal and in vitro antileukaemia activity of metal complexes with thiosemicarbazones. *Journal of cellular and molecular medicine*, 19(4), 865-878.
- Pal, I., Basuli, F., & Bhattacharya, S. (2002). Thiosemicarbazone complexes of the platinum metals. A story of variable coordination modes. *Journal of Chemical Sciences*, 114(4), 255-268.
- Park, K. C., Fouani, L., Jansson, P. J., Wooi, D., Sahni, S., Lane, D. J., ...& Kalinowski, D. S. (2016). Copper and conquer: copper complexes of di-2-pyridylketone thiosemicarbazones as novel anti-cancer therapeutics. *Metallomics*, 8(9), 874-886.
- Parsa, F. G., Feizi, M. A. H., Safaralizadeh, R., Hosseini-Yazdi, S. A., & Mahdavi, M. (2020). Molecular mechanisms of apoptosis induction in K562 and KG1a leukemia cells by a water-soluble copper (II) thiosemicarbazone complex. *Journal of Biological Inorganic Chemistry: JBIC: a Publication of the Society of Biological Inorganic Chemistry*, 25, 383-395
- Paterson, B. M., & Donnelly, P. S. (2011). Copper complexes of bis (thiosemicarbazones): from chemotherapeutics to diagnostic and therapeutic radiopharmaceuticals. *Chemical Society Reviews*, 40(5), 3005-3018..
- Pelosi, G. (2010). Thiosemicarbazone metal complexes: from structure to activity. *The Open Crystallography Journal*, 3(1).ology, 3(8), 456-458.

- Pintauer, T., & Matyjaszewski, K. (2008). Atom transfer radical addition and polymerization reactions catalyzed by ppm amounts of copper complexes. *Chemical Society Reviews*, 37(6), 1087-1097.
- Prabhu, R. N., & Ramesh, R. (2013). Synthesis and structural characterization of palladium (II) thiosemicarbazone complex: application to the Buchwald–Hartwig amination reaction. *Tetrahedron Letters*, 54(9), 1120-1124.
- Prajapati, N. P., Patel, K. D., Vekariya, R. H., Patel, H. D., & Rajani, D. P. (2019). Thiazole fused thiosemicarbazones: Microwave-assisted synthesis, biological evaluation and molecular docking study. *Journal of Molecular Structure*, 1179, 401-410.
- Qin, Q. P., Zou, B. Q., Tan, M. X., Luo, D. M., Wang, Z. F., Wang, S. L., & Liu, Y. C. (2018). High in vitro anticancer activity of a dinuclear palladium (II) complex with a 2-phenylpyridine ligand. *Inorganic Chemistry Communications*, 96, 106-110.
- Quiroga, A. G., & Ranninger, C. N. (2004). Contribution to the SAR field of metallated and coordination complexes: studies of the palladium and platinum derivatives with selected thiosemicarbazones as antitumoral drugs. *Coordination Chemistry Reviews*, 248(1-2), 119-133.
- Radev, D. D. (2012). Nickel-containing alloys for medical application obtained by methods of mechanochemistry and powder metallurgy. *International Scholarly Research Notices*, 417(3), 122-135.
- Rao, N. N., Gopichand, K., Nagaraju, R., Ganai, A. M., & Rao, P. V. (2020). Design, synthesis, spectral characterization, DNA binding, photo cleavage and antibacterial studies of transition metal complexes of benzothiazole Schiff base. *Chemical Data Collections*, 27, 100368-100379.
- Rebolledo, A. P., Vieites, M., Gambino, D., Piro, O. E., Castellano, E. E., Zani, C. L., ... & Beraldo, H. (2005). Palladium (II) complexes of 2-benzoylpyridine-derived thiosemicarbazones: spectral characterization, structural studies and cytotoxic activity. *Journal of inorganic biochemistry*, 99(3), 698-706.

- Refat, M., El-Metwaly, N., Yamany, Y. B., Althagafi, I., Hameed, A., Alharbi, A., ...& Al-Humaidi, J. Y. (2021). Electrochemical synthesis for new thiosemicarbazide complexes, spectroscopy, cyclic voltammetry, structural properties, and in silico study. *Applied Organometallic Chemistry*, 35(1), e6049.
- Roque Marques, K. M., do Desterro, M. R., de Arruda, S. M., de Araújo, N., Nascimento, L., do Carmo Alves de Lima, M., ... & de Araújo-Júnior, J. X. (2019). 5-Nitro-Thiophene-Thiosemicarbazone Derivatives Present Antitumor Activity Mediated by Apoptosis and DNA Intercalation. *Current Topics in Medicinal Chemistry*, 19(13), 1075-1091.
- Saldan, I., Semenyuk, Y., Marchuk, I., & Reshetnyak, O. (2015). Chemical synthesis and application of palladium nanoparticles. *Journal of materials science*, 50(6), 2337-2354.
- Satheesh, C. E., Kumar, P. R., Sharma, P., Lingaraju, K., Palakshamurthy, B. S., & Naika, H. R. (2016). Synthesis, characterisation and antimicrobial activity of new palladium and nickel complexes containing Schiff bases. *Inorganica Chimica Acta*, 442, 1-9.
- Schatten, H. (2018). Brief overview of prostate cancer statistics, grading, diagnosis and treatment strategies. In *Cell & Molecular Biology of Prostate Cancer* (Vol 61, pp. 1-14). Springer, Cham.
- Şen, B., Kalhan, H. K., Demir, V., Güler, E. E., Kayalı, H. A., & Subaşı, E. (2019). Crystal structures, spectroscopic properties of new cobalt (II), nickel (II), zinc (II) and palladium (II) complexes derived from 2-acetyl-5-chloro thiophene thiosemicarbazone: anticancer evaluation. *Materials Science and Engineering: C*, 98, 550-559.
- Sharma, R., Lobana, T. S., Kaur, M., Thathai, N., Hundal, G., Jasinski, J. P., & Butcher, R. J. (2016). Variable coordinating activity of sulfur in silver (I) complexes with thiophene based N 1-substituted thiosemicarbazones: First case of thiophenyl-thione sulfur bridging in a dinuclear complex. *Journal of Chemical Sciences*, 128(7), 1103-1112.
- Sibuh, B. Z., Khanna, S., Taneja, P., Sarkar, P., & Taneja, N. K. (2021). Molecular docking, synthesis and anticancer activity of thiosemicarbazone derivatives against MCF-7 human breast cancer cell line. *Life Sciences*, 273, 119305.

- SINGH, S. B. (2016). Iridium Chemistry and Its Catalytic Applications: a Brief. *Green Chem. Technol. Lett.*, 2 (206), 456-518
- Sobiesiak, M., Muzioł, T., Rozalski, M., Krajewska, U., & Budzisz, E. (2014). Co (II), Ni (II) and Cu (II) complexes with phenylthiazole and thiosemicarbazone-derived ligands: synthesis, structure and cytotoxic effects. *New Journal of Chemistry*, 38(11), 5349-5361.
- Sukhorukov, A. Y. (2020). Catalytic Reductive Amination of Aldehydes and Ketones with Nitro Compounds: New Light on an Old Reaction. *Frontiers in chemistry*, 8, 215.
- Süleymanoğlu, M., Erdem-Kuruca, S., Bal-Demirci, T., Özdemir, N., Ülküseven, B., & Yaylım, İ. (2020). Synthesis, structural, cytotoxic and pharmacokinetic evaluation of some thiosemicarbazone derivatives. *Journal of Biochemical and Molecular Toxicology*, e22512, 1-13.
- Temraz, M. G., Elzahhar, P. A., Bekhit, A. E. D. A., Bekhit, A. A., Labib, H. F., & Belal, A. S. (2018). Anti-leishmanial click modifiable thiosemicarbazones: design, synthesis, biological evaluation and in silico studies. *European journal of medicinal chemistry*, 151, 585-600.
- Trotsko, N., Golus, J., Kazimierczak, P., Paneth, A., Przekora, A., Ginalska, G., & Wujec, M. (2020). Design, synthesis and antimycobacterial activity of thiazolidine-2, 4-dione-based thiosemicarbazone derivatives. *Bioorganic chemistry*, 97, 103676.
- Totta, X., Hatzidimitriou, A. G., Papadopoulos, A. N., & Psomas, G. (2017). Nickel (II)-naproxen mixed-ligand complexes: synthesis, structure, antioxidant activity and interaction with albumins and calf-thymus DNA. *New Journal of Chemistry*, 41(11), 4478-4492.
- Tupikina, E. Y., Denisov, G. S., Melikova, S. M., Kucherov, S. Y., & Tolstoy, P. M. (2018). New look at the Badger-Bauer rule: Correlations of spectroscopic IR and NMR parameters with hydrogen bond energy and geometry. FHF complexes. *Journal of Molecular Structure*, 1164, 129-136.

- Valencia, D., Klimova, T., & García-Cruz, I. (2012). Aromaticity of five- and six-membered heterocycles present in crude oils—An electronic description for hydrotreatment process. *Fuel*, *100*, 177-185.
- Valentini, A., Conforti, F., Crispini, A., De Martino, A., Condello, R., Stelitano, C., ... & Pucci, D. (2008). Synthesis, oxidant properties, and antitumoral effects of a heteroleptic palladium (II) complex of curcumin on human prostate cancer cells. *Journal of medicinal chemistry*, *52*(2), 484-491.
- Walzl, A., Unger, C., Kramer, N., Unterleuthner, D., Scherzer, M., Hengstschläger, M., & Dolznig, H. (2014). The resazurin reduction assay can distinguish cytotoxic from cytostatic compounds in spheroid screening assays. *Journal of biomolecular screening*, *19*(7), 1047-1059.
- Weiss, H., & Mohr, F. (2011). Cyclopalladation of thiophene-substituted thiosemicarbazones. *Journal of Organometallic Chemistry*, *696*(20), 3150-3154.
- Wiedermann, J., Mereiter, K., & Kirchner, K. (2006). Palladium imine and amine complexes derived from 2-thiophenecarboxaldehyde as catalysts for the Suzuki cross-coupling of aryl bromides. *Journal of Molecular Catalysis A: Chemical*, *257*(1-2), 67-72.
- Wilson, B. E., Jacob, S., Yap, M. L., Ferlay, J., Bray, F., & Barton, M. B. (2019). Estimates of global chemotherapy demands and corresponding physician workforce requirements for 2018 and 2040: a population-based study. *The Lancet Oncology*, *20*(6), 769-780.
- Wu, C. P., Hsieh, C. H., & Wu, Y. S. (2011). The emergence of drug transporter-mediated multidrug resistance to cancer chemotherapy. *Molecular pharmaceuticals*, *8*(6), 1996-2011.
- Wu, Q., Cui, Y., Li, Q., & Sun, J. (2015). Effective removal of heavy metals from industrial sludge with the aid of a biodegradable chelating ligand GLDA. *Journal of hazardous materials*, *283*, 748-754.
- Yu, X., Wang, J., Xu, Z., Yamamoto, Y., & Bao, M. (2016). Copper-Catalyzed Aza-Diels–Alder Reaction and Halogenation: An Approach To Synthesize 7-Halogenated Chromenoquinolines. *Organic letters*, *18*(10), 2491-2494.

- Zamani, H. A. (2008). Construction of strontium PVC-membrane sensor based on salicylaldehyde thiosemicarbazone. *Analytical letters*, 41(10), 1850-1866.
- Zhang, G., Yin, Z., & Zheng, S. (2016). Cobalt-catalyzed N-alkylation of amines with alcohols. *Organic letters*, 18(2), 300-303.
- Zhao, L., Wang, F., An, Q. Q., & Zhao, J. X. (2016). Crystal structure of (E)-1-(4-(((E)-3, 5-dichloro-2-hydroxybenzylidene) amino) phenyl) ethan-1-one O-ethyl oxime, C₁₇H₁₆Cl₂N₂O₂. *Zeitschrift für Kristallographie-New Crystal Structures*, 231(4), 1045-1046.

APPENDICES

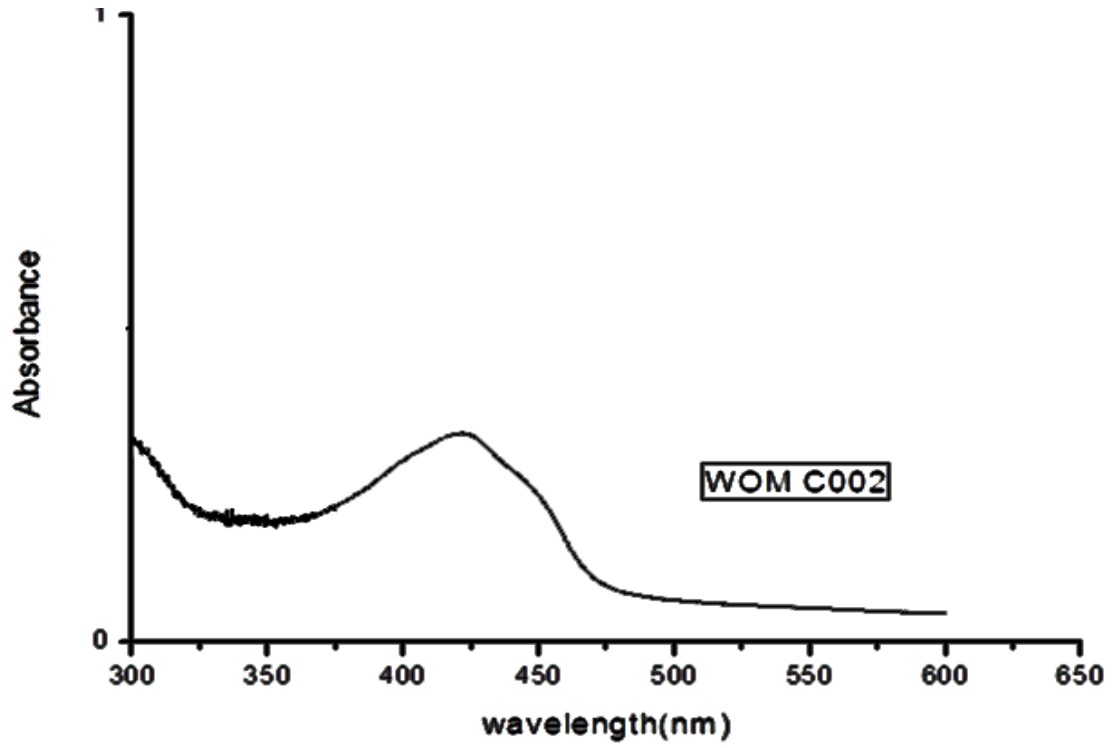


Figure 3: UV-Vis spectra for C2

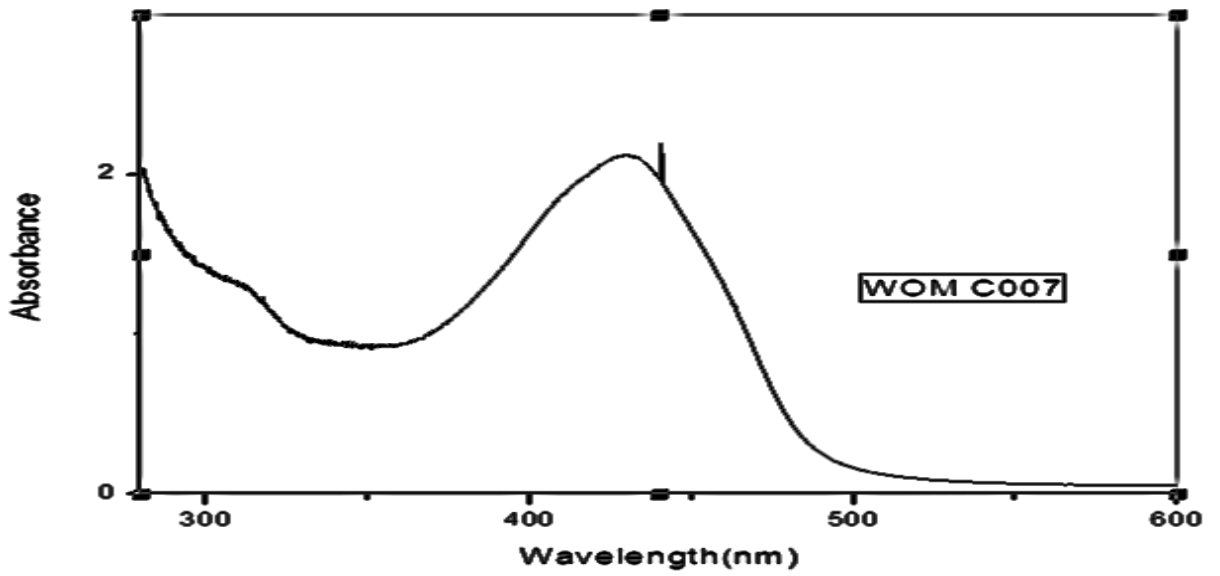


Figure 2: UV-Vis spectra for C3

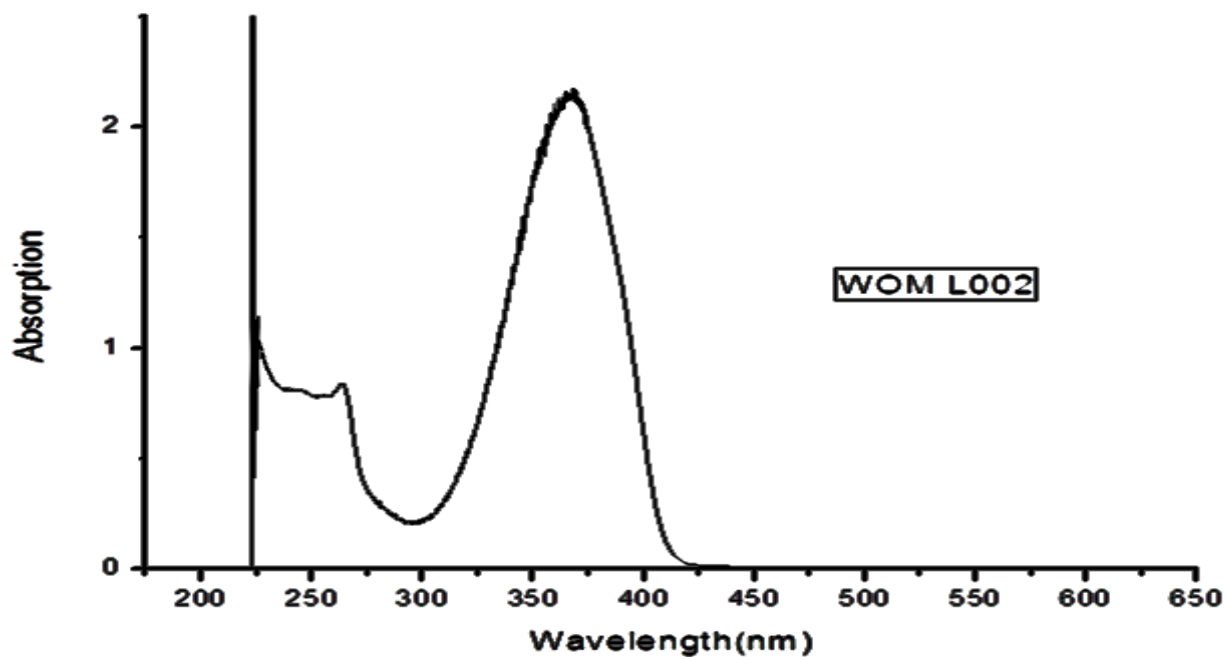


Figure 3:UV-Vis spectra for L2

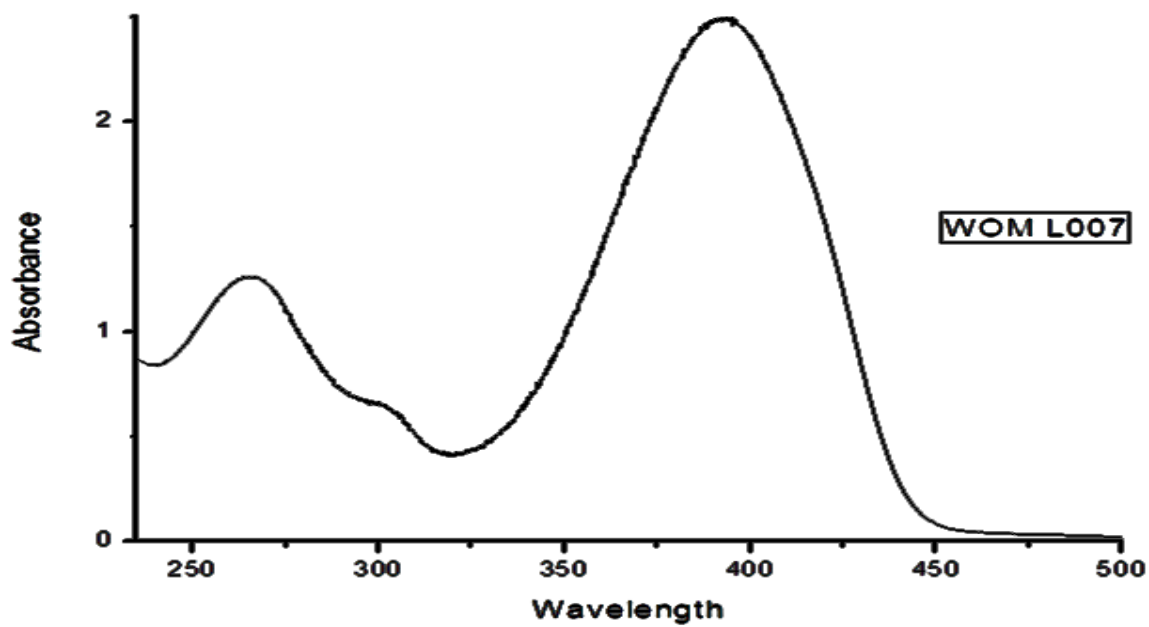


Figure 4:UV-Vis spectra for L3

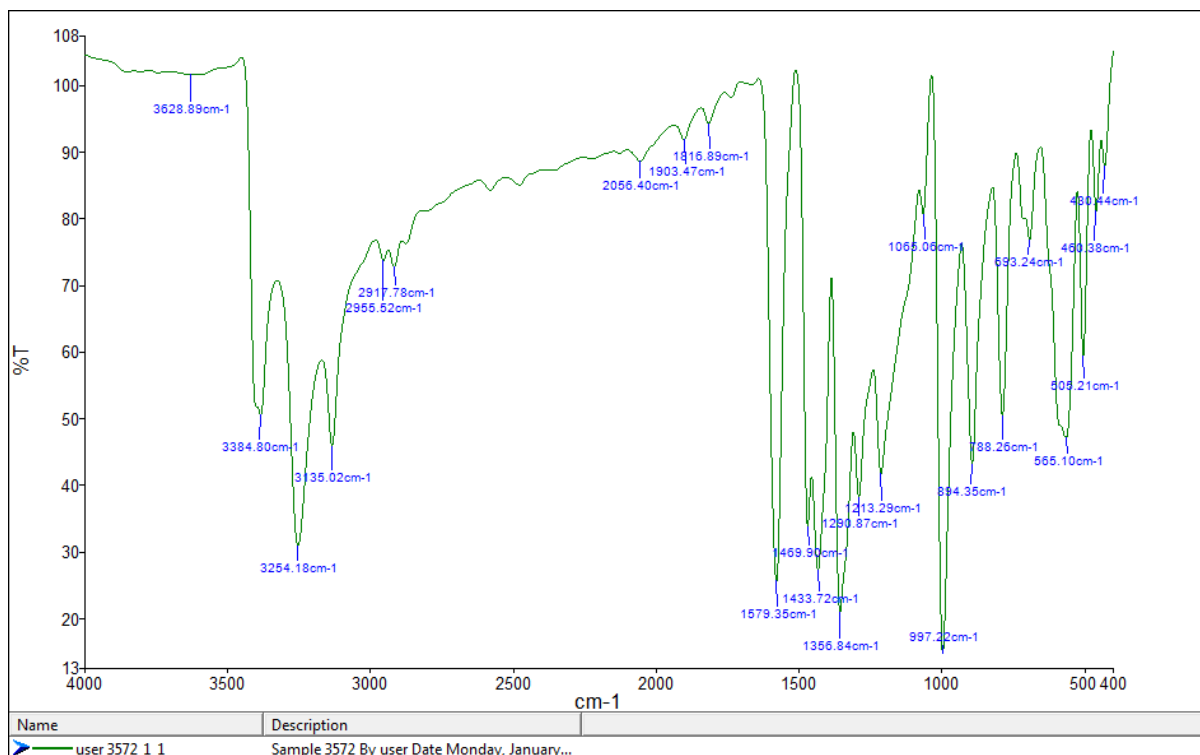


Figure 5: FTIR spectra for L3

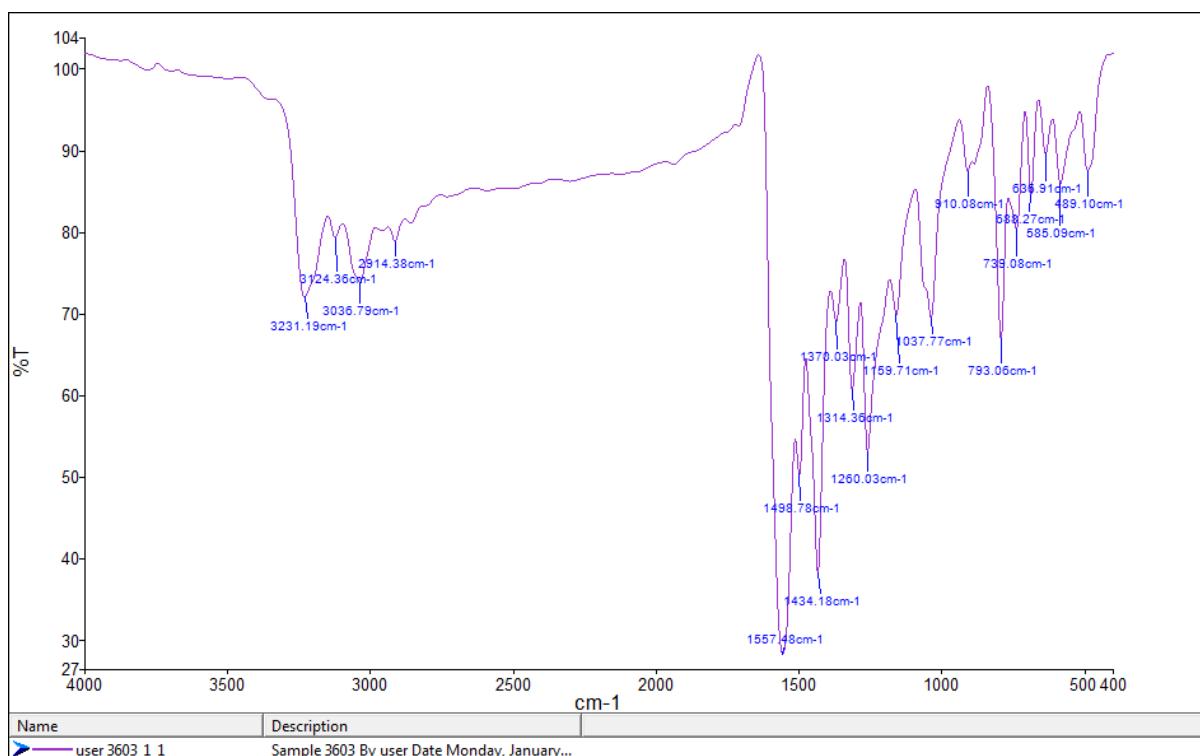


Figure 6: FTIR spectra for C3

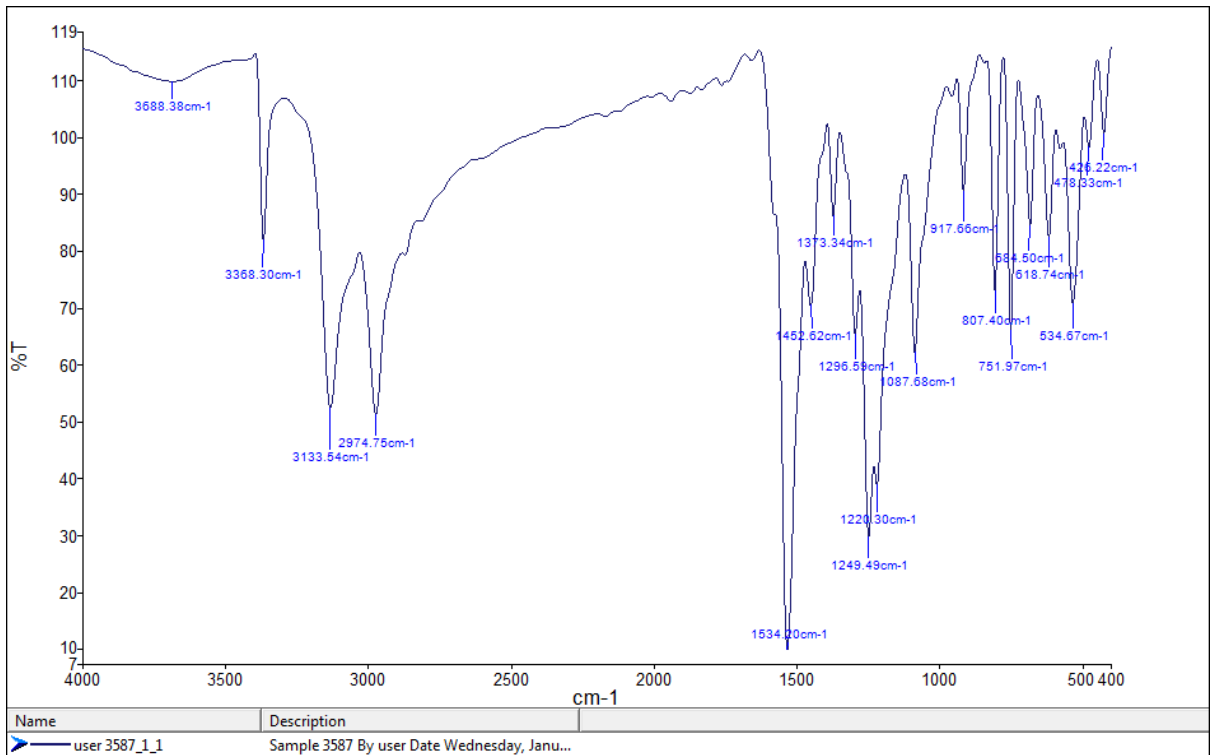


Figure 7: FTIR spectra for L2

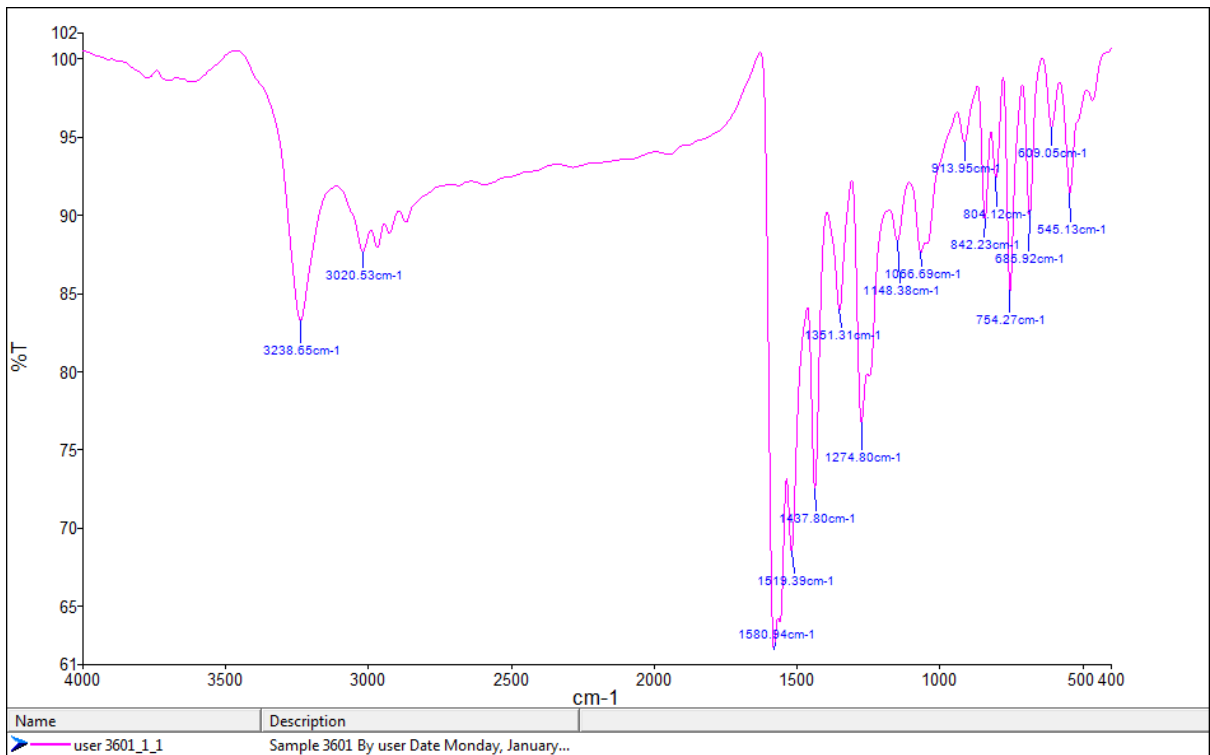


Figure 8: FTIR spectra for C2

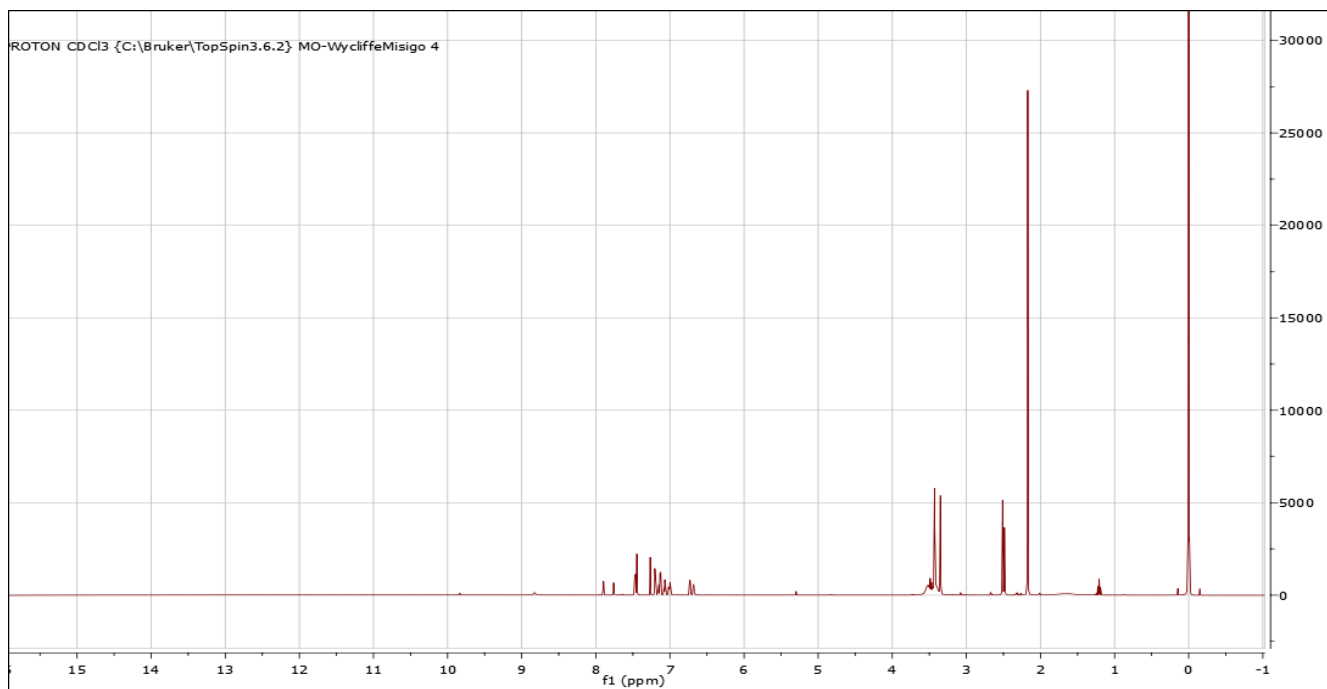


Figure 9: ¹H NMR for L1

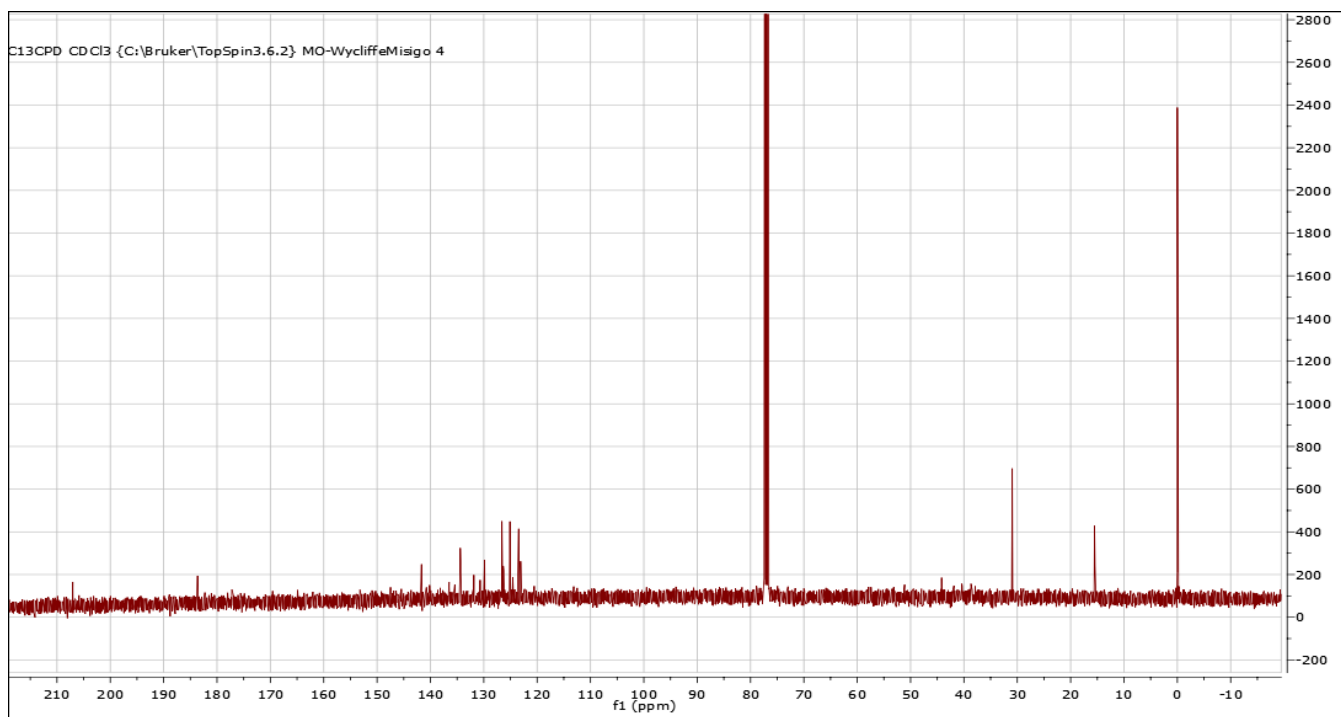


Figure 10: ¹³C NMR spectra for L1

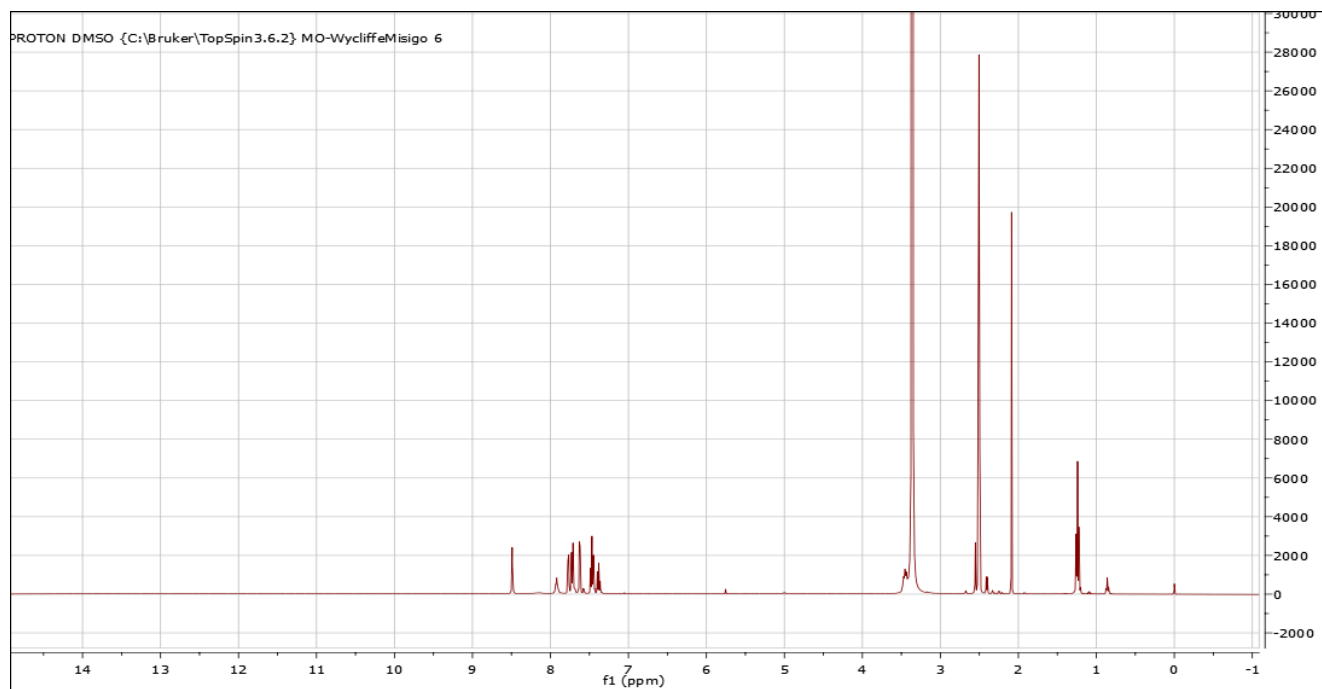


Figure 11: ¹H NMR spectra for C2

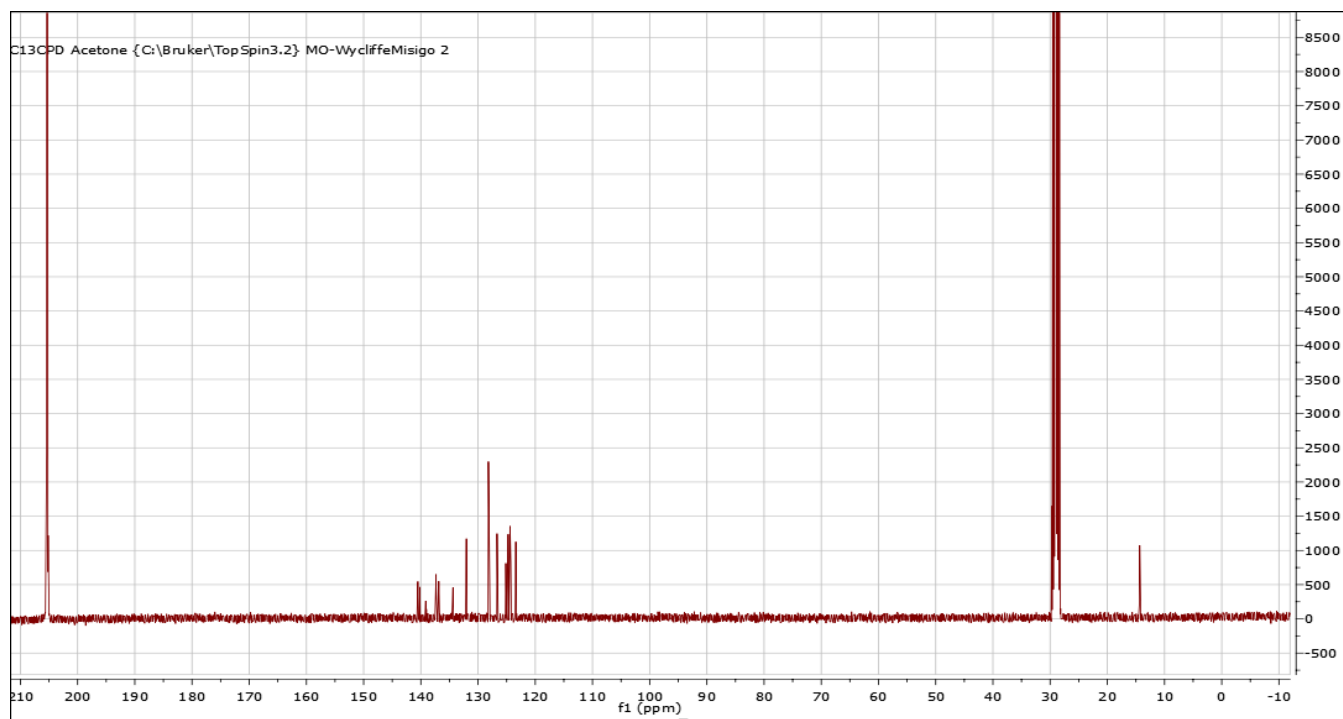


Figure 4: ¹³C NMR spectra for L3

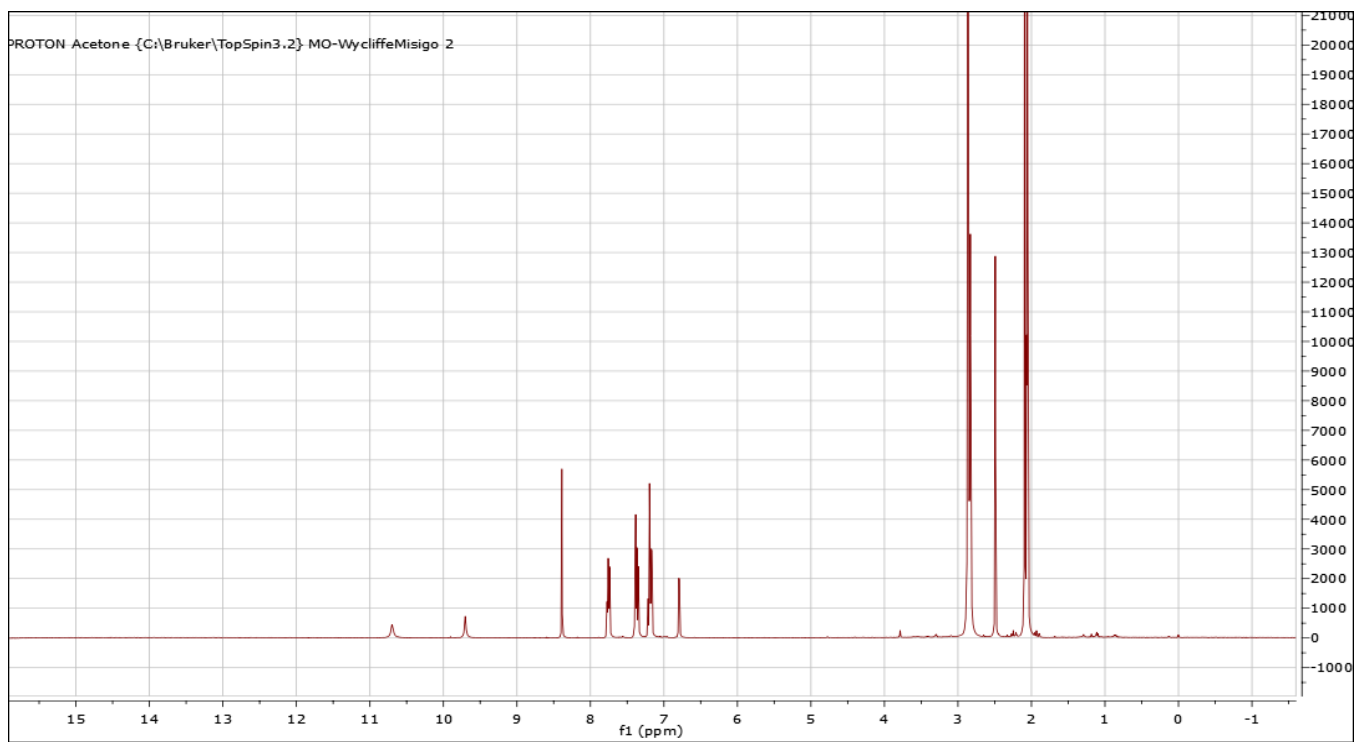


Figure 13: ^1H NMR spectra for L3

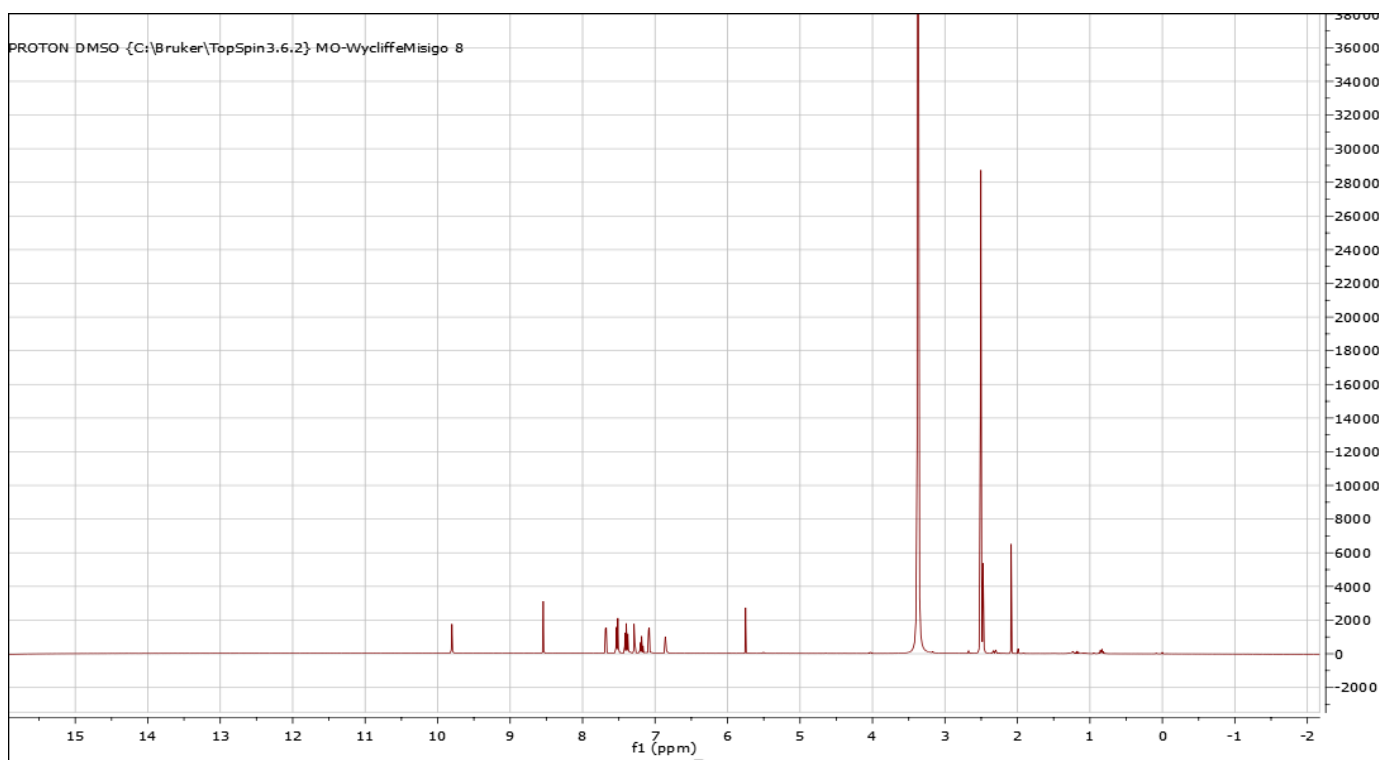


Figure 14: ^1H NMR spectra for C3